US012355328B2

(12) **United States Patent**
Sarlioglu et al.

(10) **Patent No.: US 12,355,328 B2**
(45) **Date of Patent: Jul. 8, 2025**

(54) **ELECTRICAL MACHINE COOLING WITH AXIAL AND RADIAL INLETS AND OUTLETS**

(71) Applicant: **Wisconsin Alumni Research Foundation**, Madison, WI (US)

(72) Inventors: **Bulent Sarlioglu**, Madison, WI (US); **Gregory F. Nellis**, Waunakee, WI (US); **Leyue Zhang**, Madison, WI (US); **Hao Ding**, Carson, CA (US)

(73) Assignee: **Wisconsin Alumni Research Foundation**, Madison, WI (US)

(*) Notice: Subject to any disclaimer, the term of this patent is extended or adjusted under 35 U.S.C. 154(b) by 299 days.

(21) Appl. No.: **17/937,798**

(22) Filed: **Oct. 4, 2022**

(65) **Prior Publication Data**

US 2023/0112852 A1 Apr. 13, 2023

Related U.S. Application Data

(60) Provisional application No. 63/253,634, filed on Oct. 8, 2021.

(51) **Int. Cl.**
H02K 5/20 (2006.01)
H02K 1/20 (2006.01)
H02K 1/32 (2006.01)

(52) **U.S. Cl.**
CPC ***H02K 5/20*** (2013.01); ***H02K 1/20*** (2013.01); ***H02K 1/32*** (2013.01)

(58) **Field of Classification Search**
CPC .. H02K 5/20; H02K 1/20; H02K 1/32; H02K 5/207; H02K 2201/03; H02K 9/06; H02K 1/276
See application file for complete search history.

(56) **References Cited**

U.S. PATENT DOCUMENTS

7,021,905 B2 4/2006 Torrey et al.
8,248,302 B2 8/2012 Tsai et al.
(Continued)

FOREIGN PATENT DOCUMENTS

DE 202008015895 U1 * 3/2009 ..... H02K 11/33
WO WO-2021199376 A1 * 10/2021 ..... H02K 1/32

OTHER PUBLICATIONS

DE202008015895U1 English translation (Year: 2024).*
(Continued)

Primary Examiner — Christopher M Koehler
Assistant Examiner — Viswanathan Subramanian
(74) *Attorney, Agent, or Firm* — Bell & Manning, LLC

(57) **ABSTRACT**

An electrical machine includes a rotor, a stator, and a winding mounted within a housing. The rotor includes a rotor core mounted to a shaft and a plurality of blades extending radially away from the rotor core. Each blade of the plurality of blades is curved axially along the rotor core. The stator includes a stator core and a plurality of teeth extending from the stator core toward the rotor core to define a plurality of slots between successive teeth. The winding is wound through at least two slots of the plurality of slots. The stator is mounted radially relative to the rotor. The housing includes a front wall, a back wall, and a radial sidewall mounted between the front wall and the back wall to define an enclosure. A radial inlet aperture wall is formed circumferentially through the radial sidewall to form an opening through the radial sidewall.

20 Claims, 55 Drawing Sheets
(12 of 55 Drawing Sheet(s) Filed in Color)

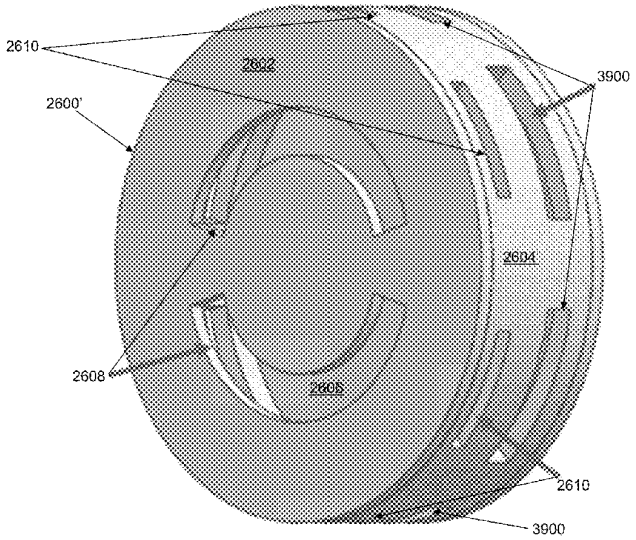

(56) **References Cited**

U.S. PATENT DOCUMENTS

8,790,236	B2	7/2014	LaRose et al.	
10,539,147	B2	1/2020	Sarlioglu et al.	
2010/0117475	A1	5/2010	Leonardi et al.	
2017/0149308	A1 *	5/2017	Sayre	H02K 5/207

OTHER PUBLICATIONS

WO2021199376A1 English translation (Year: 2024).*
NPLDing (Year: 2024).*
NPLZhang (Year: 2024).*
N. Rotevatn, Design and testing of Flux Switched Permanent Magnet (FSPM) Machines, Master of Science in Energy and Environment, Norwegian University of Science and Technology, Department of Electrical Power Engineering, Jun. 2009.
Wang et al., Reduction of Cogging Torque in Permanent Magnet Flux-Switching Machines, J. Electromagnetic Analysis & Applications 1, Mar. 2009, pp. 11-14.
Yang et al., Acoustic Noise/Vibration Reduction of a Single-Phase SRM Using Skewed Stator and Rotor, IEEE Transactions On Industrial Electronics, vol. 60, No. 10, Sep. 6, 2012, pp. 4292-4300.
Zhang, Leyue, et al. "Radial and Axial Inlet and Outlet Design for End Winding Cooling of High-Speed Integrated Flux-Switching Motor-Compressor." 2021 IEEE Energy Conversion Congress and Exposition (Ecce). IEEE, Oct. 2021.
Sayed, Ehab, et al. "A comprehensive review of flux barriers in interior permanent magnet synchronous machines." IEEE Access 7 (2019): 149168-149181.
Mccluskey, F. Patrick, et al. "Cooling for electric aircraft motors." 2019 18th IEEE Intersociety Conference on Thermal and Thermomechanical Phenomena in Electronic Systems (ITherm). IEEE, May 2019. pp. 1134-1138.
Cui, Shumei, et al. "A thermal-electromagnetic coupled motor design flow for electric aircraft propeller drive application." 2017 IEEE Transportation Electrification Conference and Expo, Asia-Pacific (ITEC Asia-Pacific). IEEE, 2017.

* cited by examiner

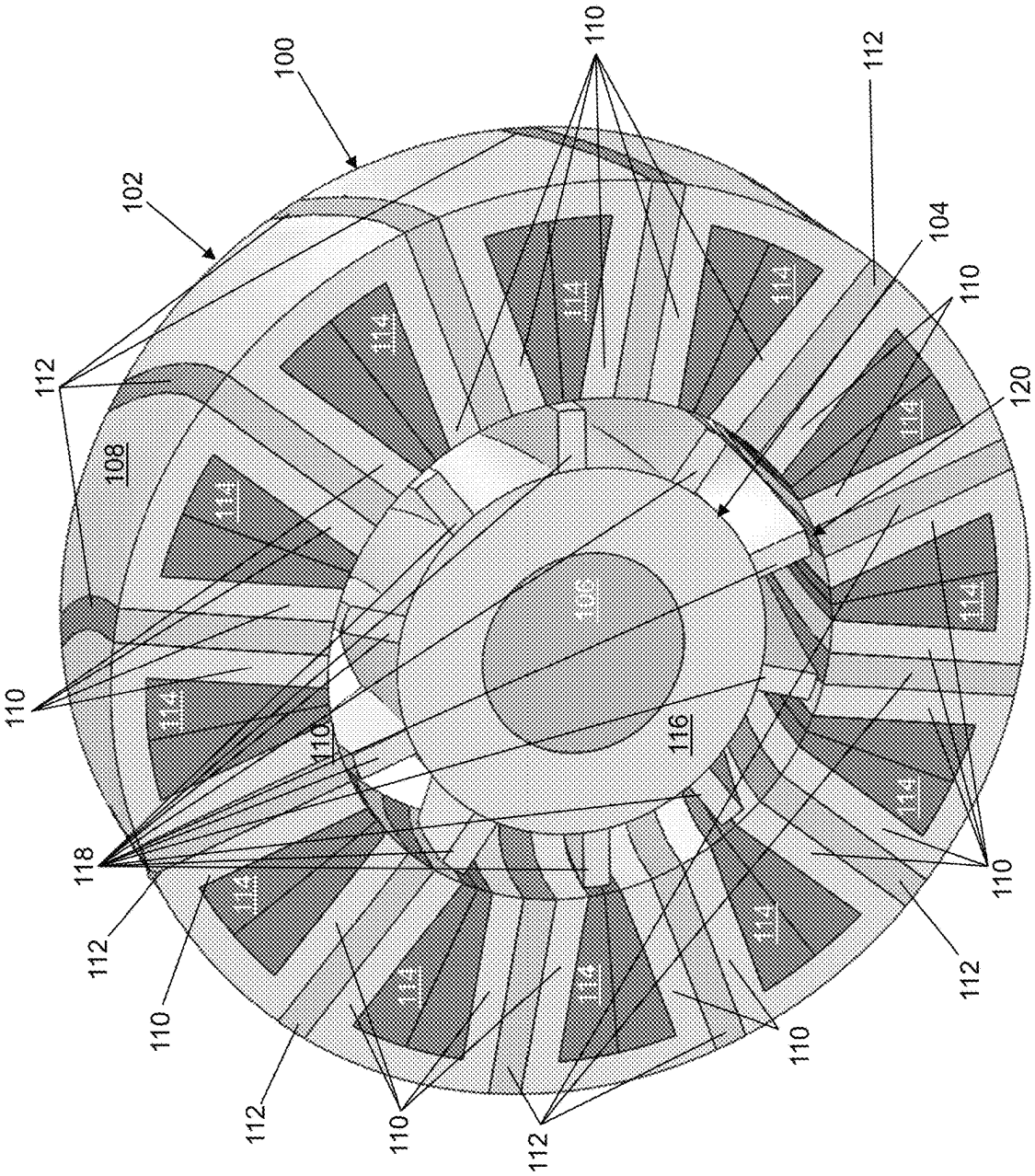

FIG. 1

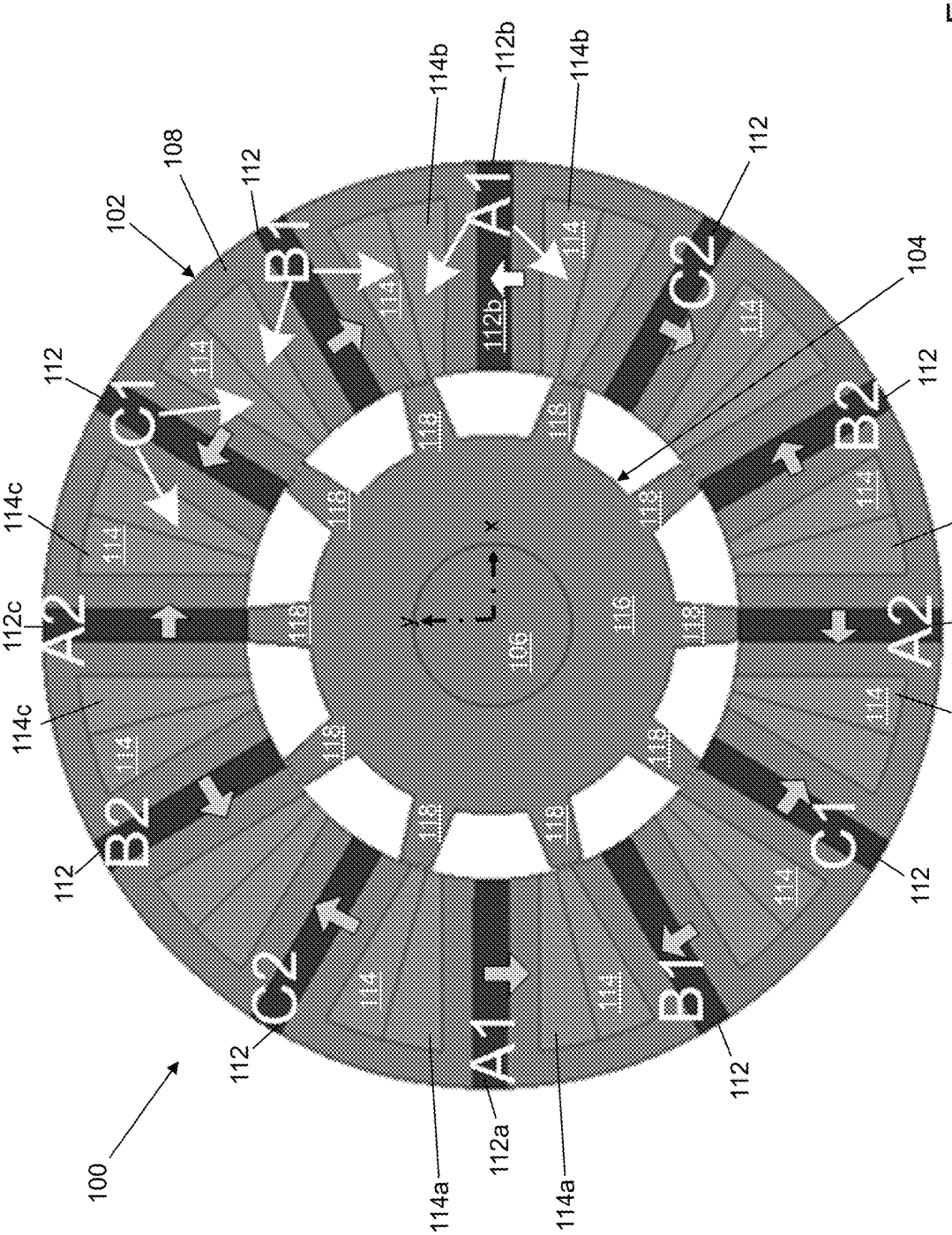
100
102
104
106
108
112
112a
112b
112c
112d
114
114a
114b
114c
114d
116
118
A1
A2
B1
B2
C1
C2
y
x

FIG. 2

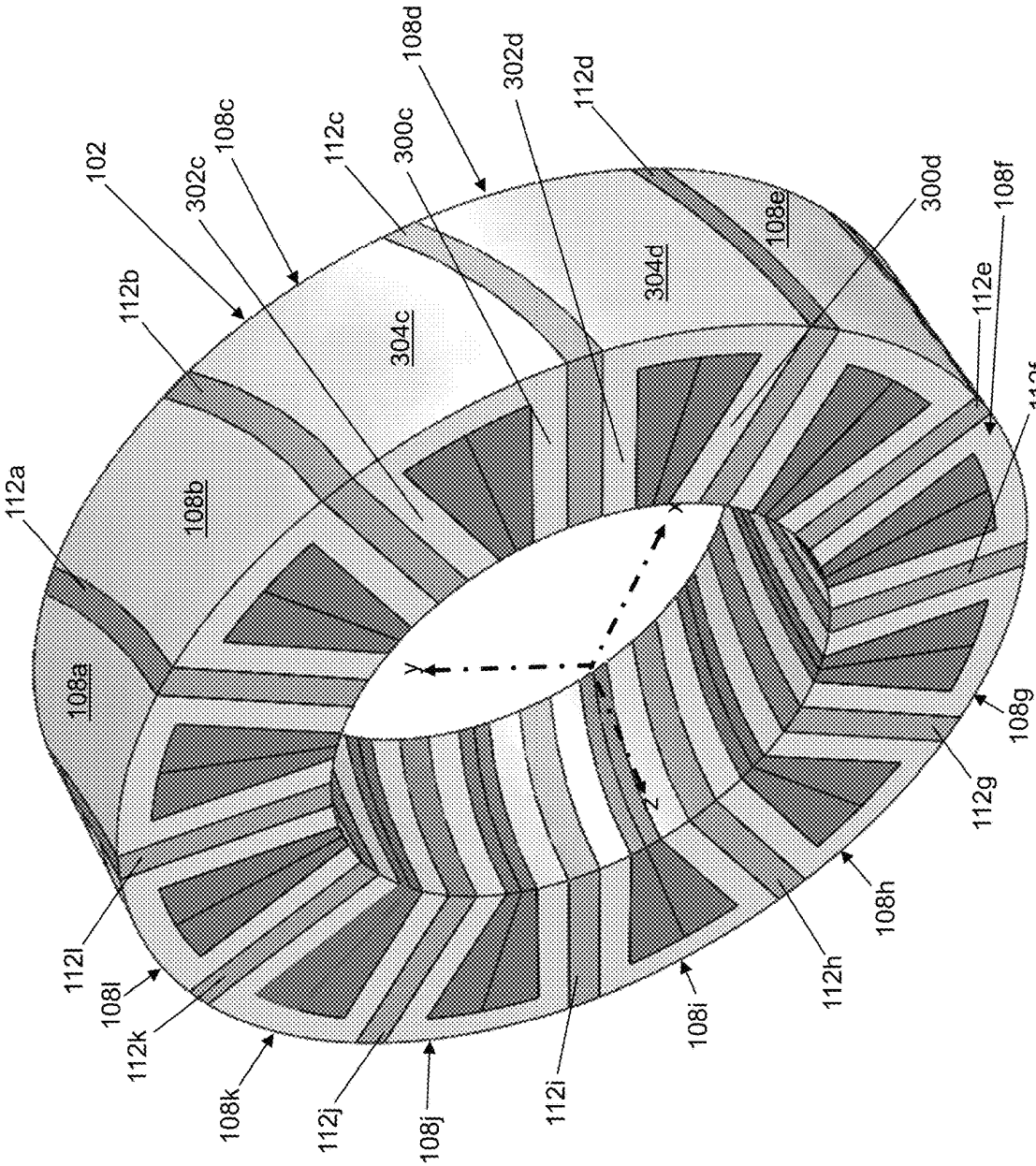
102
112a
112b
112c
112d
112e
112f
112g
112h
112i
112j
112k
112l
108a
108b
108c
108d
108e
108f
108g
108h
108i
108j
108k
108l
300c
300d
302c
302d
304c
304d
x
y
z

FIG. 3

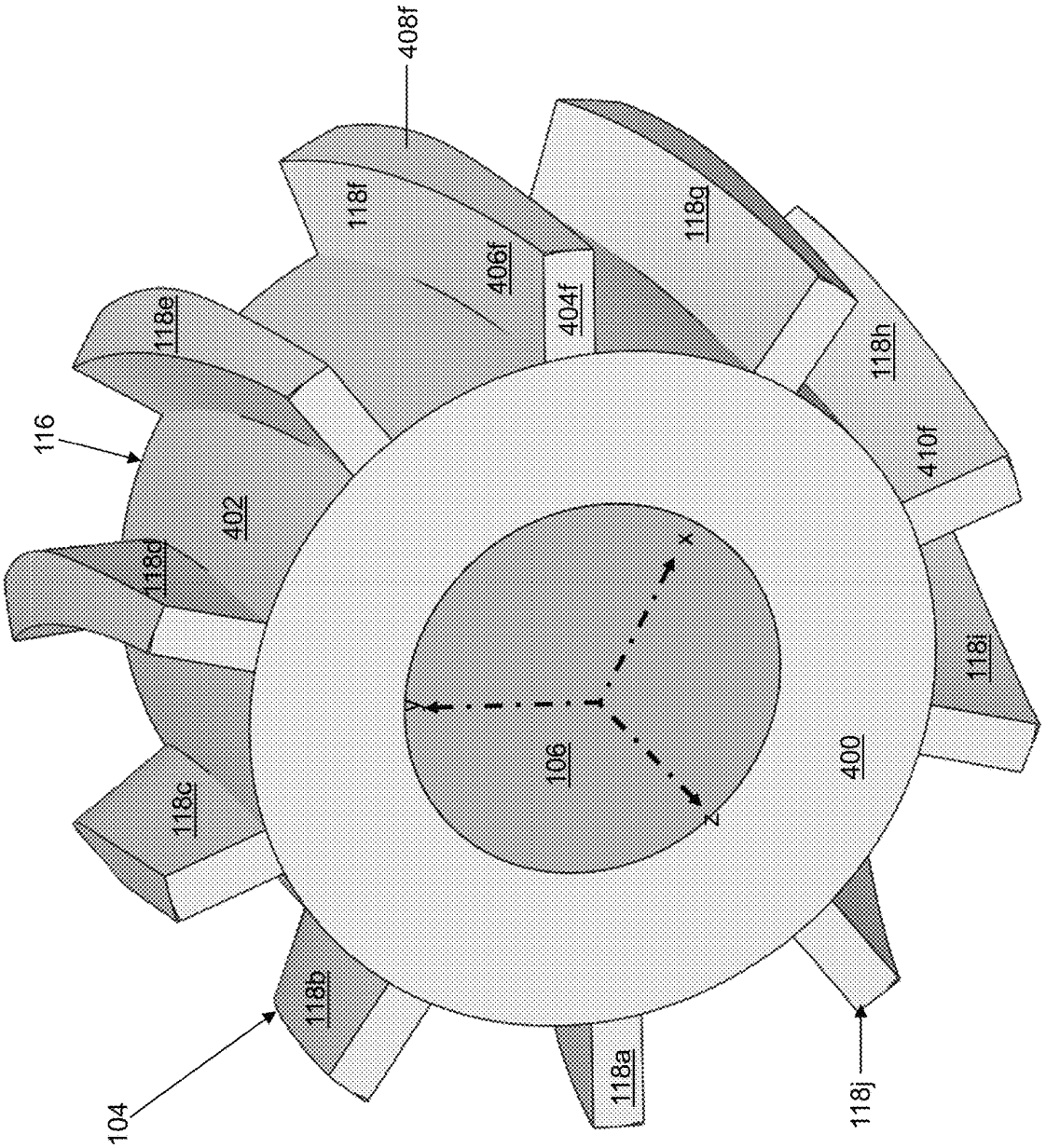
408f
118f
406f
404f
118g
118h
410f
118e
116
402
118d
118i
106
400
118c
118b
118a
118j
104
x
y
z

FIG. 4

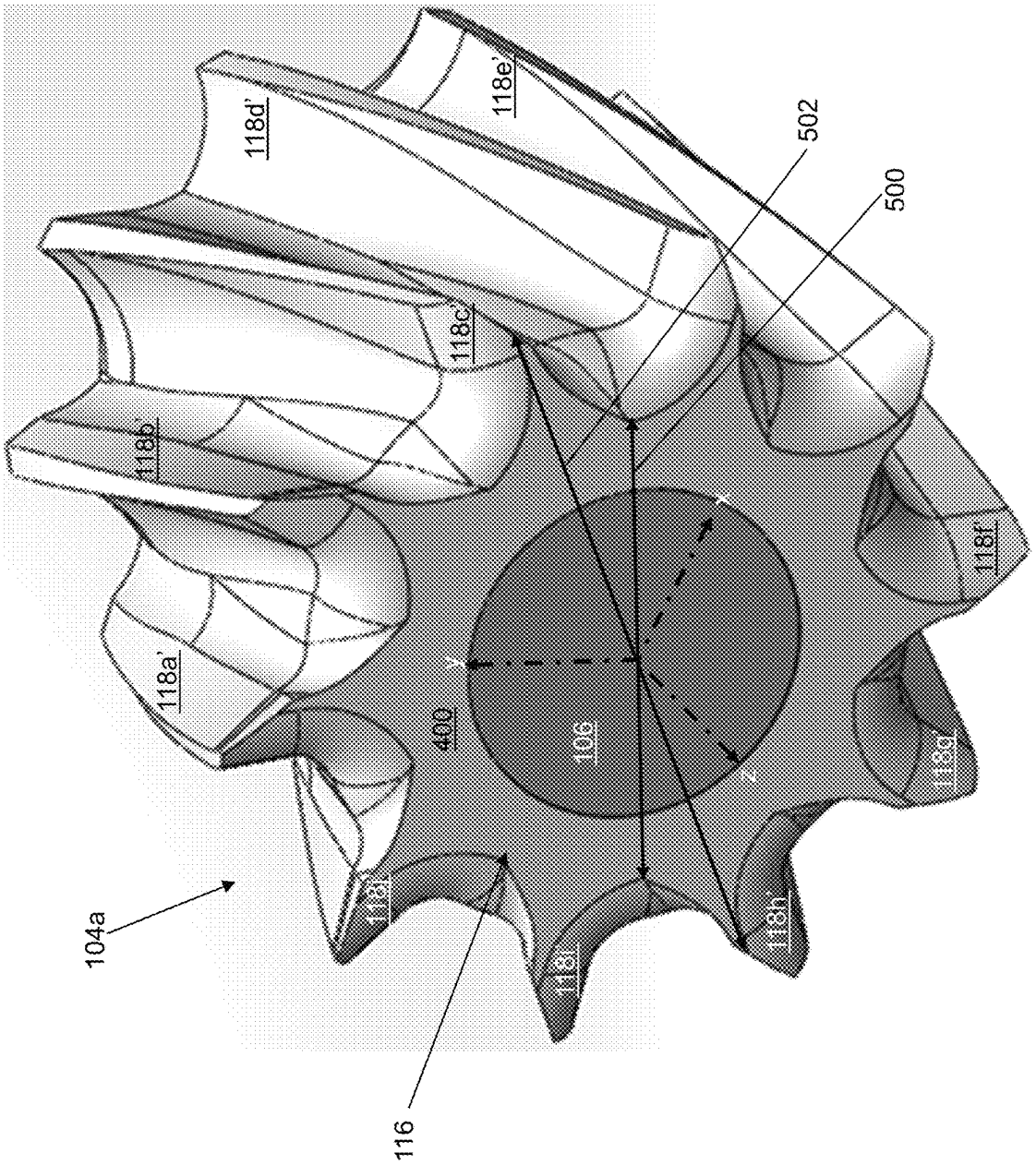
104a
116
118a'
118b'
118c'
118d'
118e'
118f'
118g
118h
118i
118j
106
400
500
502

FIG. 5

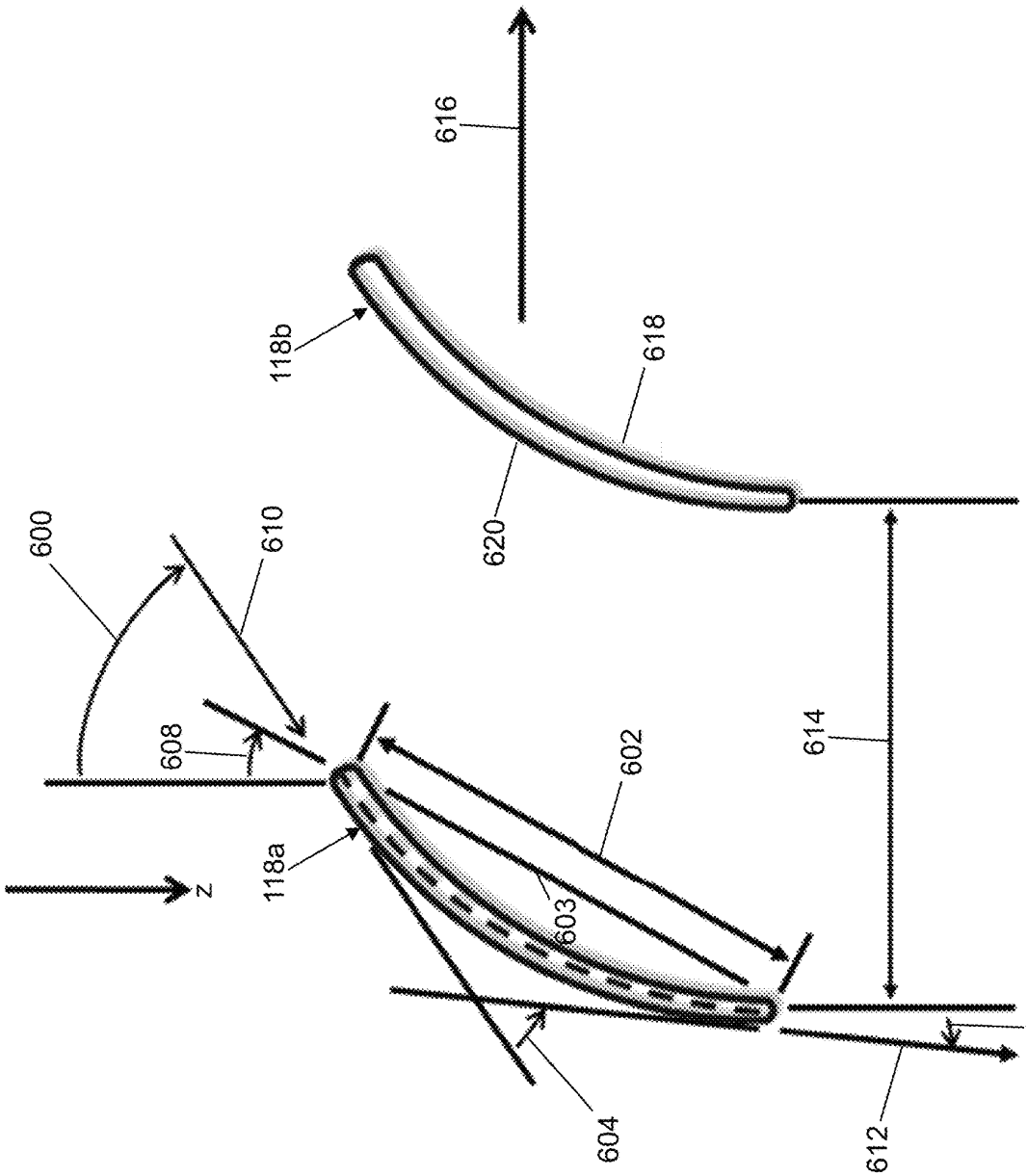

FIG. 6

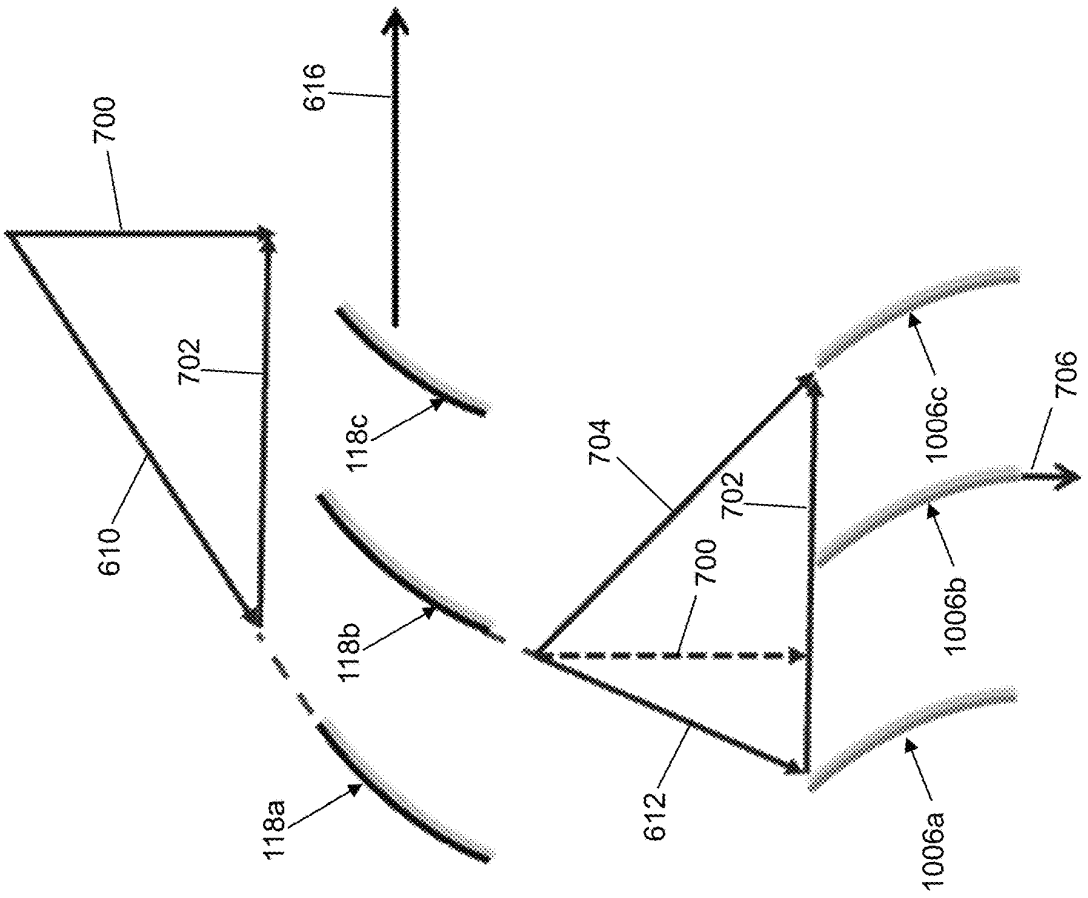
700
610
702
118a
118b
118c
616
704
612
700
702
1006a
1006b
1006c
706

FIG. 7

FIG. 8

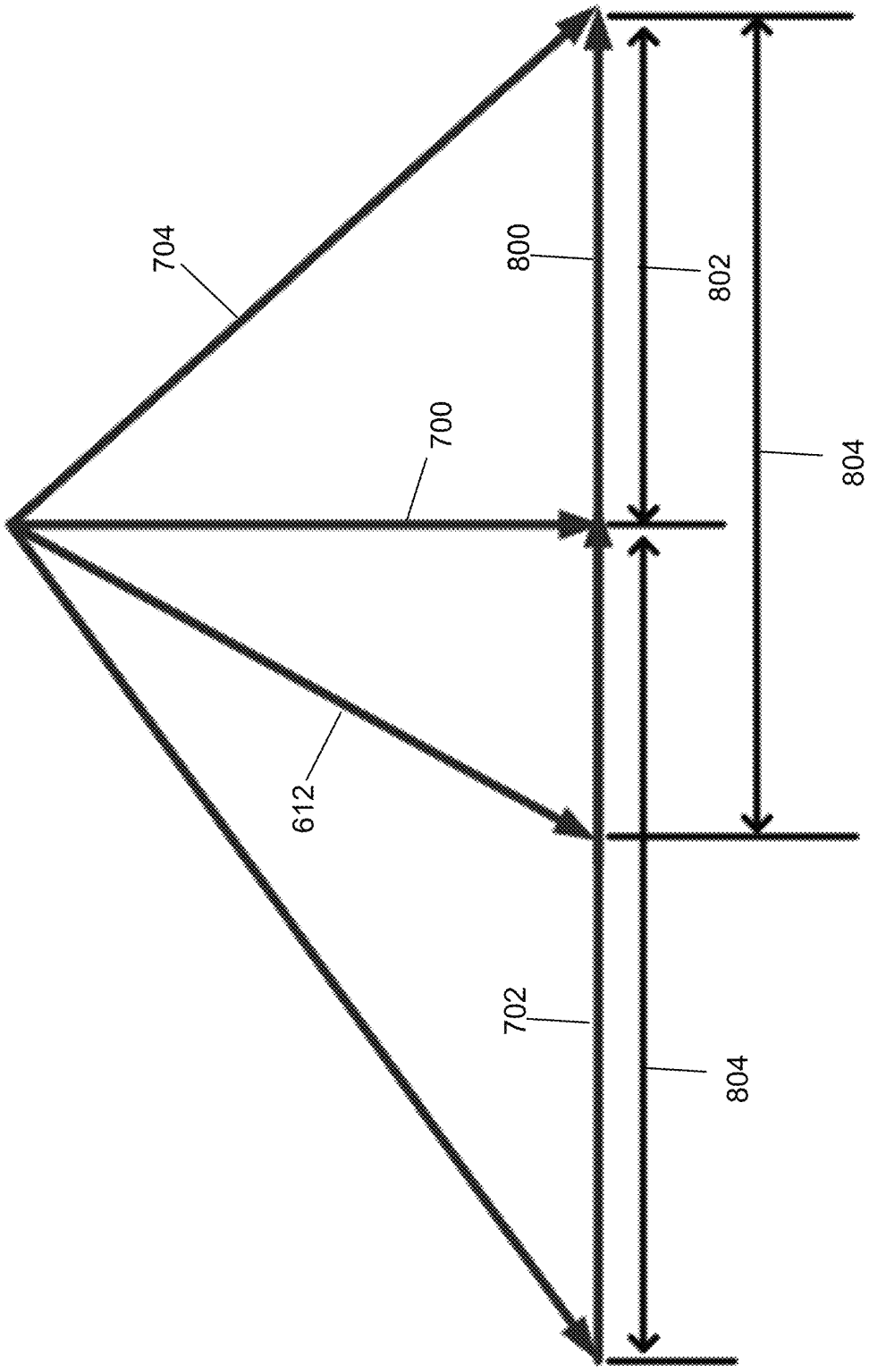

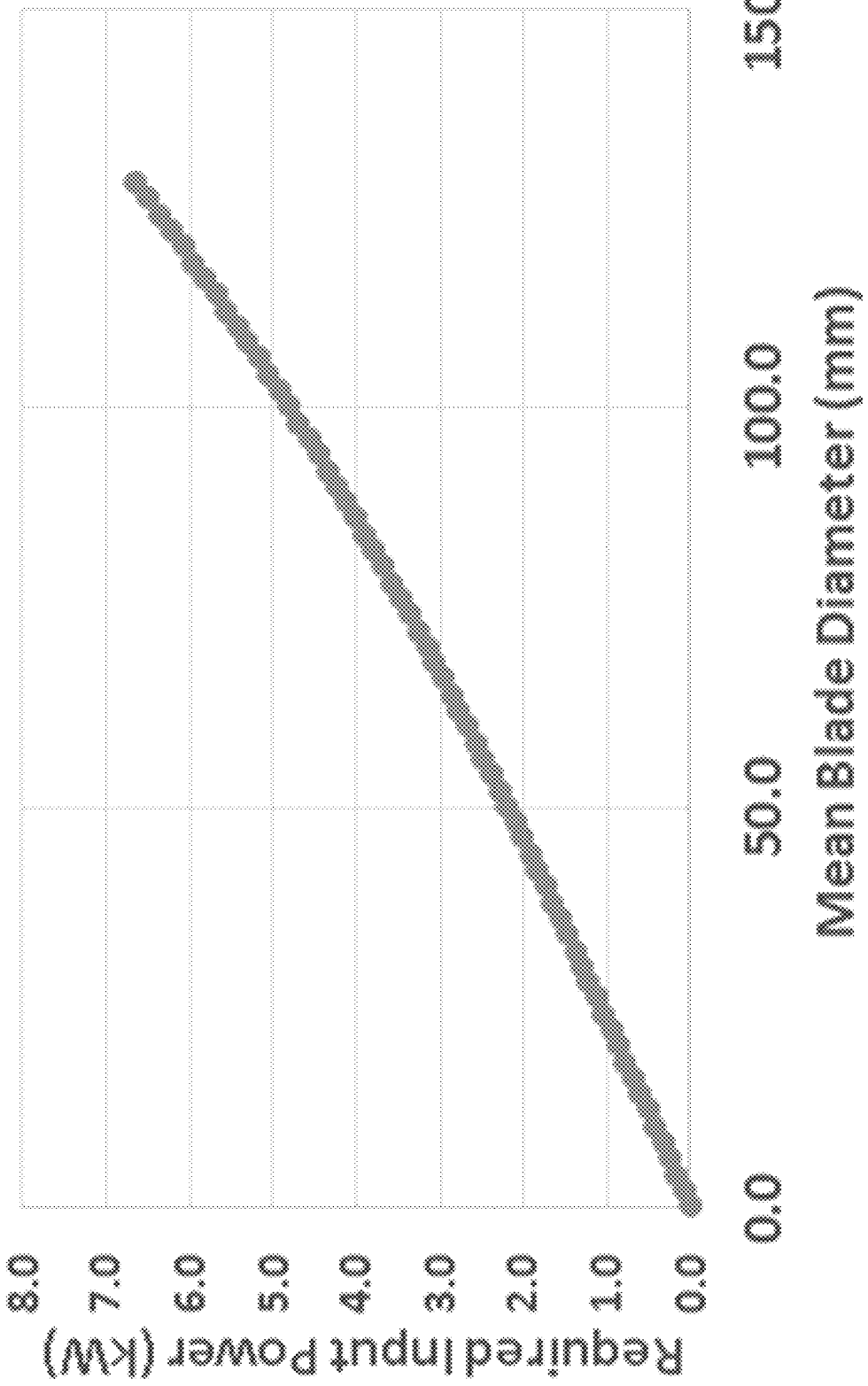
Required Input Power (kW)
8.0
7.0
6.0
5.0
4.0
3.0
2.0
1.0
0.0
Mean Blade Diameter (mm)
0.0
50.0
100.0
150.0

FIG. 9

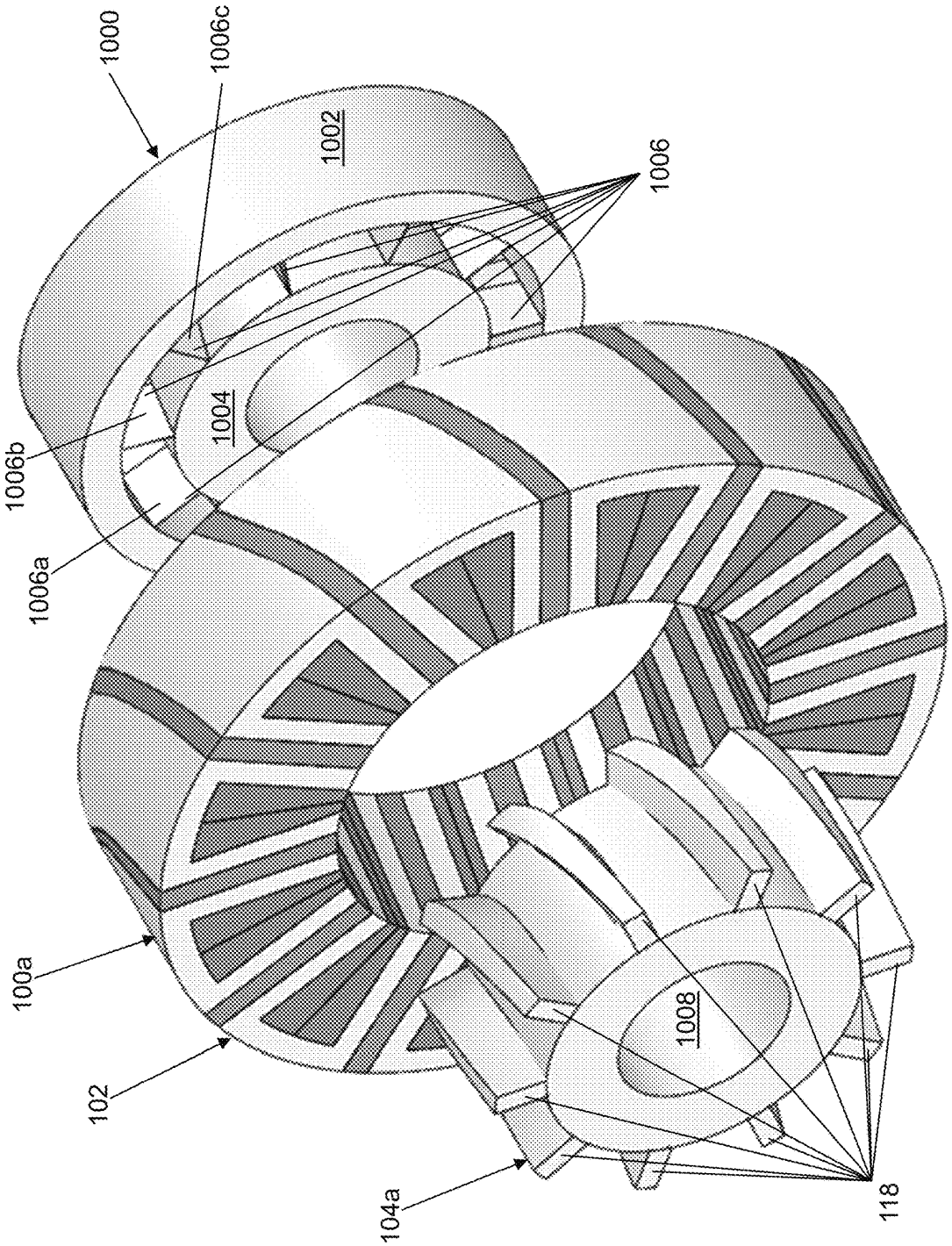

FIG. 10

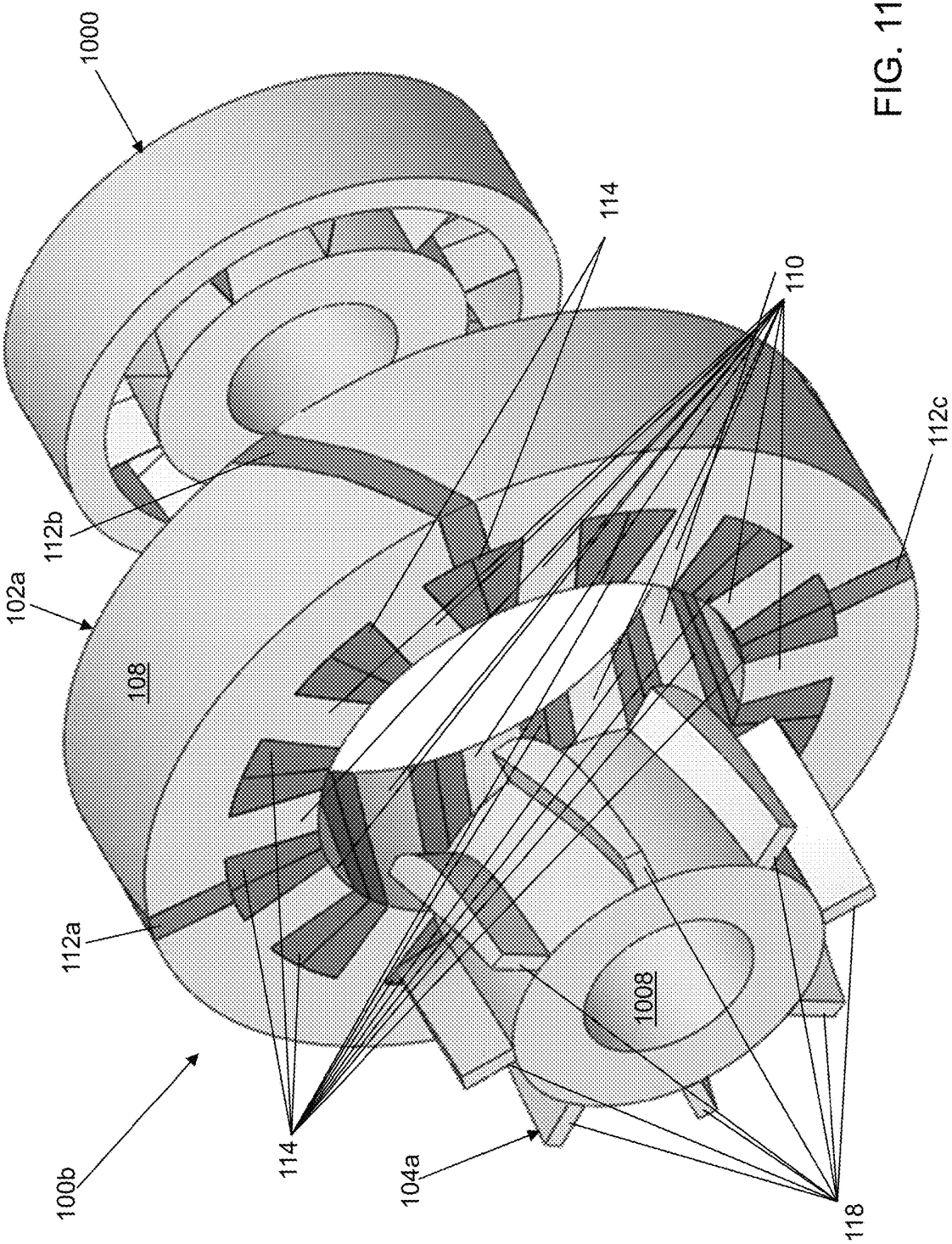

FIG. 11

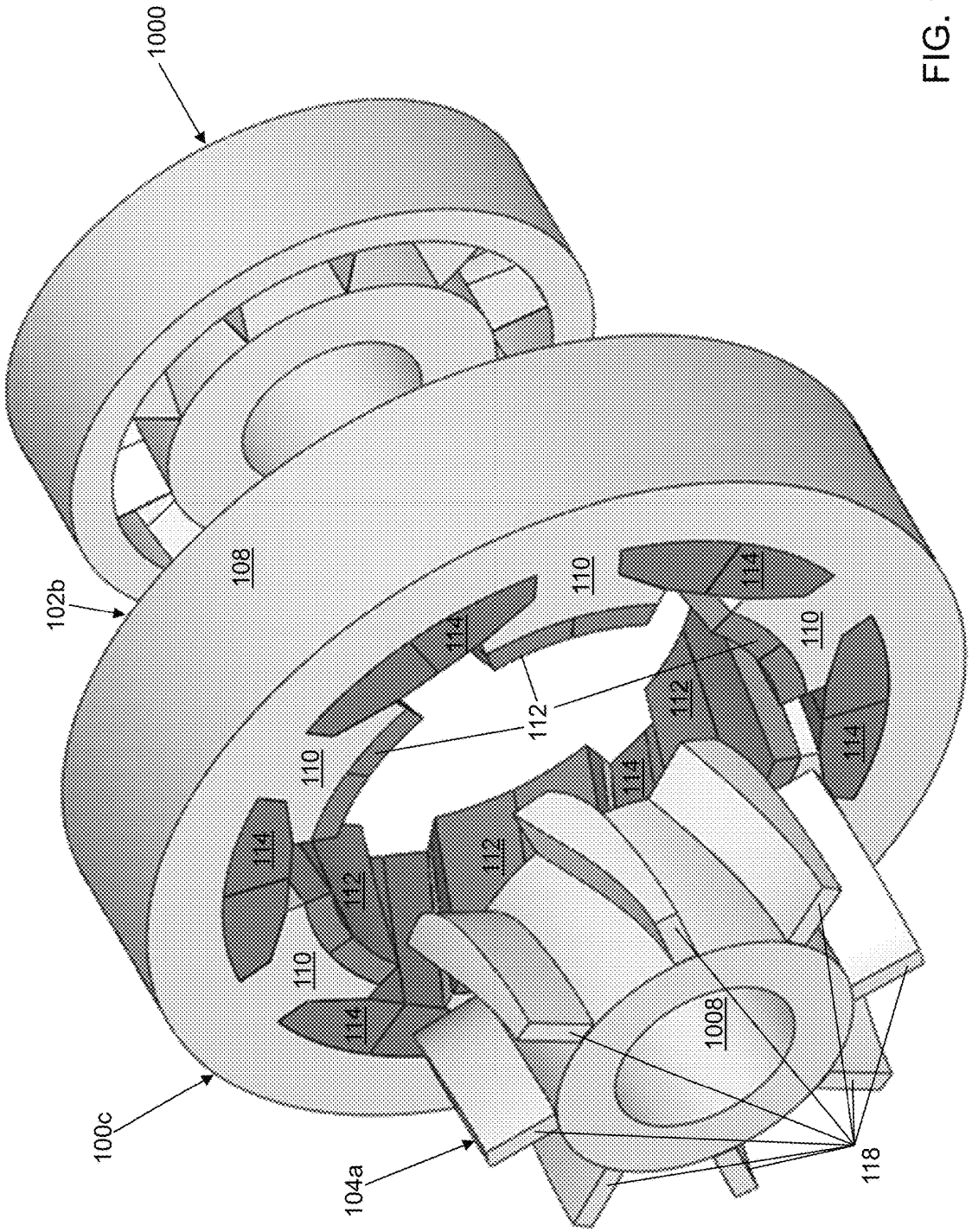

FIG. 12

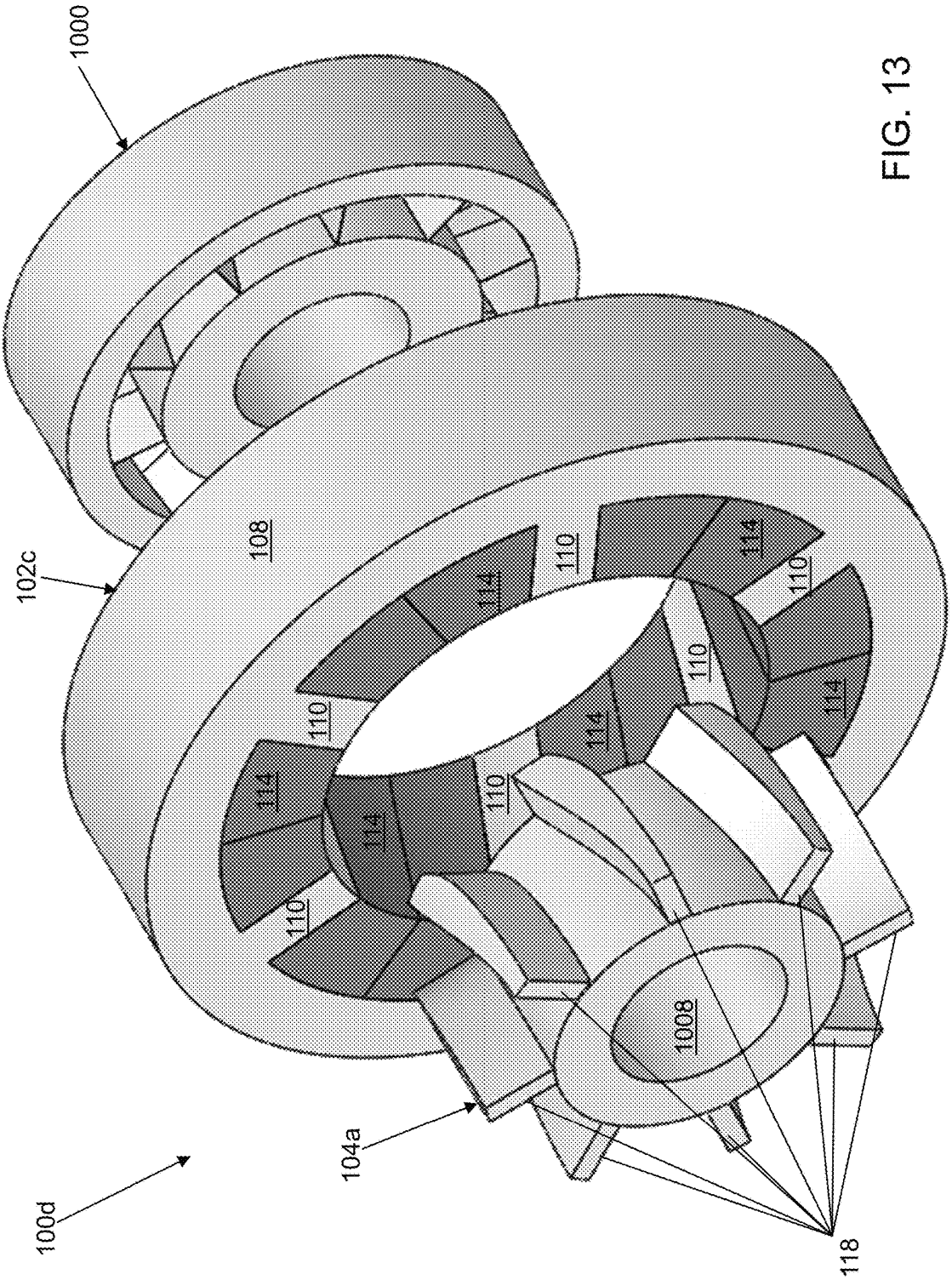

FIG. 13

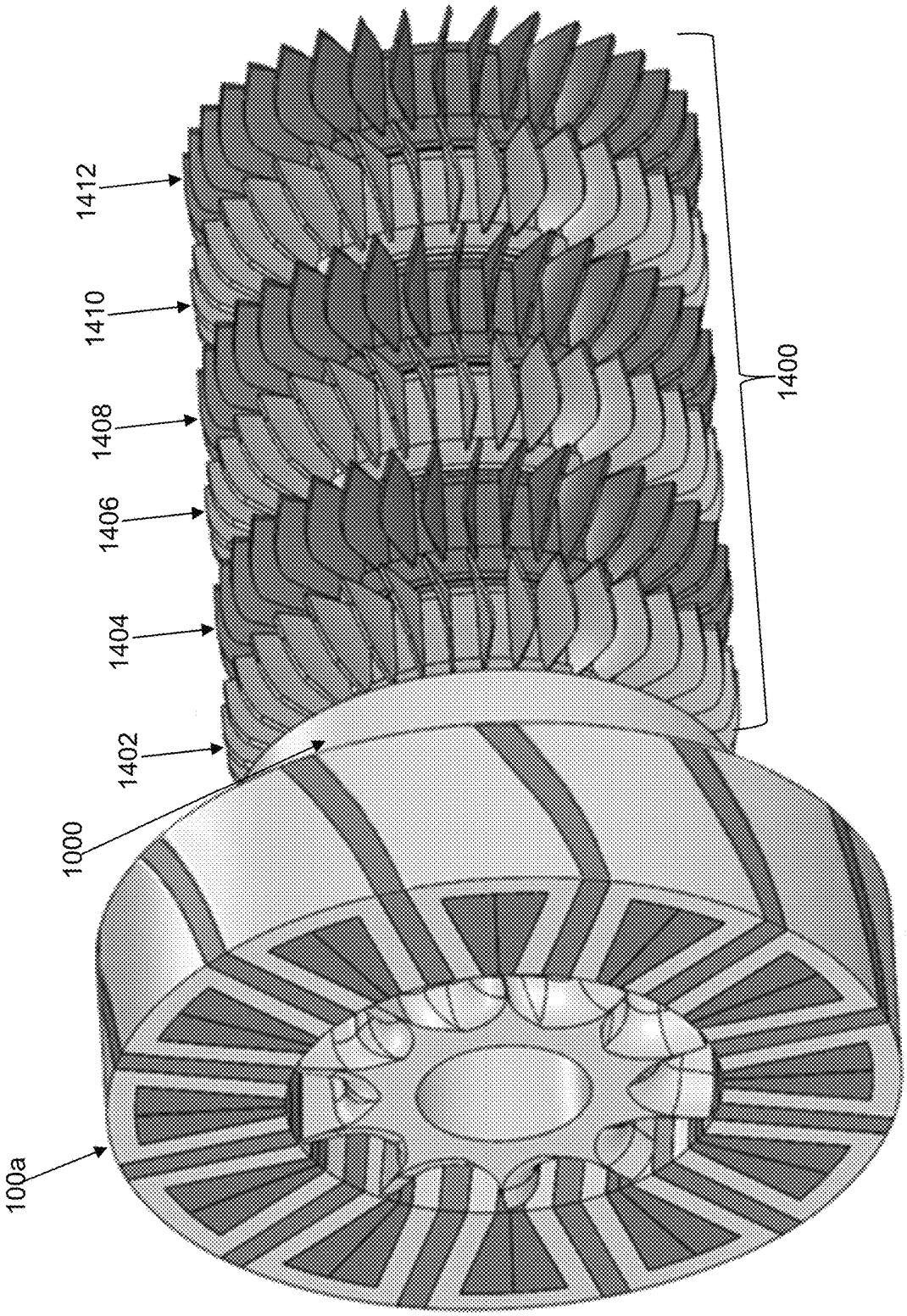

FIG. 14

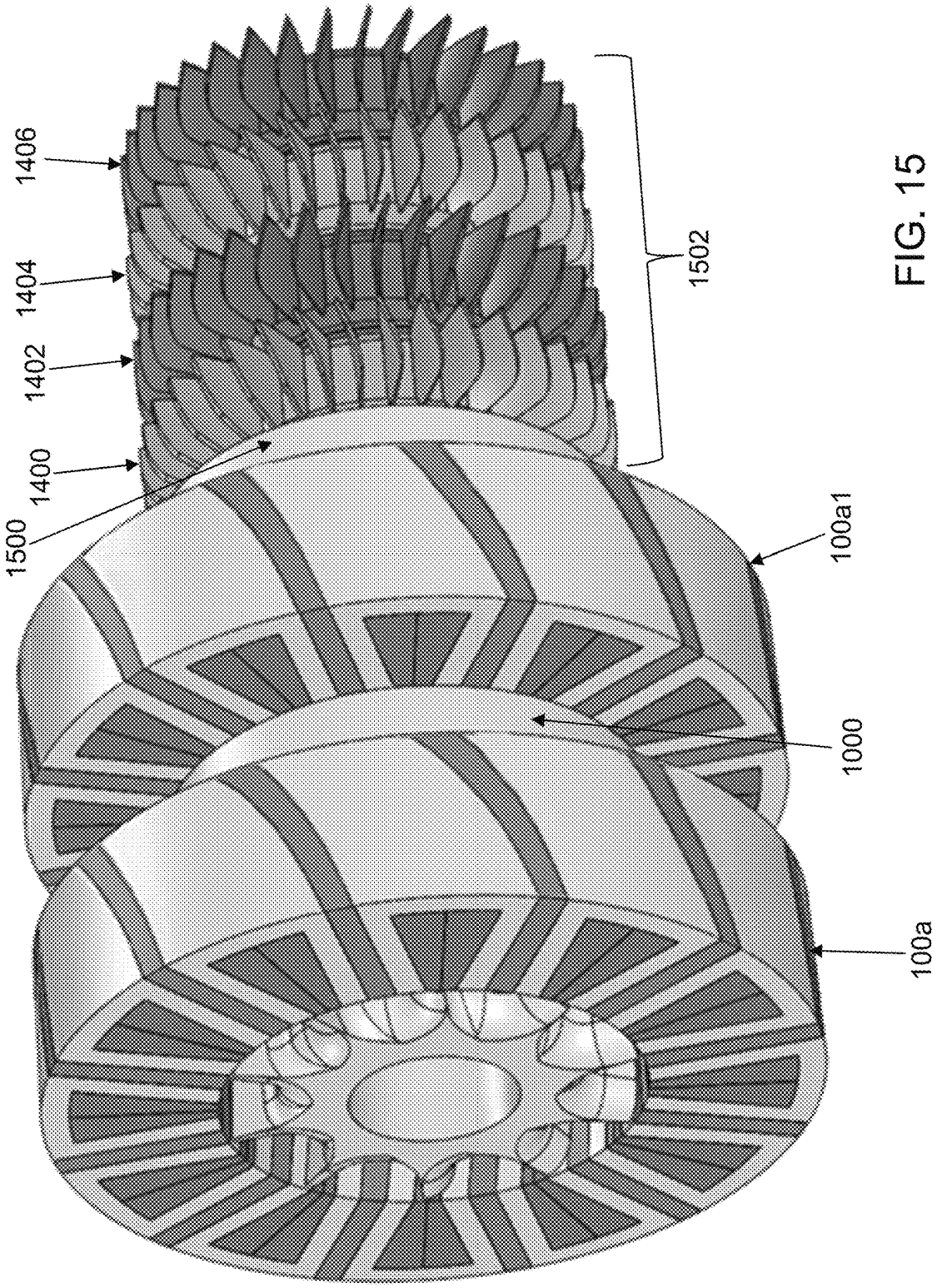

FIG. 15

FIG. 16

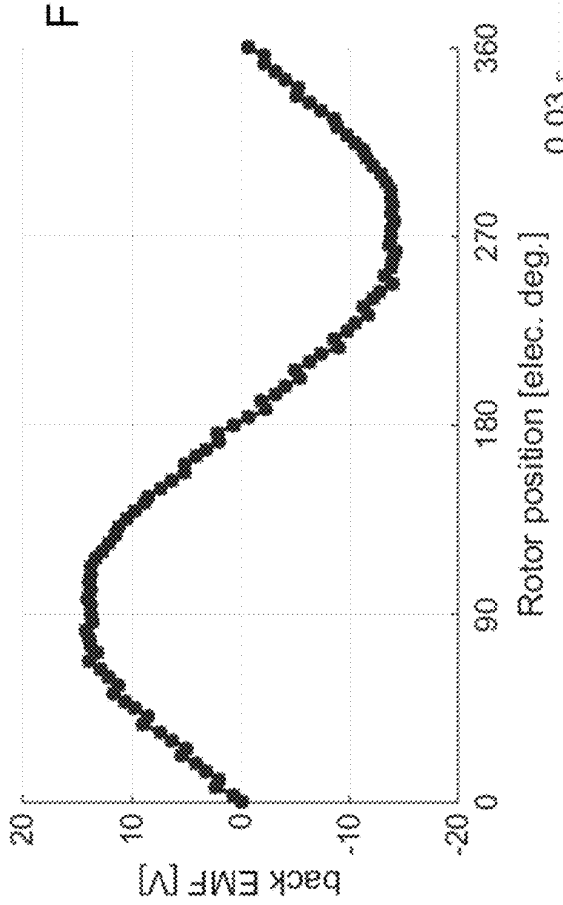
back EMF [V]
20
10
0
-10
-20
0
90
180
270
360
Rotor position [elec. deg.]

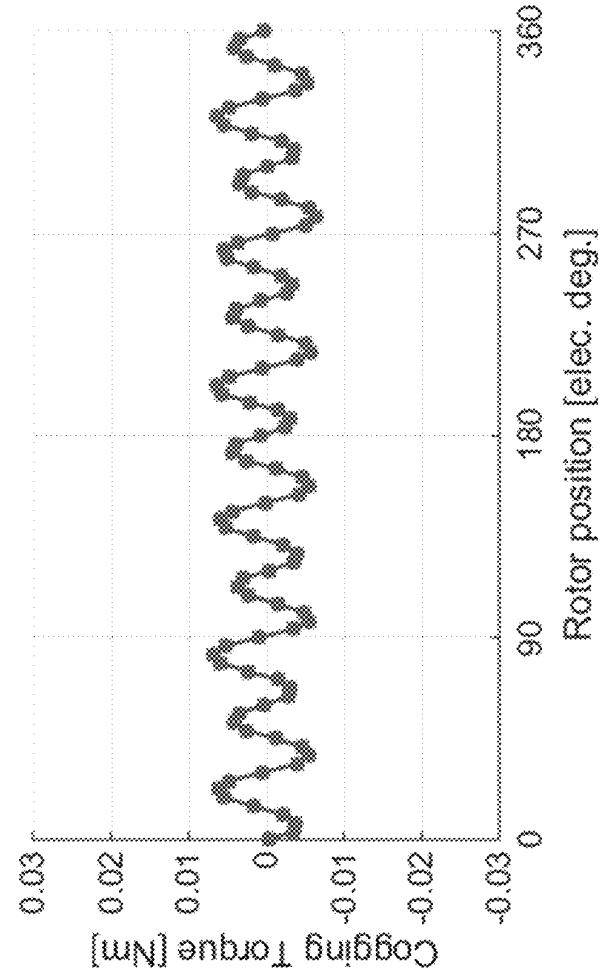
Cogging Torque [Nm]
0.03
0.02
0.01
0
-0.01
-0.02
-0.03
0
90
180
270
360
Rotor position [elec. deg.]

FIG. 17

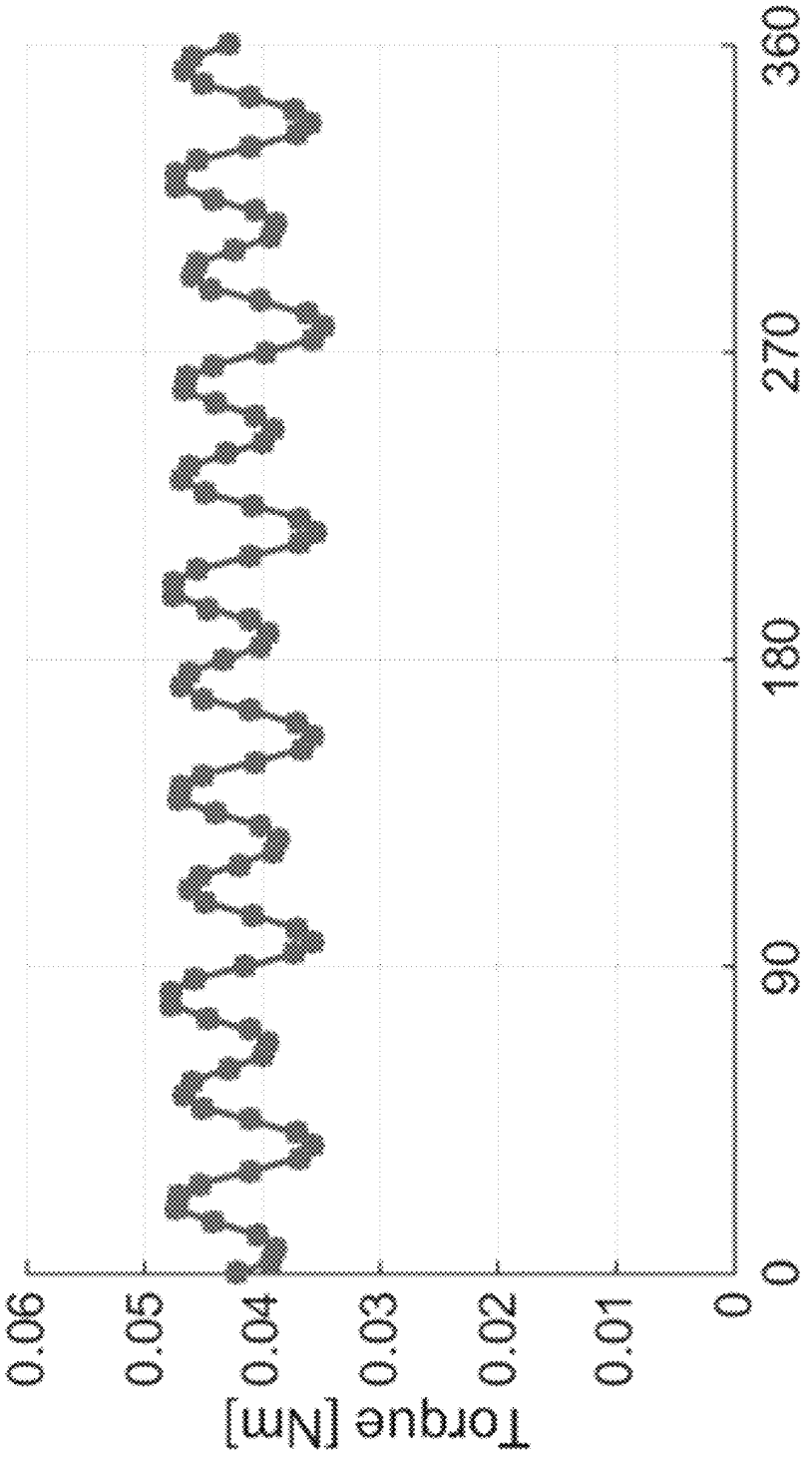
Torque [Nm]
0.06
0.05
0.04
0.03
0.02
0.01
0
0
90
180
270
360
Rotor position [elec. deg.]

FIG. 18

FIG. 19

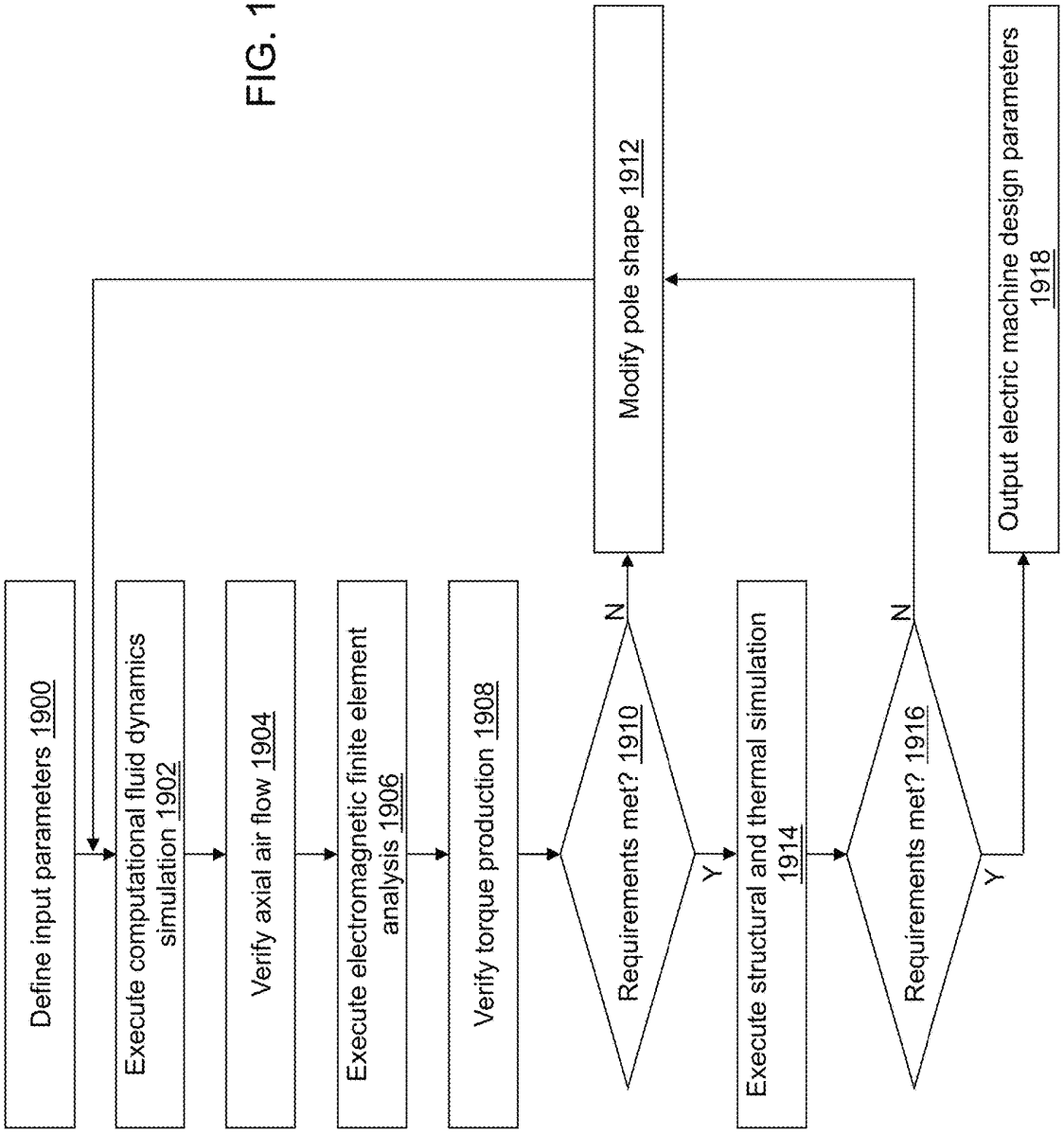
Define input parameters 1900
Execute computational fluid dynamics simulation 1902
Verify axial air flow 1904
Execute electromagnetic finite element analysis 1906
Verify torque production 1908
Requirements met? 1910
N
Y
Modify pole shape 1912
Execute structural and thermal simulation 1914
Requirements met? 1916
N
Y
Output electric machine design parameters 1918

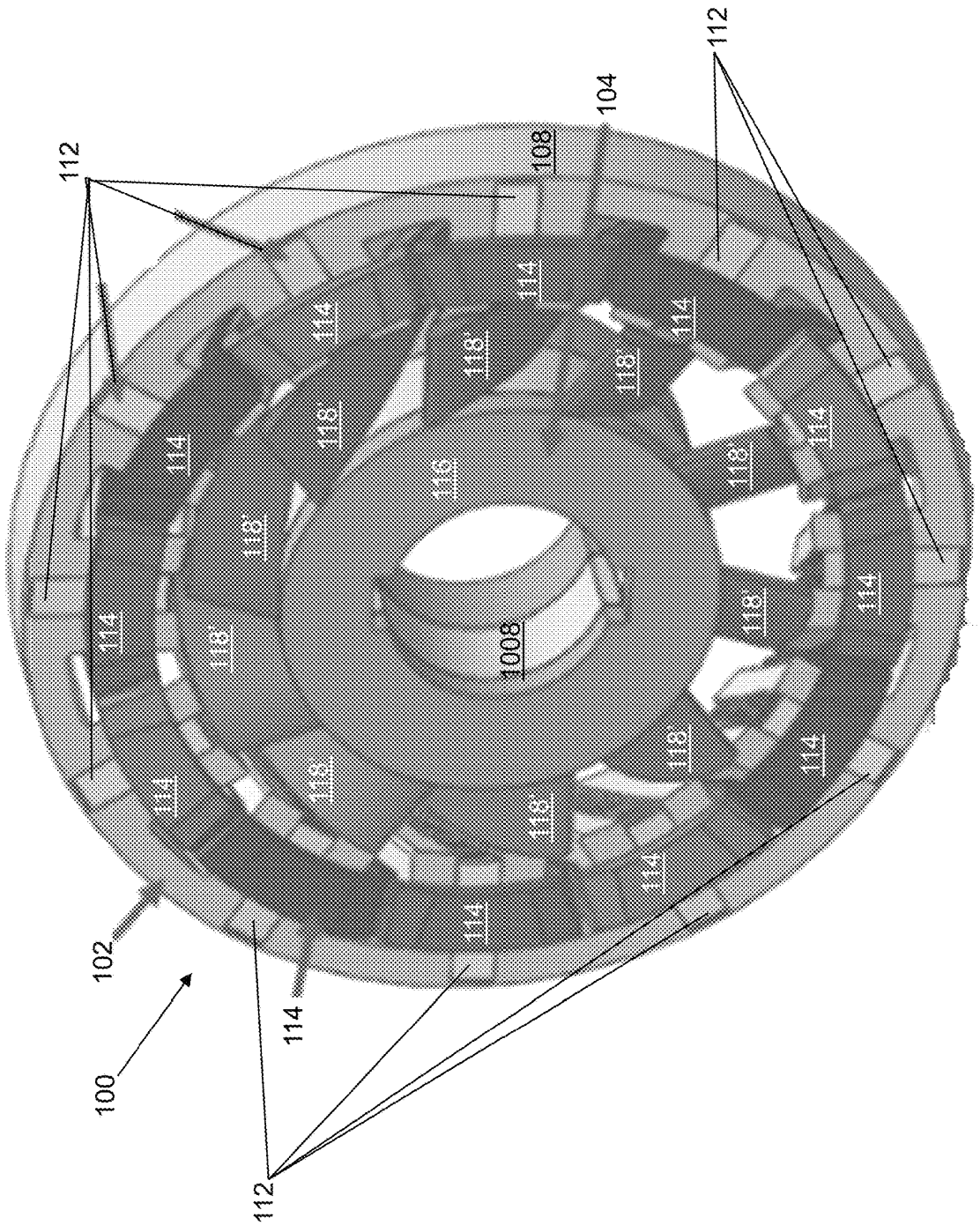

FIG. 20

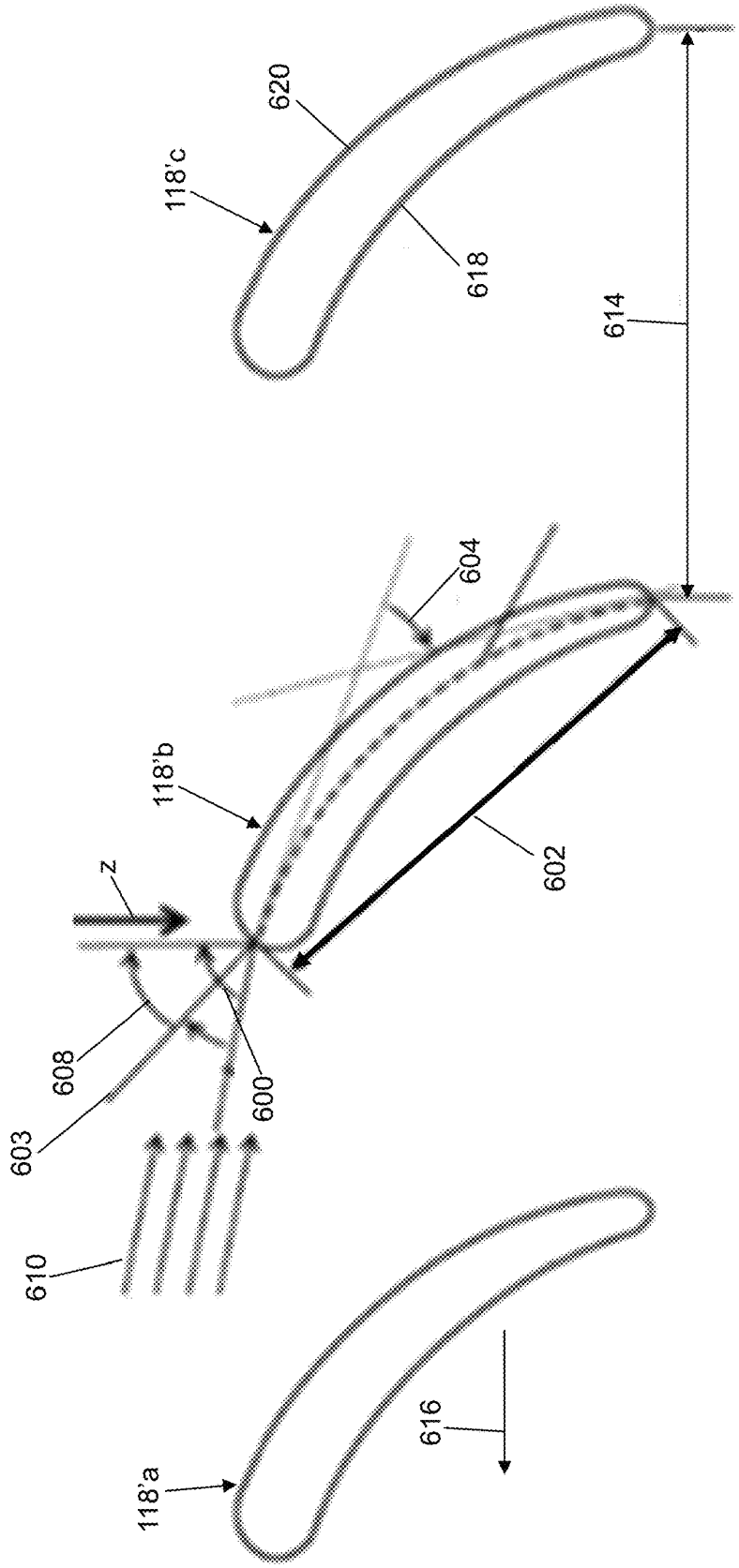

FIG. 21

FIG. 22

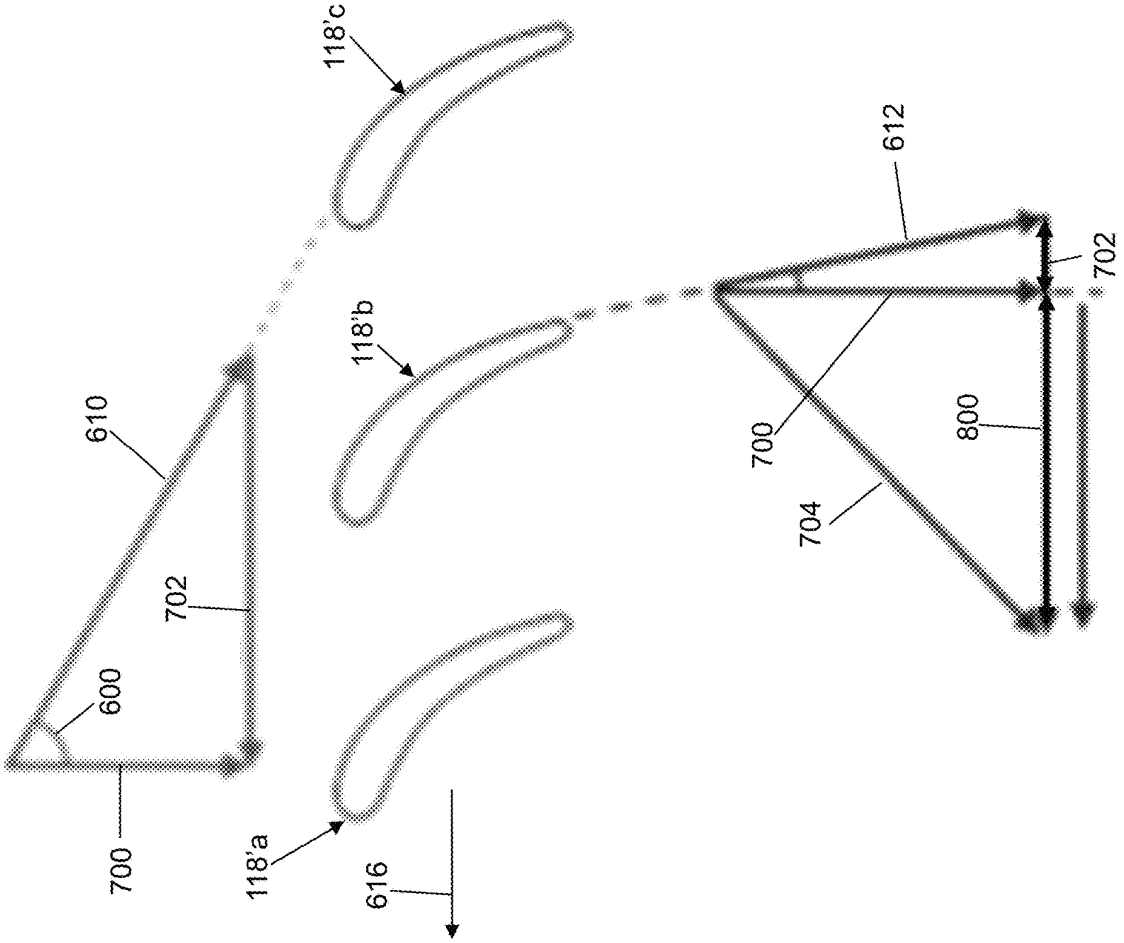

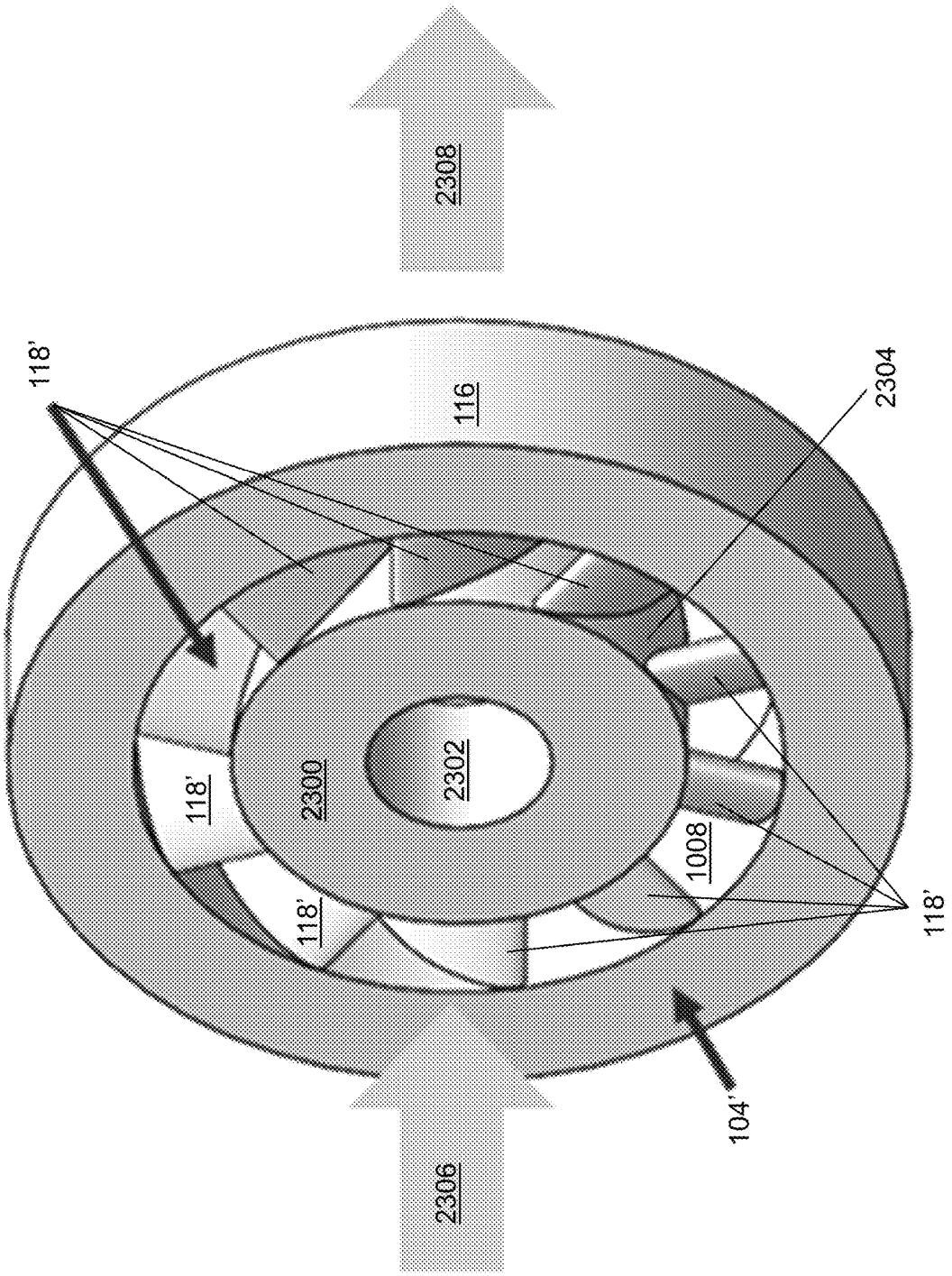

FIG. 23

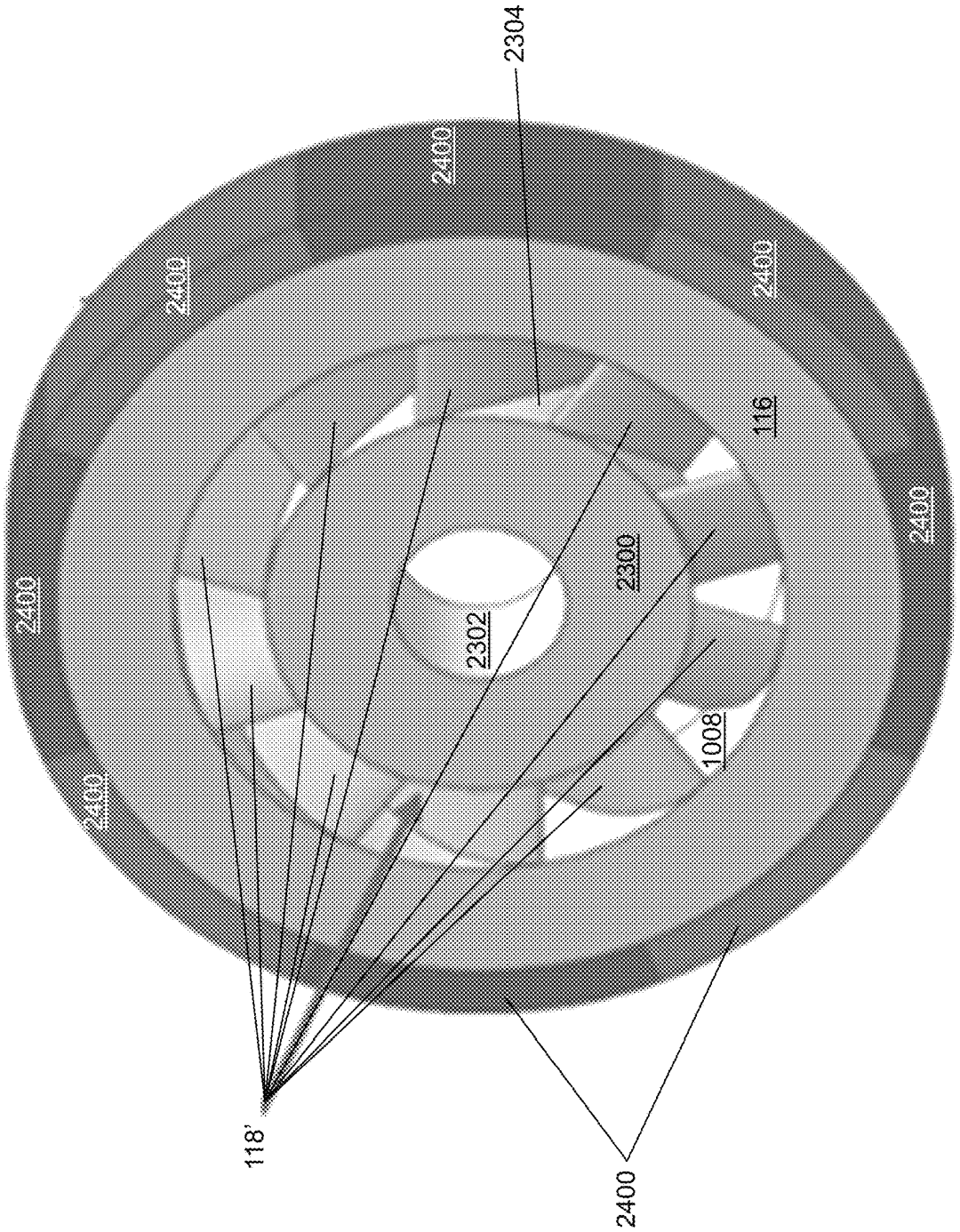
2304
2400
2400
2400
2400
2400
2400
116
2300
2302
1008
118'
2400

FIG. 24

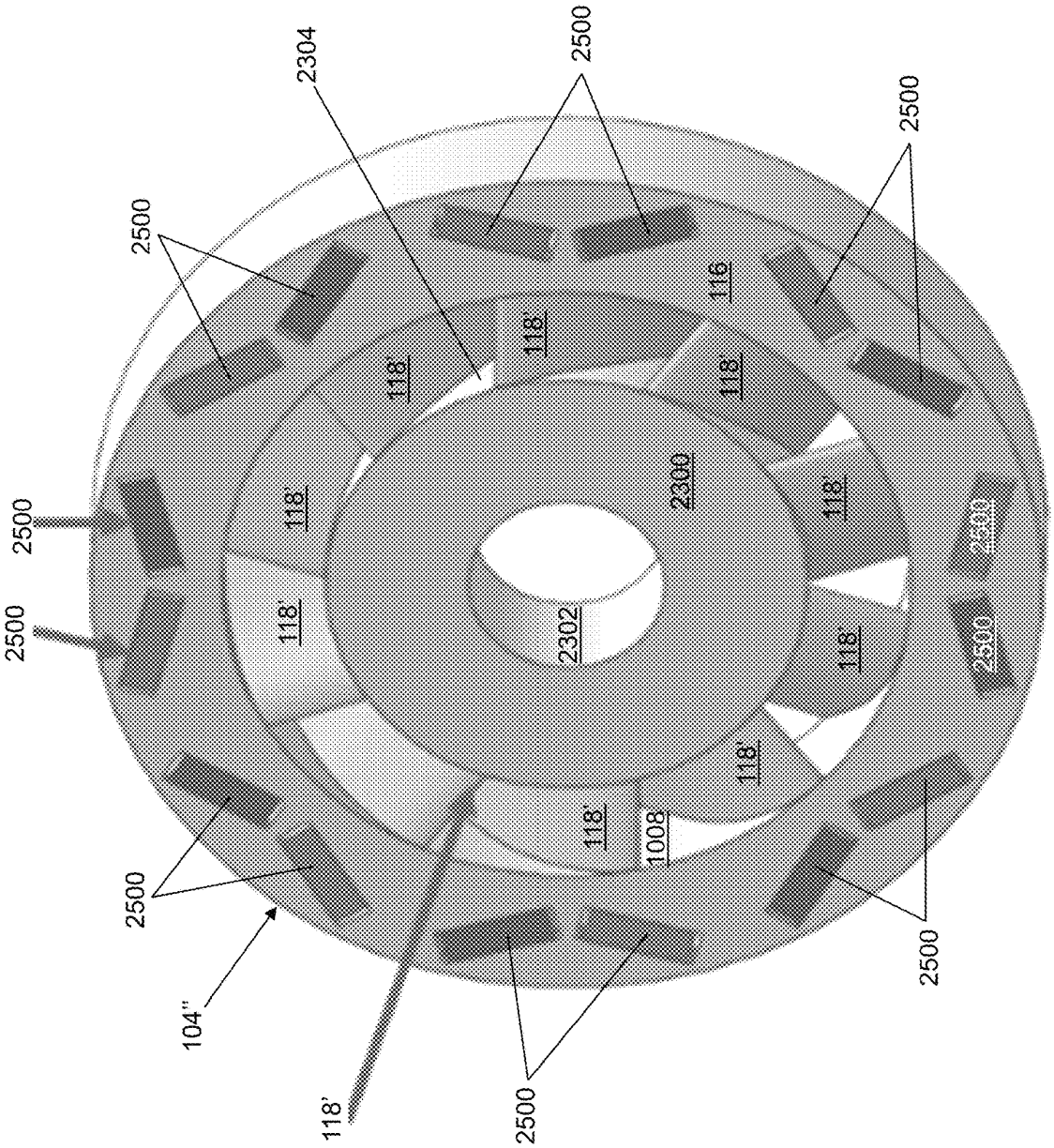
2304
2500
2500
2500
2500
2500
2500
2500
2500
2500
2500
2500
2500
118'
118'
118'
118'
118'
118'
118'
118'
118'
118'
116
2300
2302
1008
104''

FIG. 25

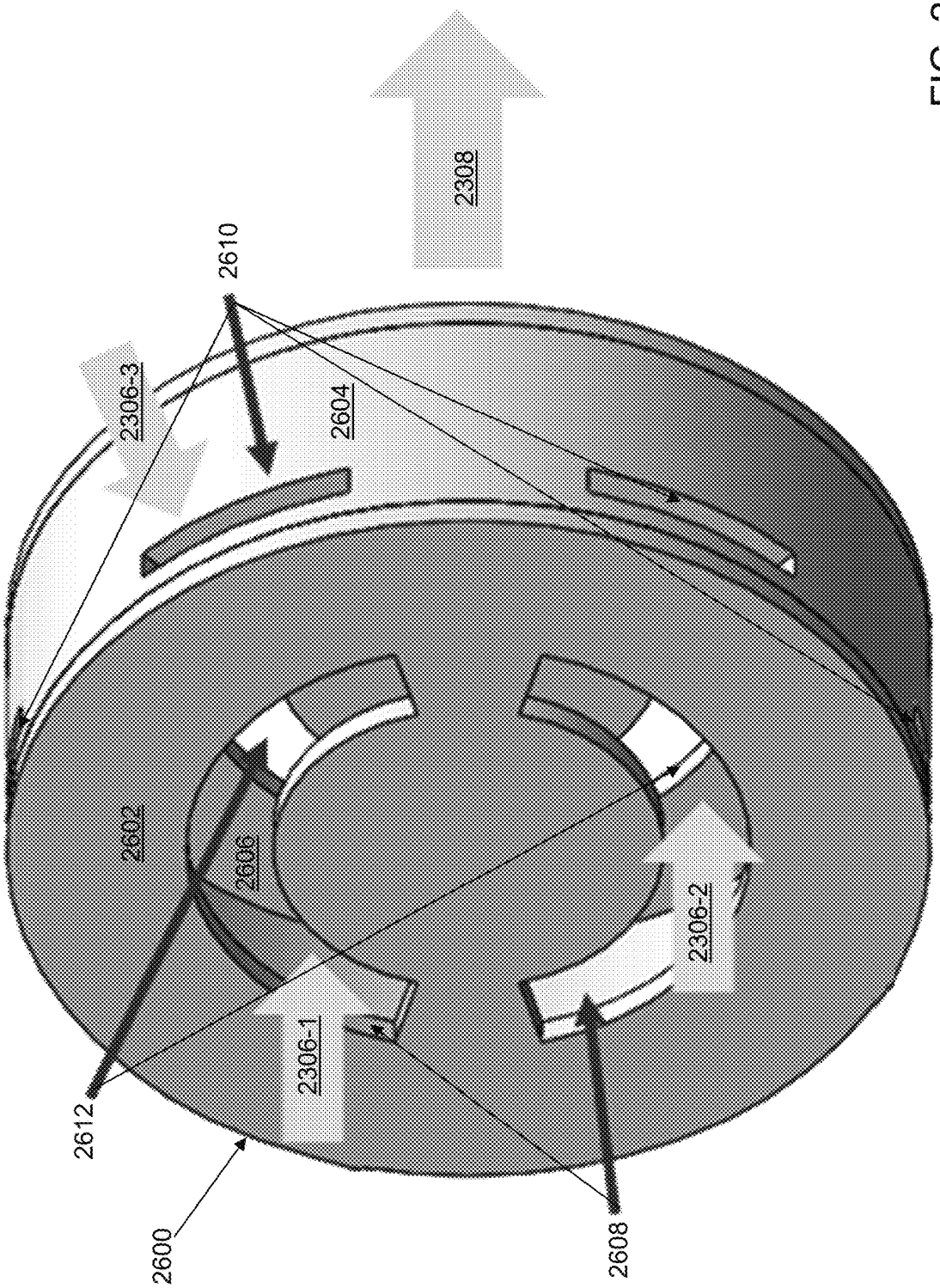

FIG. 26

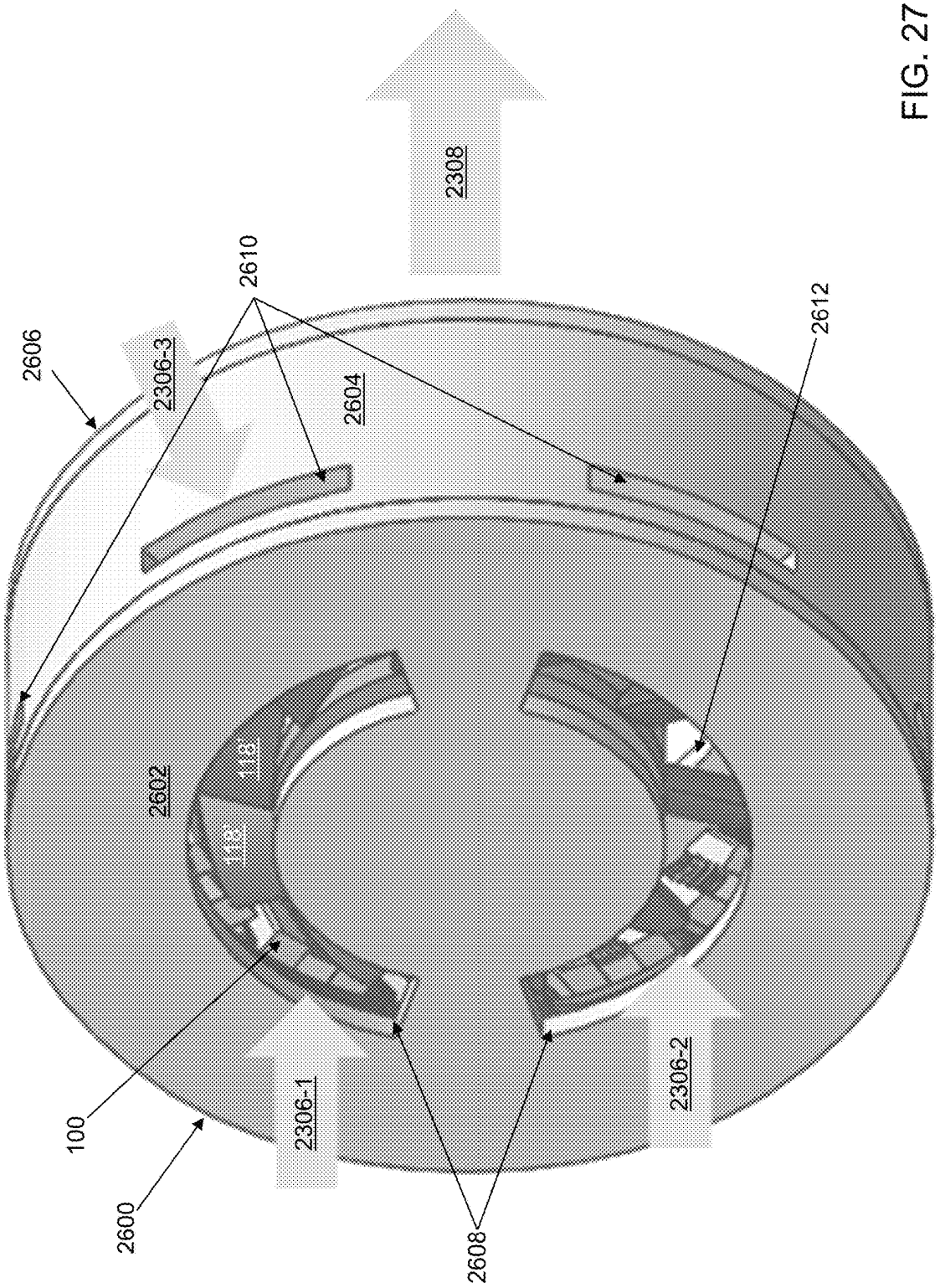
2308
2610
2606
2306-3
2604
2612
2602
113
113
100
2600
2306-1
2608
2306-2

FIG. 27

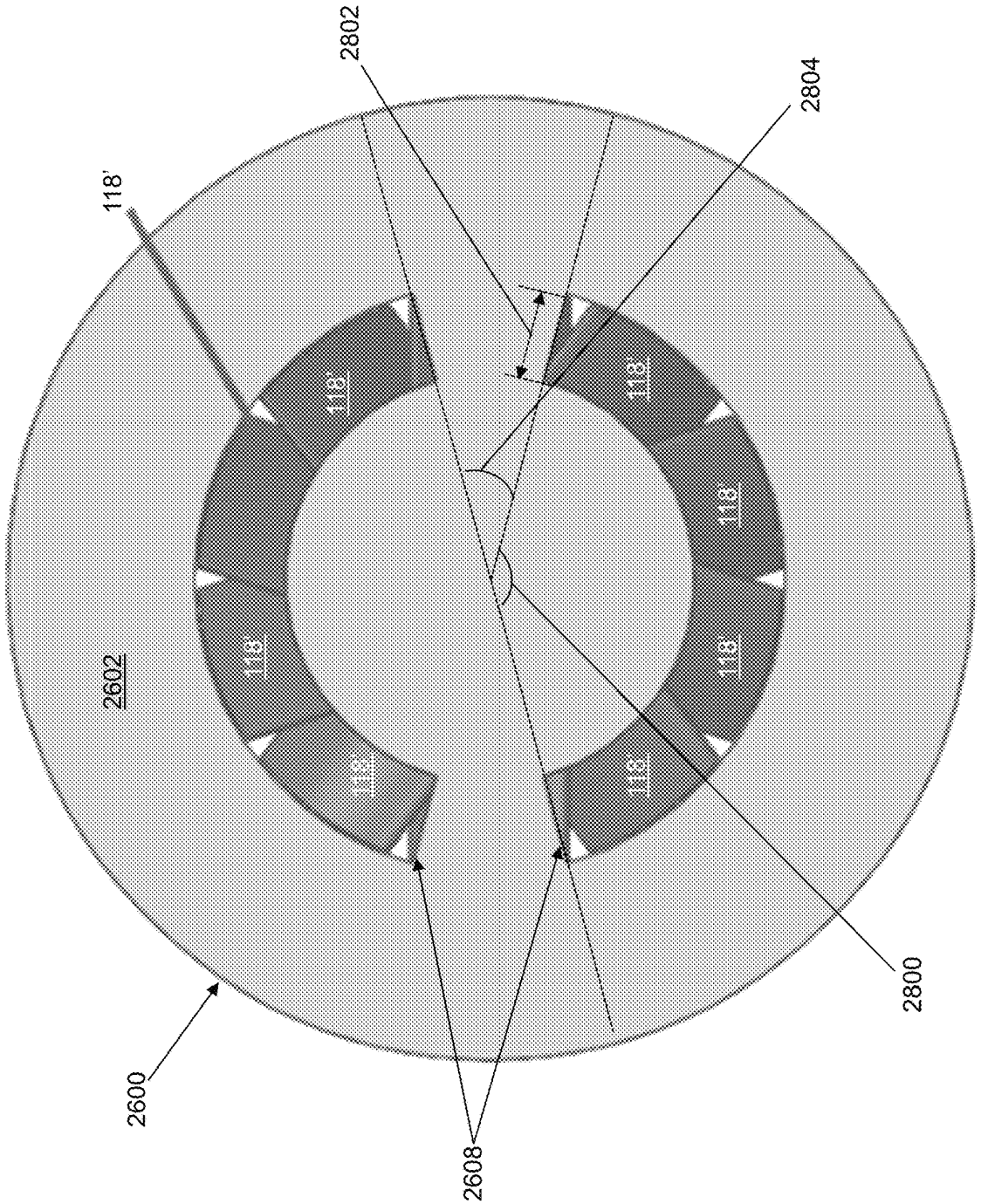

FIG. 28A

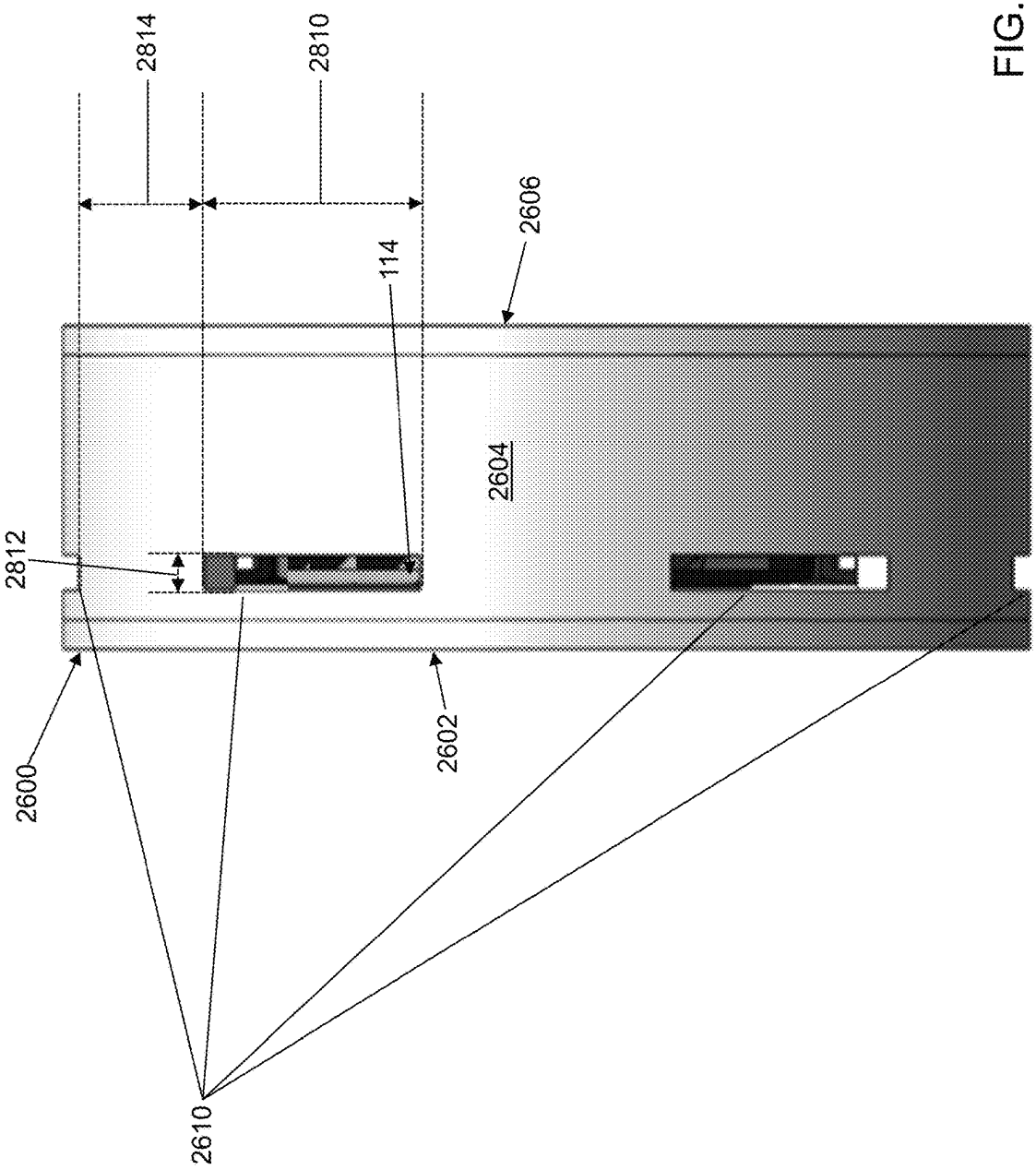

FIG. 28B

FIG. 29

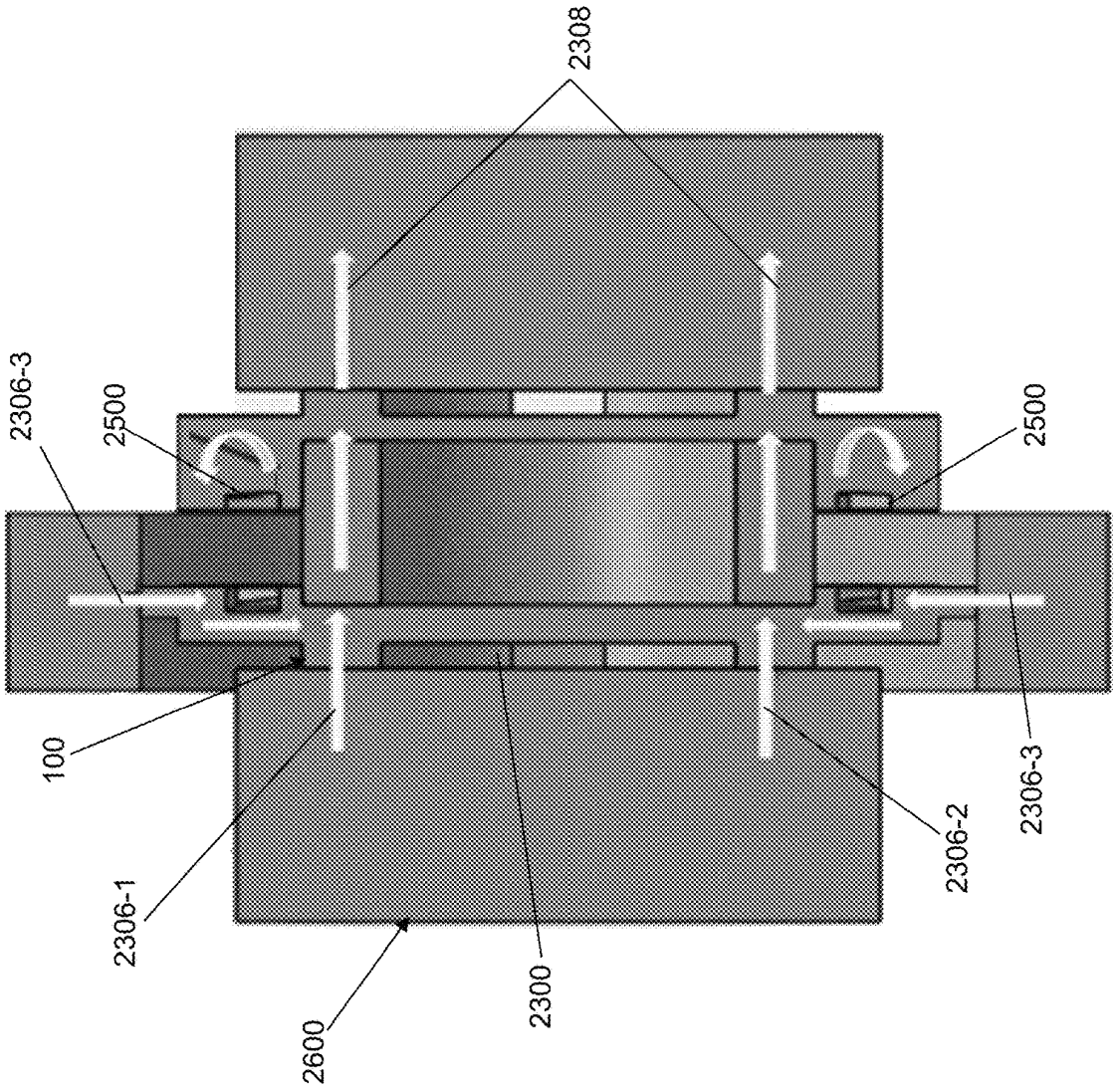

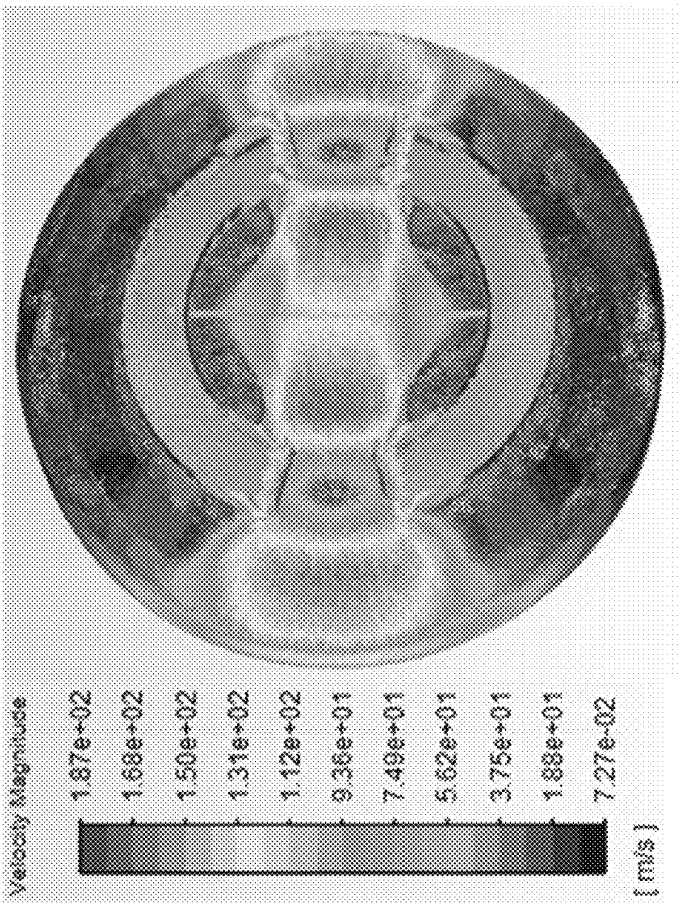
Velocity Magnitude
1.87e+02
1.68e+02
1.50e+02
1.31e+02
1.12e+02
9.36e+01
7.49e+01
5.62e+01
3.75e+01
1.88e+01
7.27e-02
[m/s]

FIG. 31

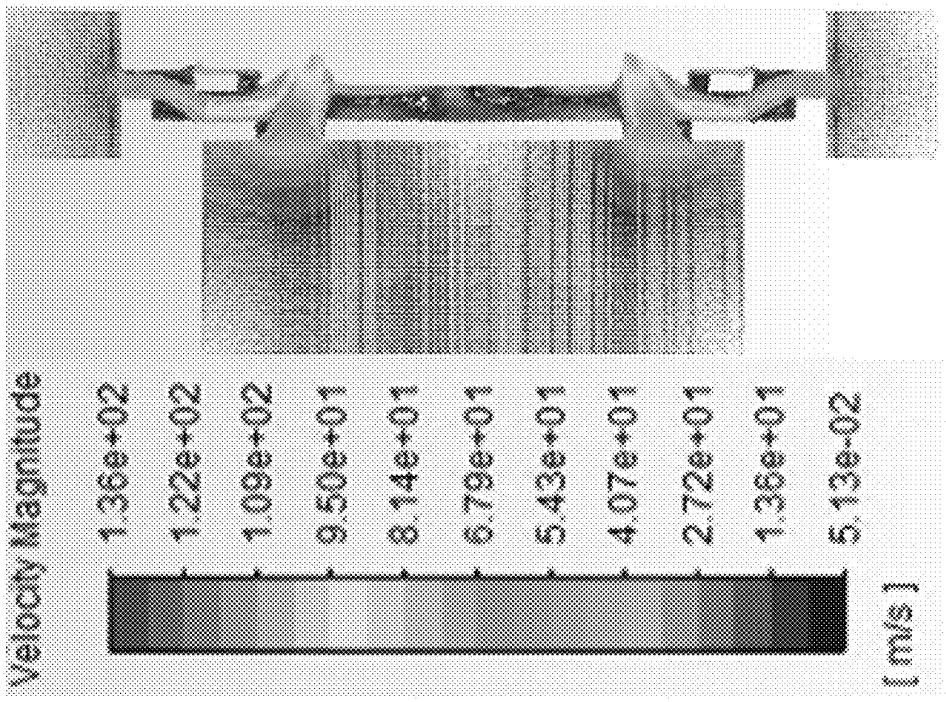
Velocity Magnitude
1.36e+02
1.22e+02
1.09e+02
9.50e+01
8.14e+01
6.79e+01
5.43e+01
4.07e+01
2.72e+01
1.36e+01
5.13e-02
[m/s]

FIG. 30

FIG. 32

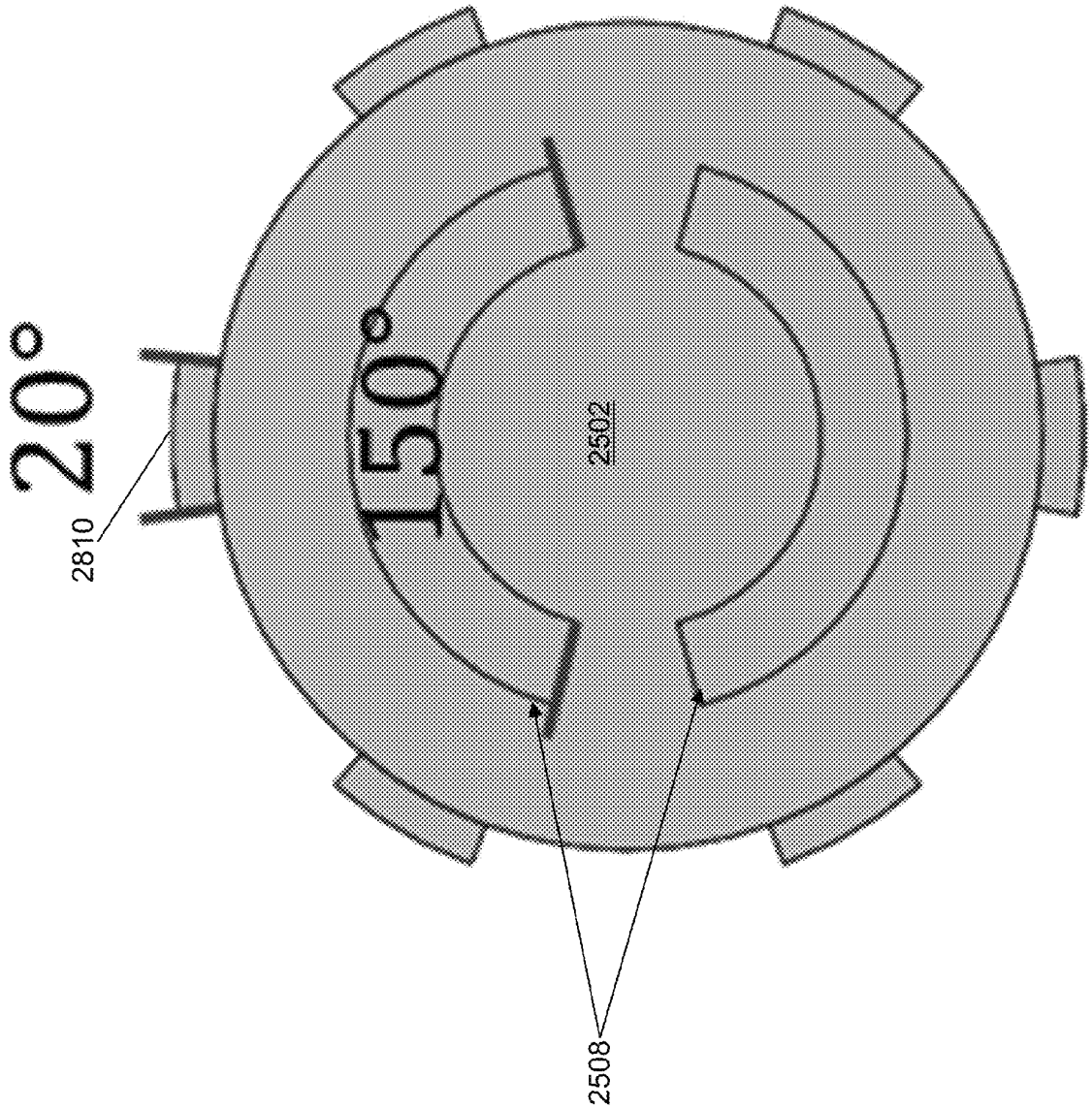

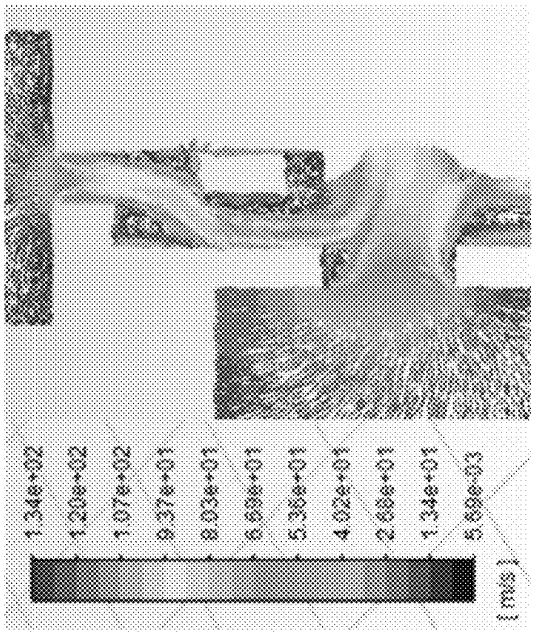

FIG. 33B

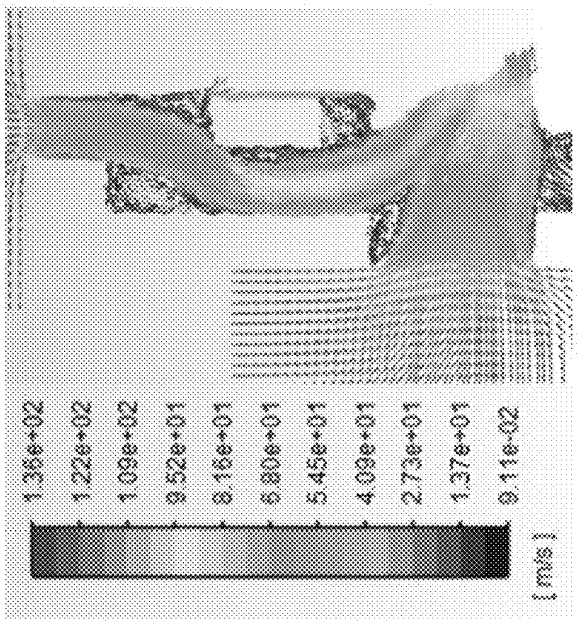

FIG. 33D

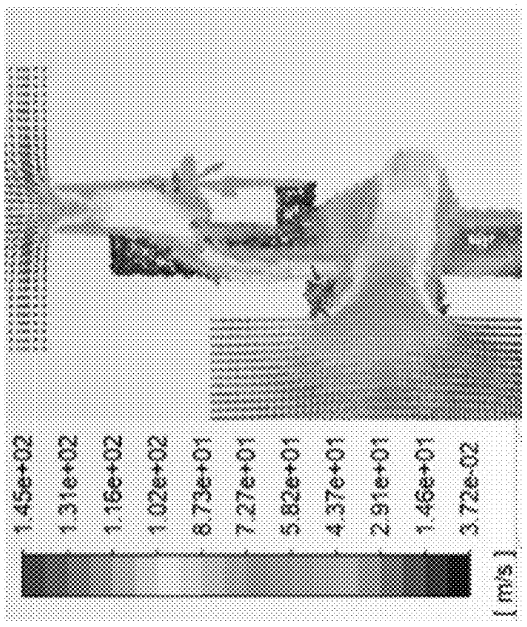

FIG. 33A

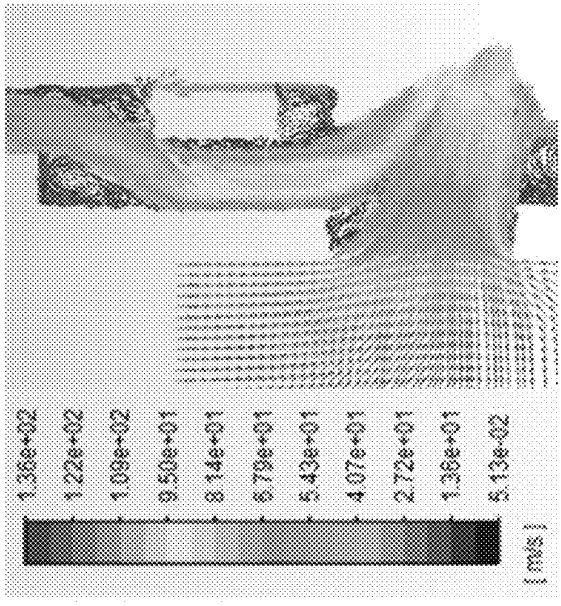

FIG. 33C

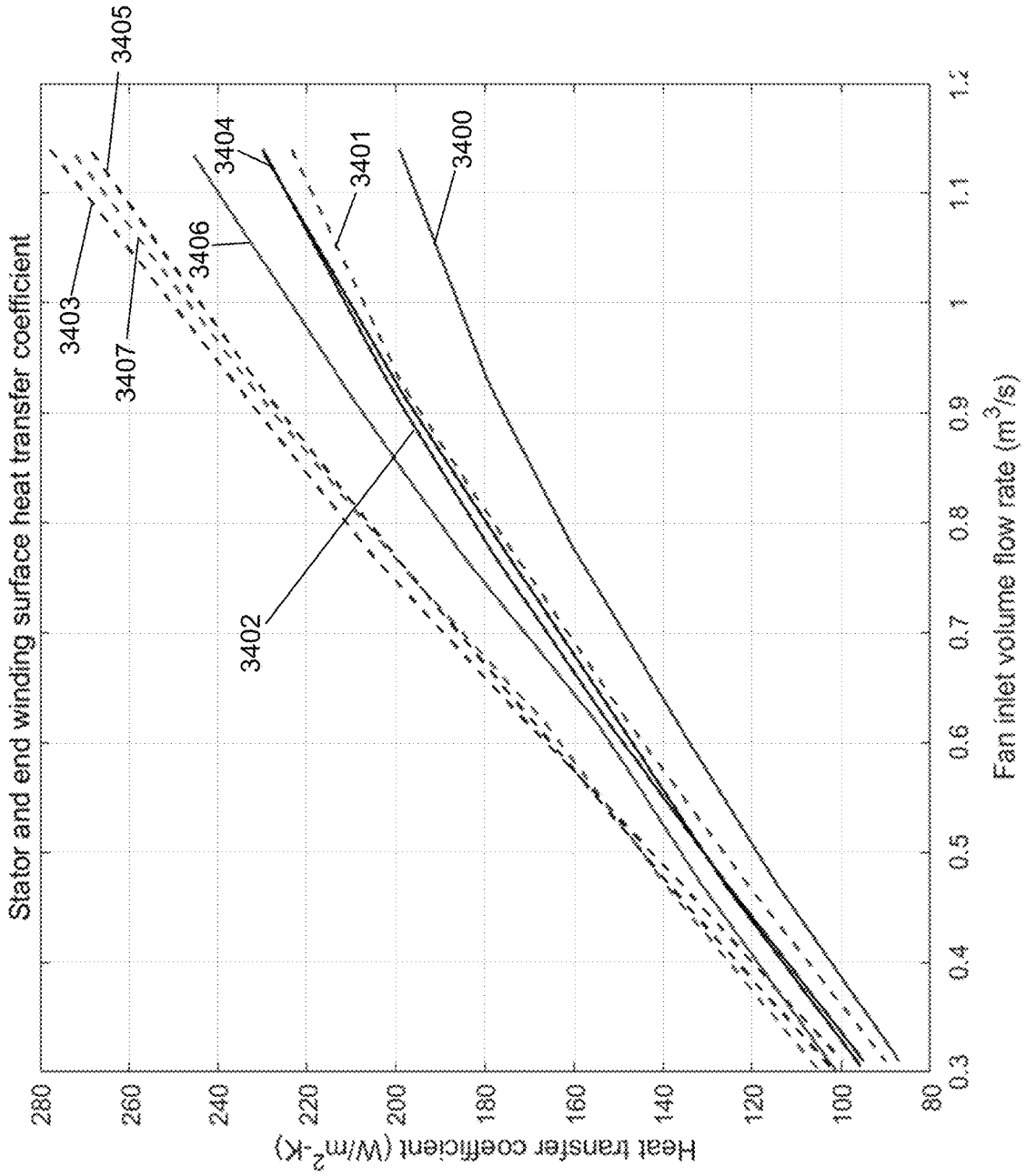
Stator and end winding surface heat transfer coefficient
Heat transfer coefficient (W/m^2-K)
Fan inlet volume flow rate (m^3/s)
280
260
240
220
200
180
160
140
120
100
80
0.3
0.4
0.5
0.6
0.7
0.8
0.9
1
1.1
3400
3401
3402
3403
3404
3405
3406
3407

FIG. 34

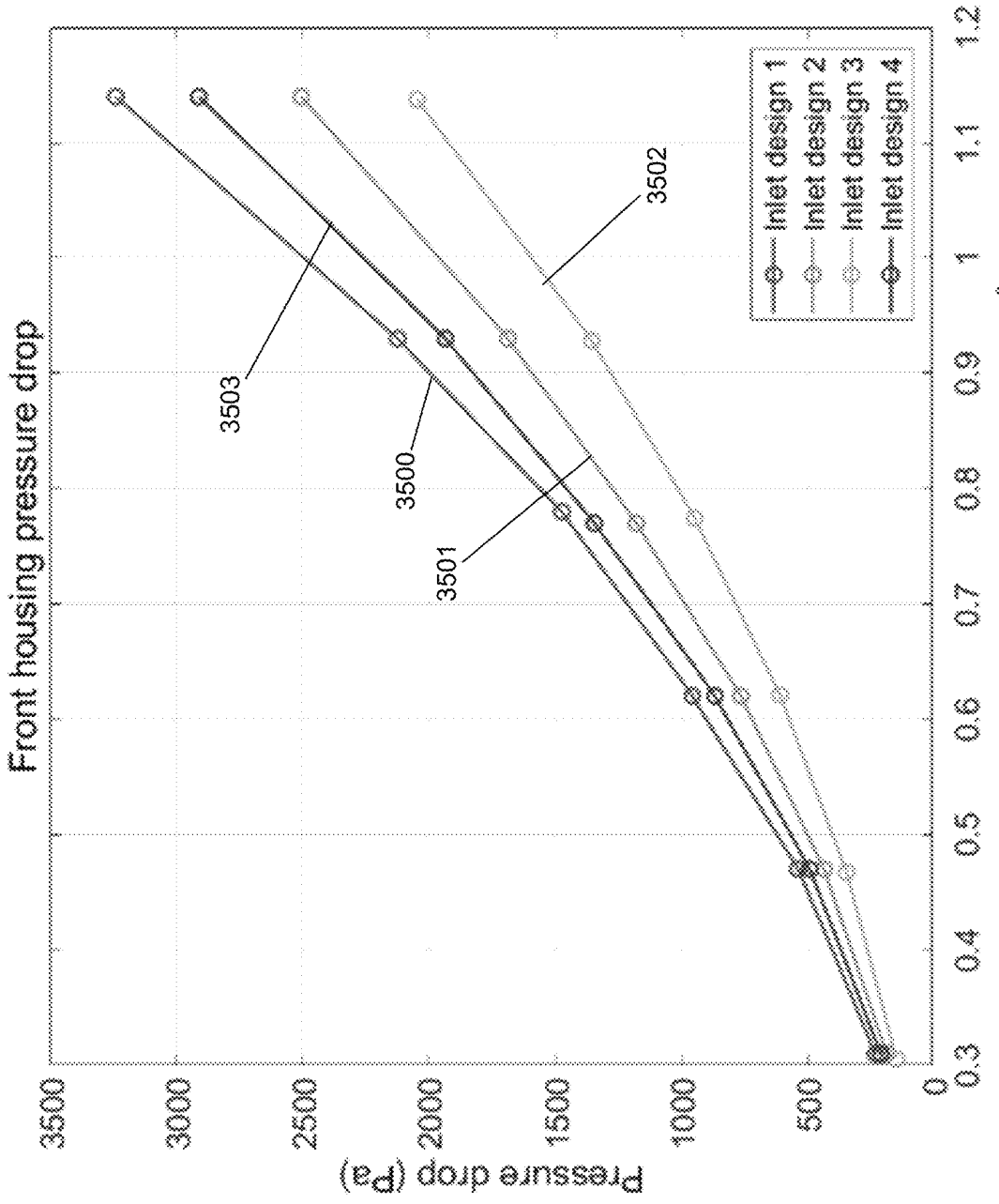
Front housing pressure drop
Pressure drop (Pa)
Fan zone inlet volume flow rate (m3/s)
Inlet design 1
Inlet design 2
Inlet design 3
Inlet design 4
3500
3501
3502
3503
0
500
1000
1500
2000
2500
3000
3500
0.3
0.4
0.5
0.6
0.7
0.8
0.9
1
1.1
1.2

FIG. 35A

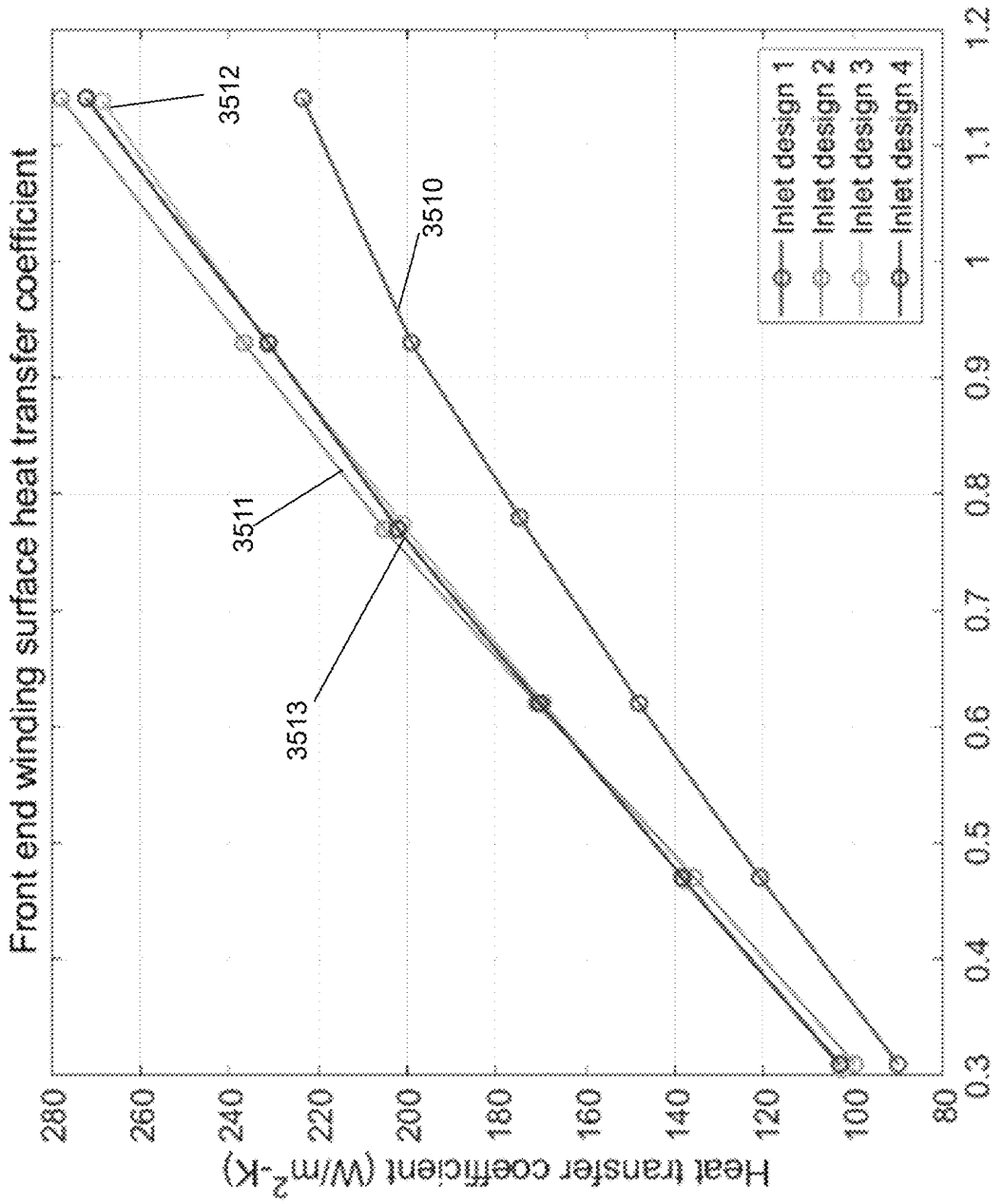
Front end winding surface heat transfer coefficient
Heat transfer coefficient (W/m²-K)
Fan zone inlet volume flow rate (m³/s)
Inlet design 1
Inlet design 2
Inlet design 3
Inlet design 4
3510
3511
3512
3513
280
260
240
220
200
180
160
140
120
100
80
0.3
0.4
0.5
0.6
0.7
0.8
0.9
1
1.1
1.2

FIG. 35B

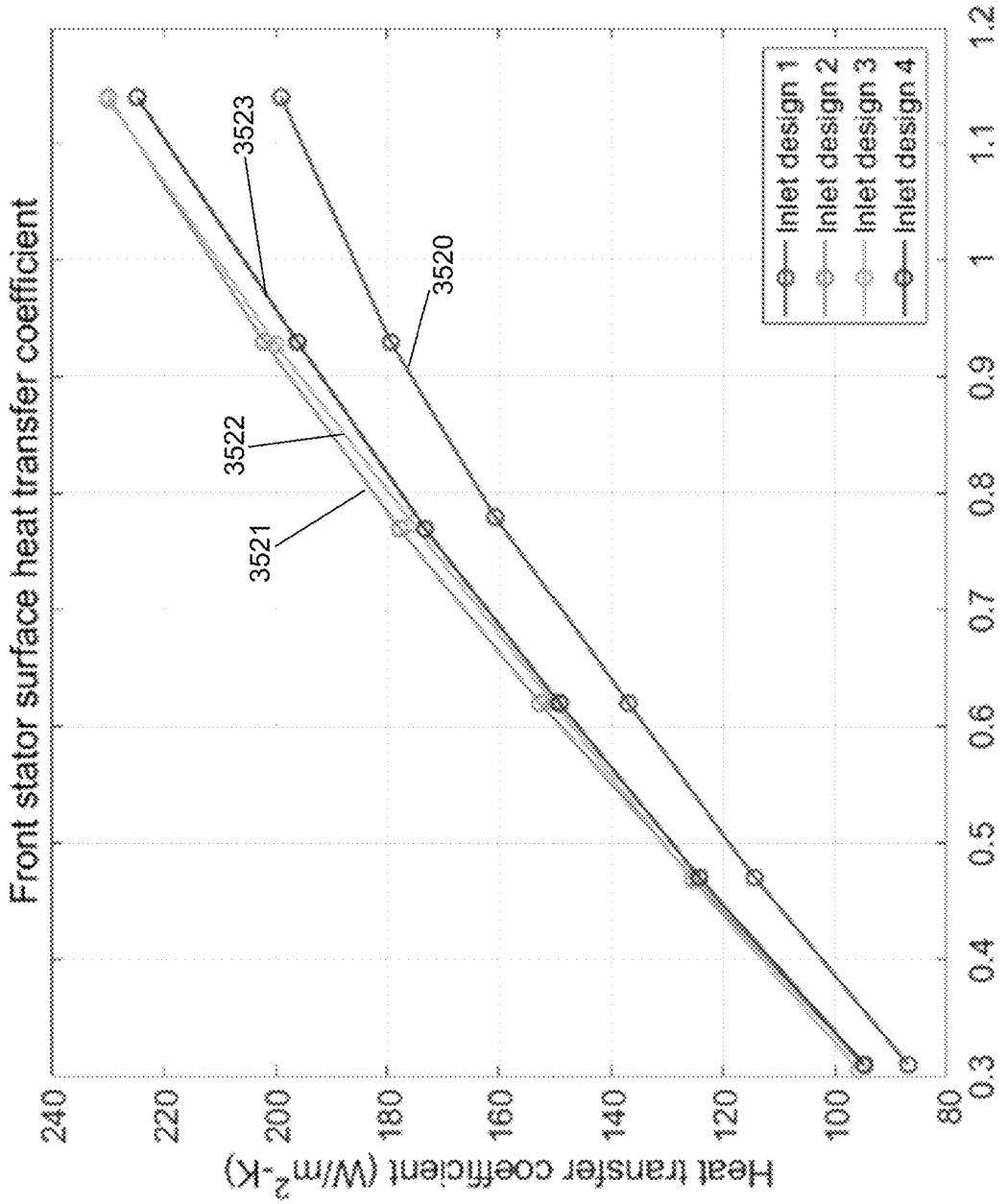
Front stator surface heat transfer coefficient
Heat transfer coefficient (W/m²-K)
Fan zone inlet volume flow rate (m³/s)
Inlet design 1
Inlet design 2
Inlet design 3
Inlet design 4
3520
3521
3522
3523
240
220
200
180
160
140
120
100
80
0.3
0.4
0.5
0.6
0.7
0.8
0.9
1
1.1
1.2

FIG. 35C

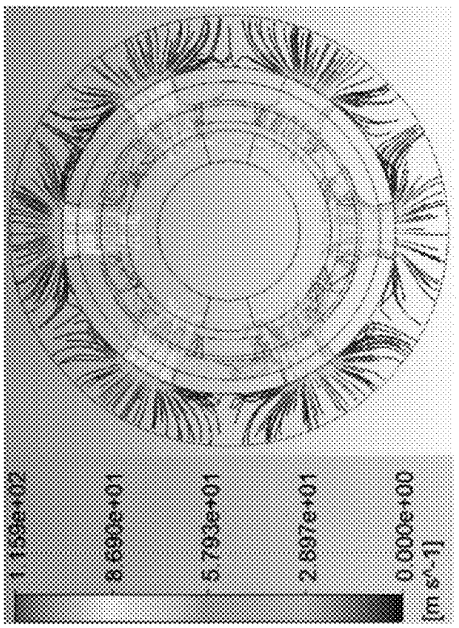

FIG. 36A

FIG. 36B

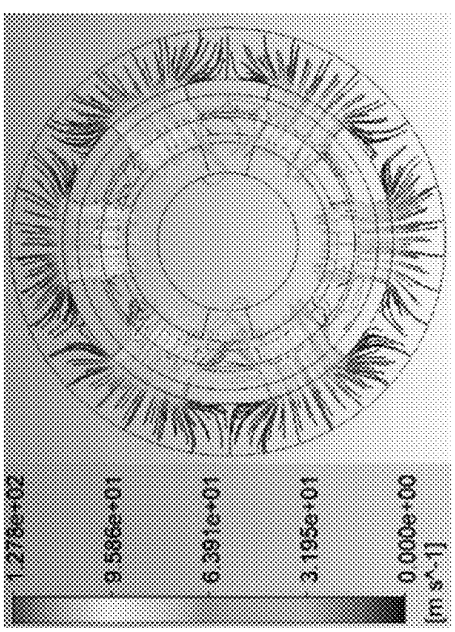

FIG. 36C

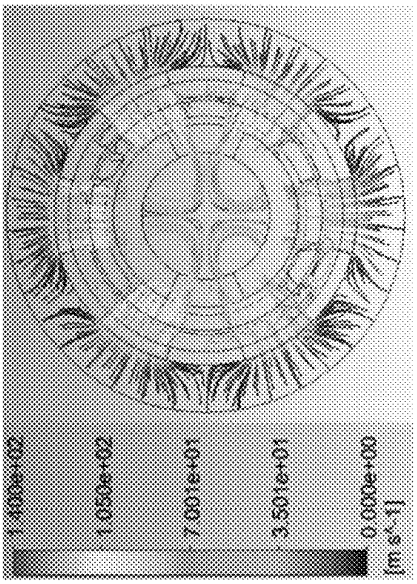

FIG. 36D

FIG. 37

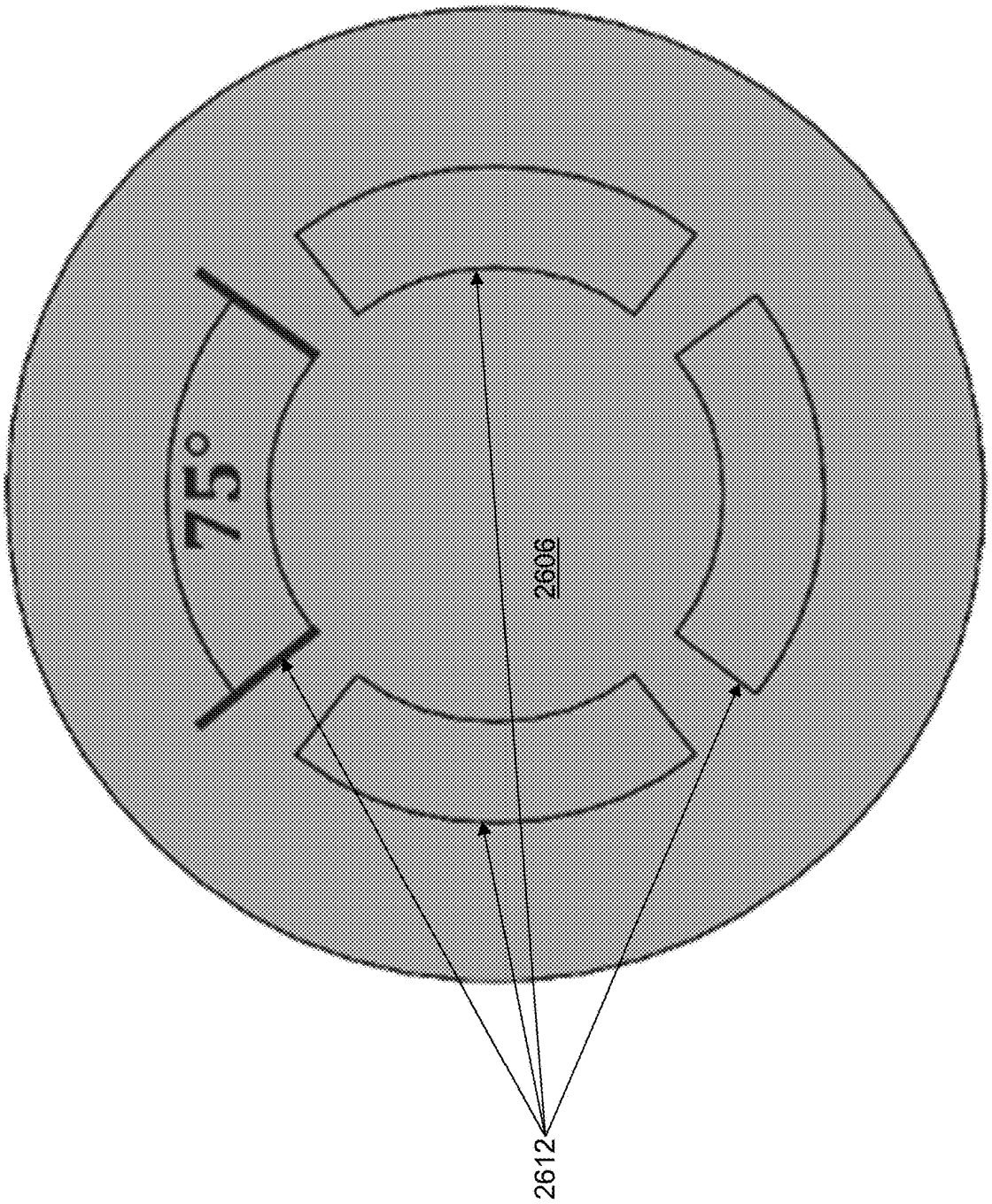

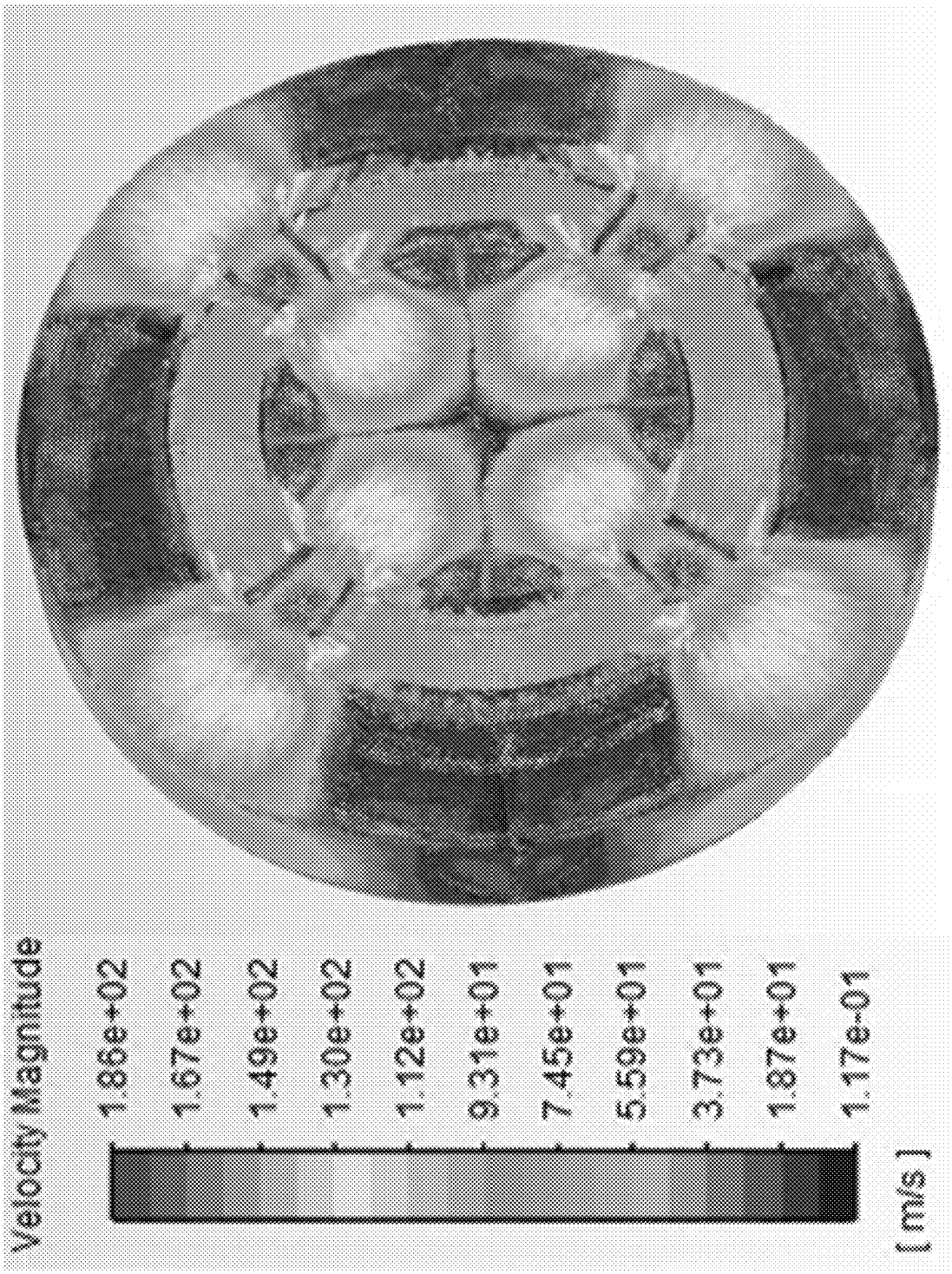
Velocity Magnitude
1.86e+02
1.67e+02
1.49e+02
1.30e+02
1.12e+02
9.31e+01
7.45e+01
5.59e+01
3.73e+01
1.87e+01
1.17e-01
[m/s]

FIG. 38A

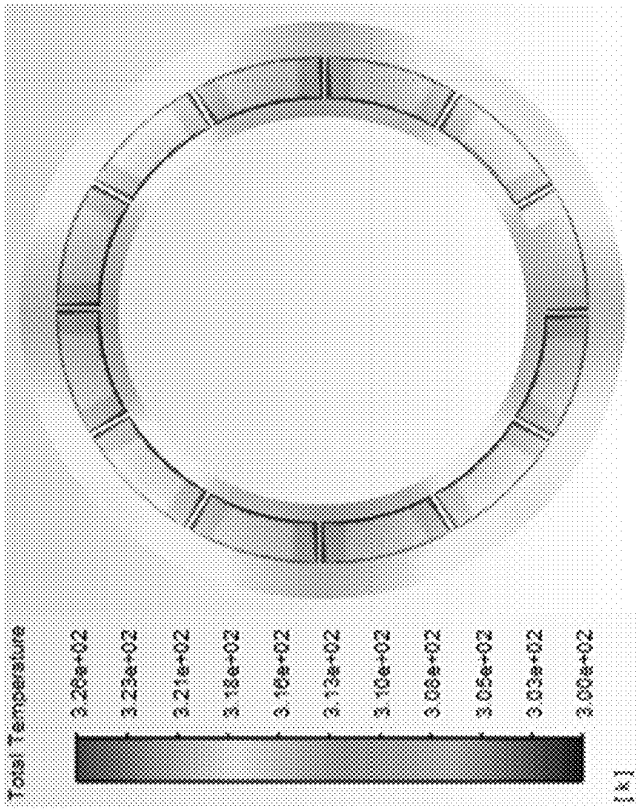

FIG. 38C

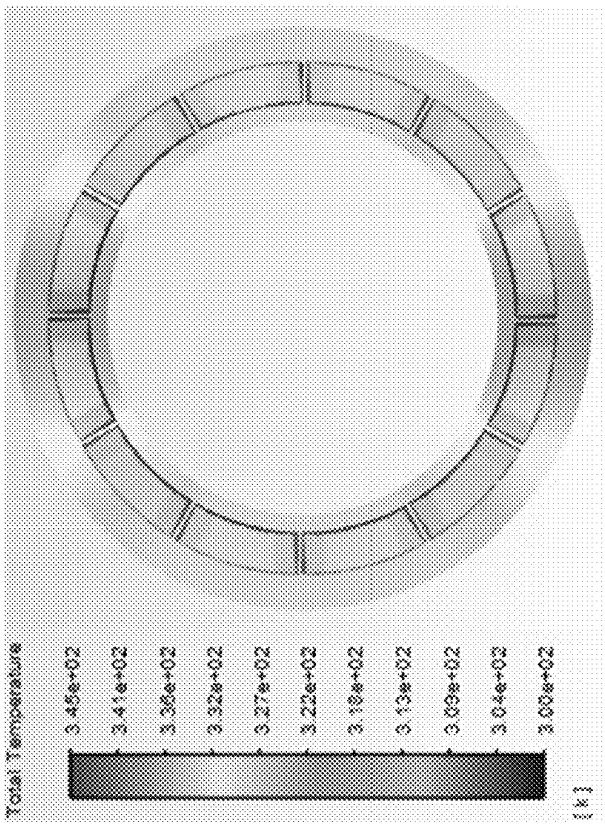

FIG. 38B

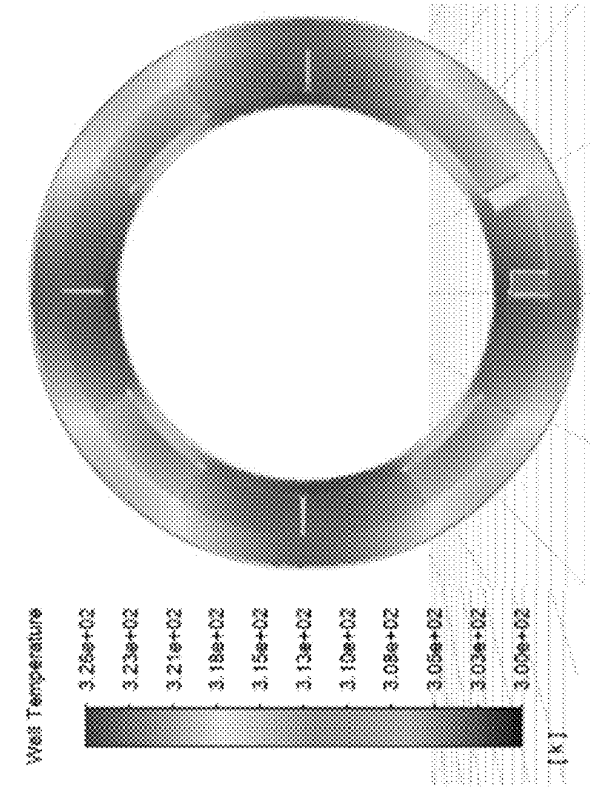

FIG. 38E

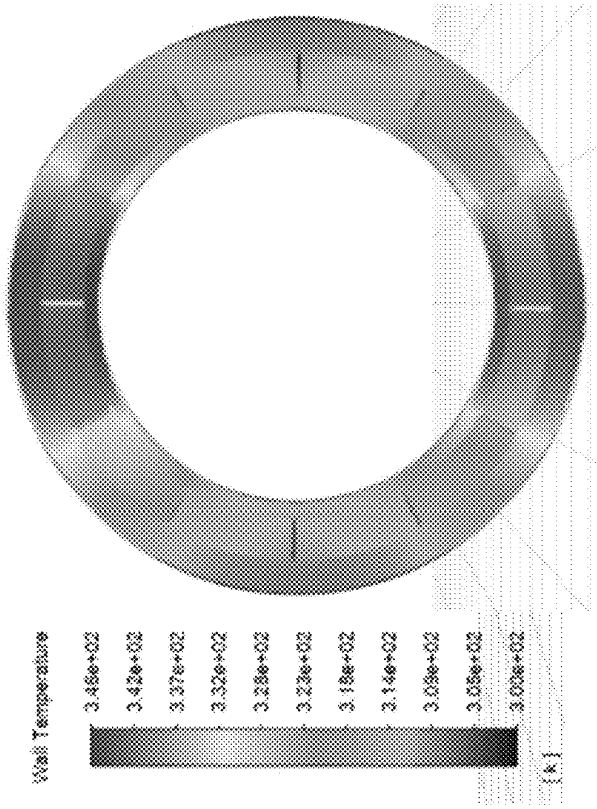

FIG. 38D

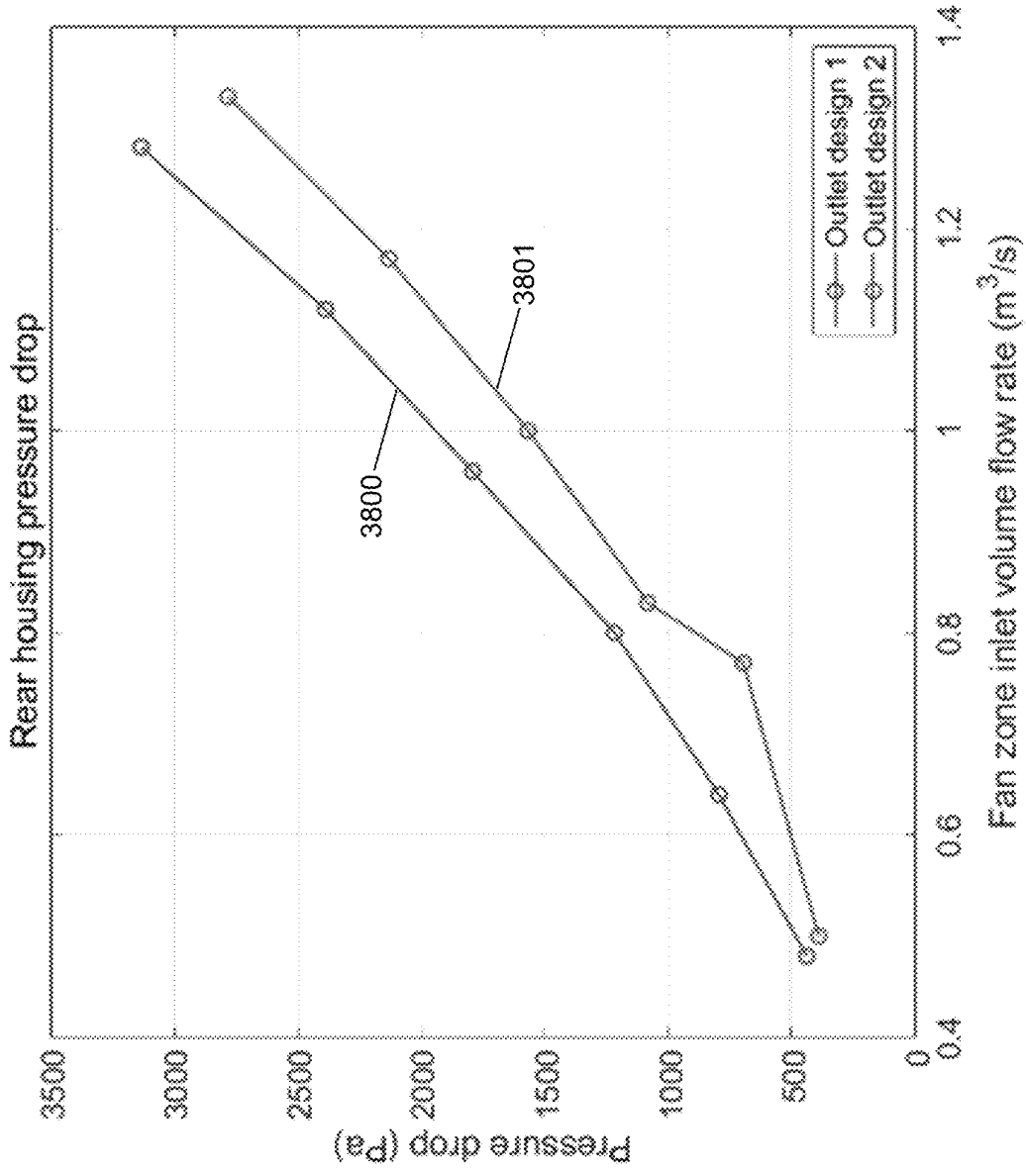
Rear housing pressure drop
Pressure drop (Pa)
Fan zone inlet volume flow rate (m3/s)
Outlet design 1
Outlet design 2
3800
3801
3500
3000
2500
2000
1500
1000
500
0
0.4
0.6
0.8
1
1.2
1.4

FIG. 38F

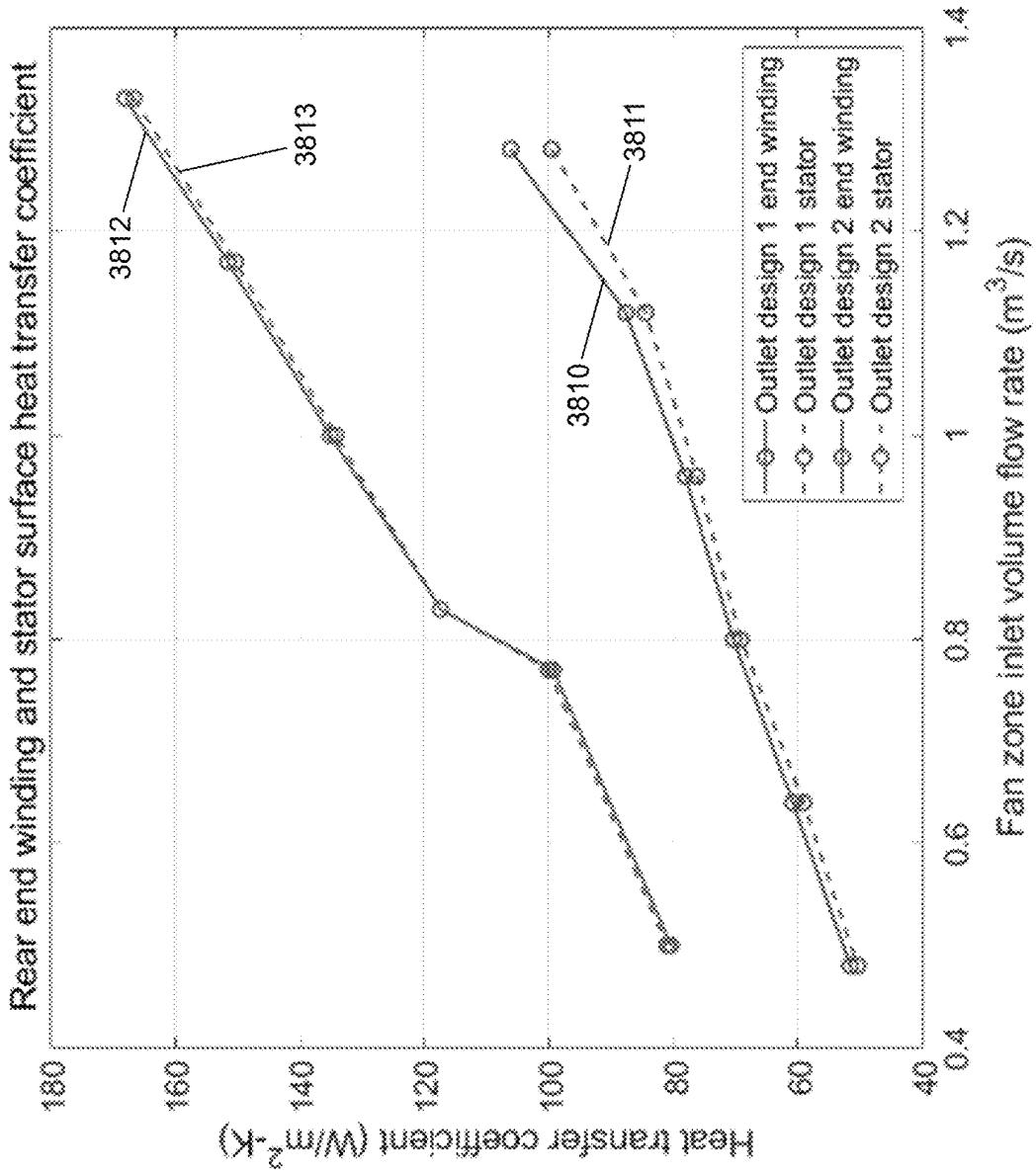
Rear end winding and stator surface heat transfer coefficient
Heat transfer coefficient (W/m²-K)
Fan zone inlet volume flow rate (m³/s)
180
160
140
120
100
80
60
40
0.4
0.6
0.8
1
1.2
1.4
3812
3813
3810
3811
Outlet design 1 end winding
Outlet design 1 stator
Outlet design 2 end winding
Outlet design 2 stator

FIG. 38G

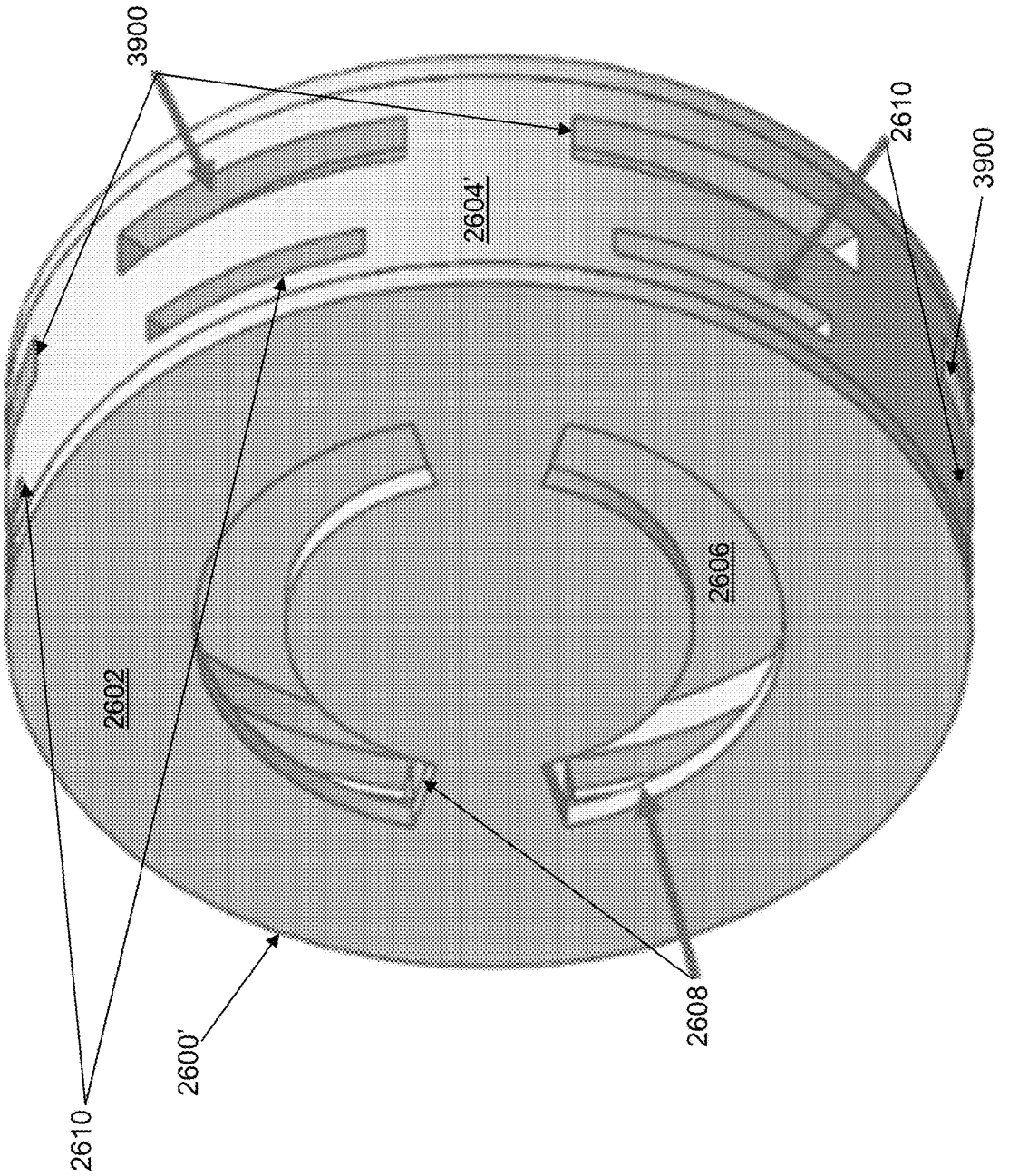

FIG. 39

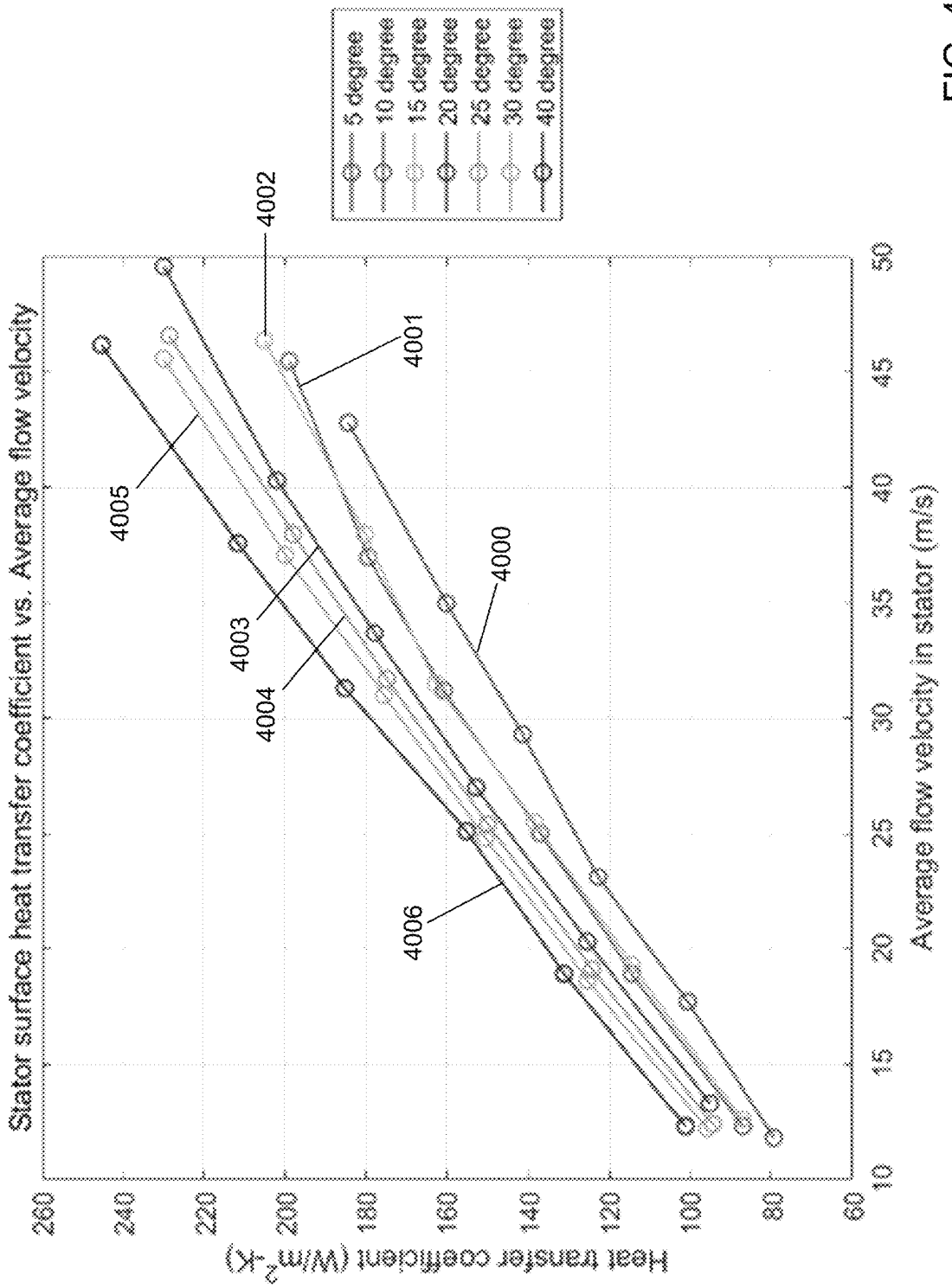
Stator surface heat transfer coefficient vs. Average flow velocity
Heat transfer coefficient (W/m²-K)
Average flow velocity in stator (m/s)
5 degree
10 degree
15 degree
20 degree
25 degree
30 degree
40 degree
4000
4001
4002
4003
4004
4005
4006

FIG. 40A

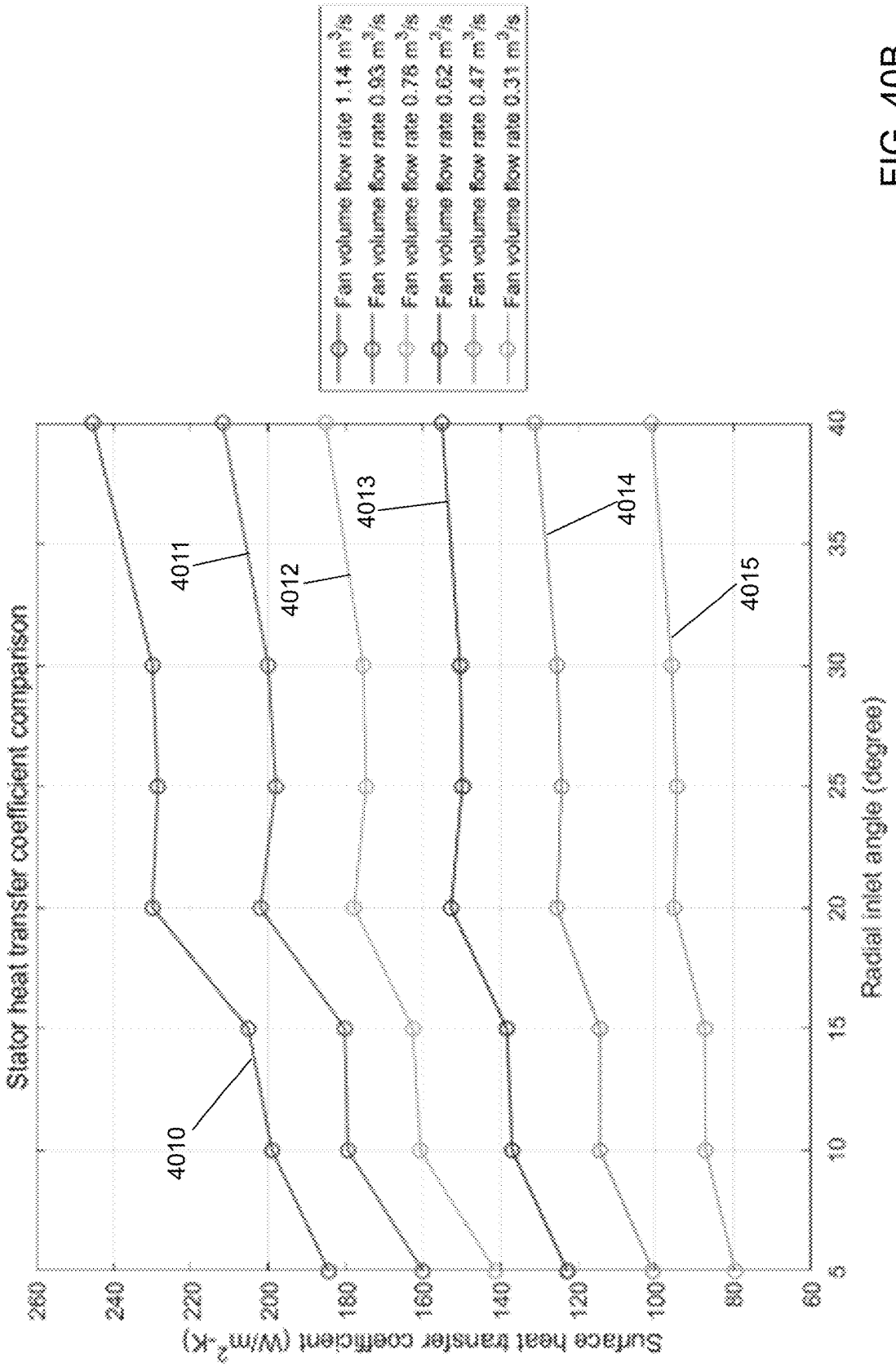
Stator heat transfer coefficient comparison
Surface heat transfer coefficient (W/m²-K)
Radial inlet angle (degree)
Fan volume flow rate 1.14 m³/s
Fan volume flow rate 0.93 m³/s
Fan volume flow rate 0.78 m³/s
Fan volume flow rate 0.62 m³/s
Fan volume flow rate 0.47 m³/s
Fan volume flow rate 0.31 m³/s
4010
4011
4012
4013
4014
4015
260
240
220
200
180
160
140
120
100
80
60
5
10
15
20
25
30
35
40

FIG. 40B

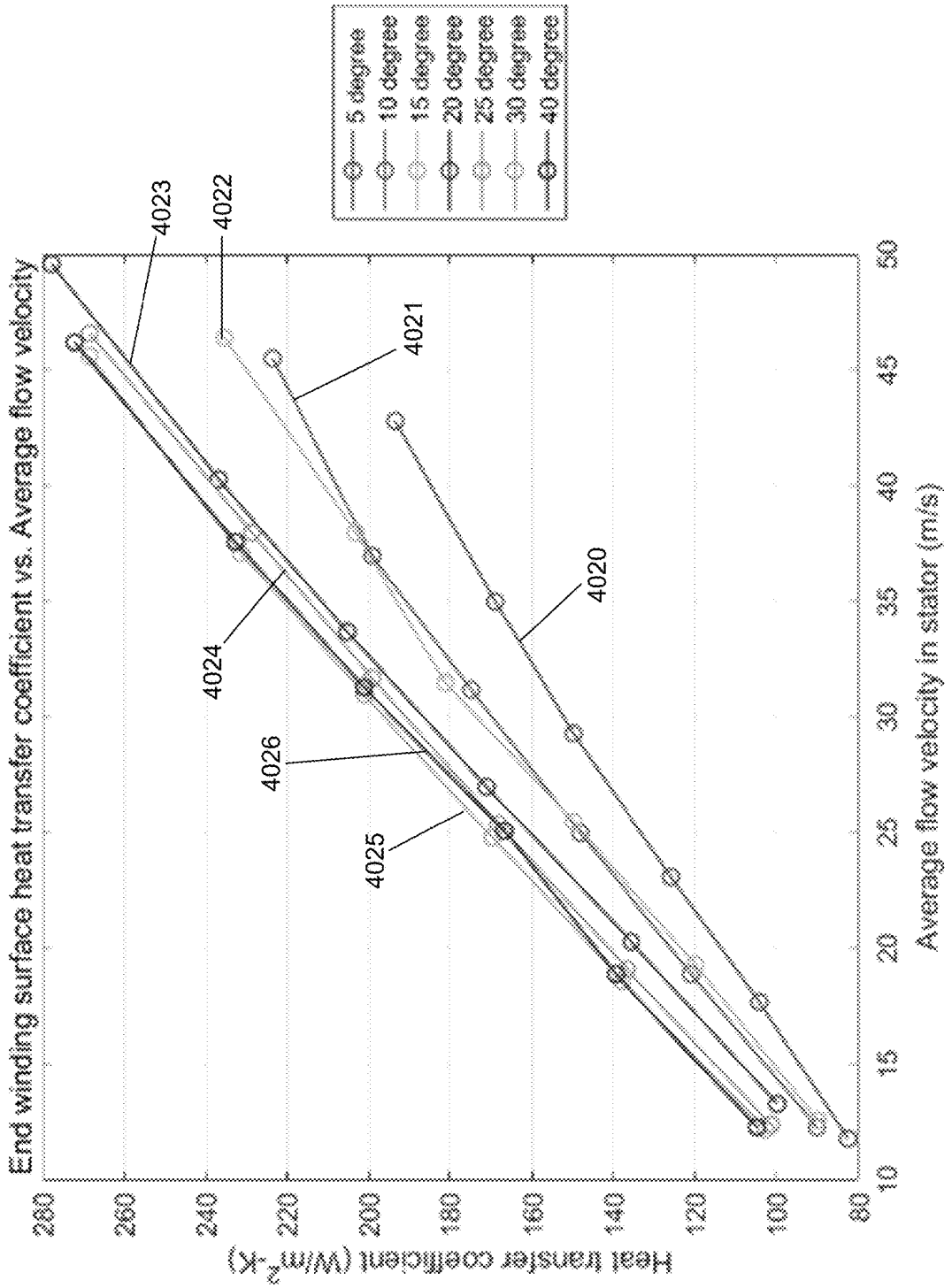
End winding surface heat transfer coefficient vs. Average flow velocity
Heat transfer coefficient (W/m²-K)
Average flow velocity in stator (m/s)
5 degree
10 degree
15 degree
20 degree
25 degree
30 degree
40 degree
4020
4021
4022
4023
4024
4025
4026

FIG. 40C

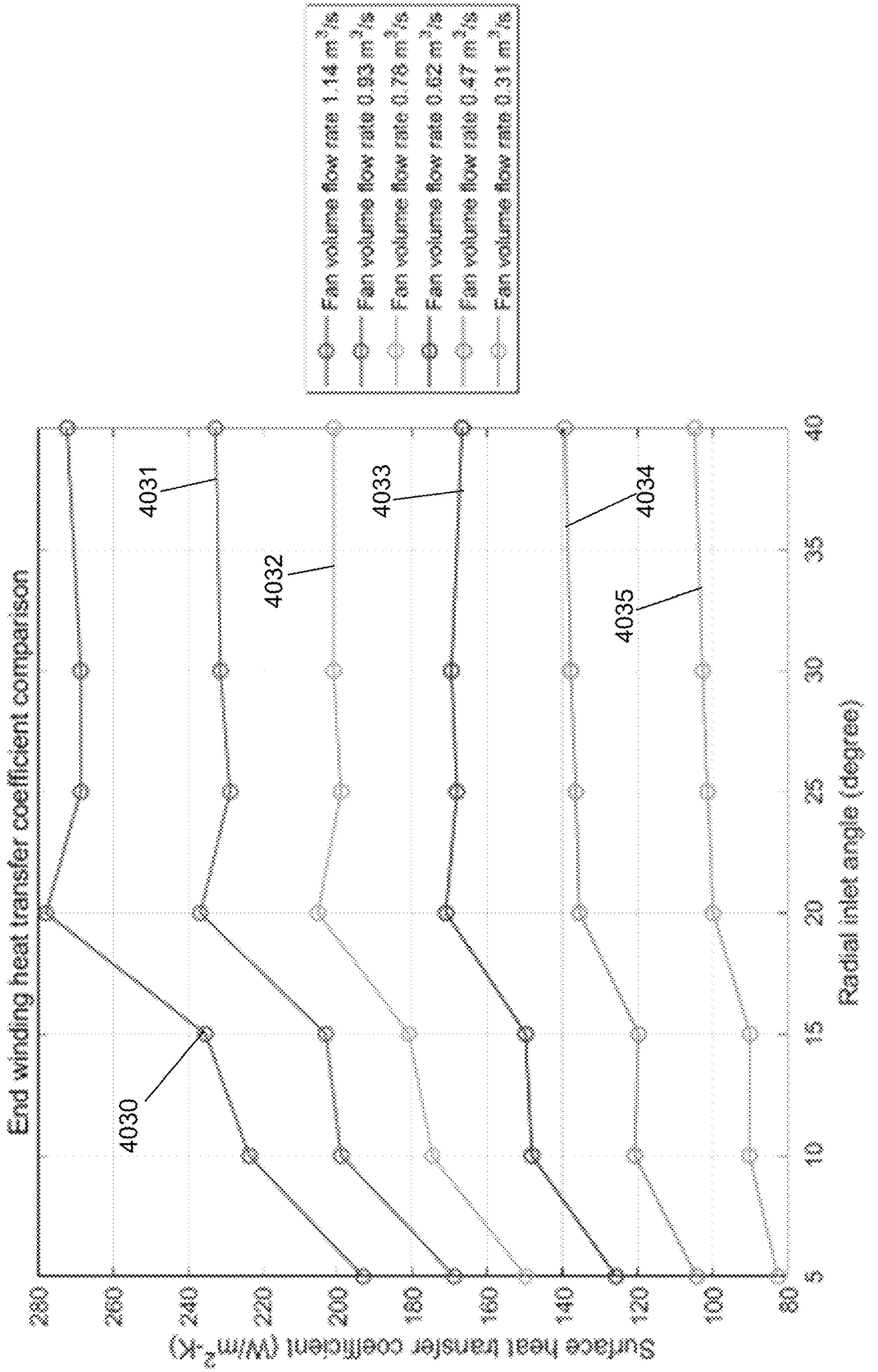
End winding heat transfer coefficient comparison
Surface heat transfer coefficient (W/m²-K)
Radial inlet angle (degree)
Fan volume flow rate 1.14 m³/s
Fan volume flow rate 0.93 m³/s
Fan volume flow rate 0.78 m³/s
Fan volume flow rate 0.62 m³/s
Fan volume flow rate 0.47 m³/s
Fan volume flow rate 0.31 m³/s
4030
4031
4032
4033
4034
4035
280
260
240
220
200
180
160
140
120
100
80
5
10
15
20
25
30
35
40

FIG. 40D

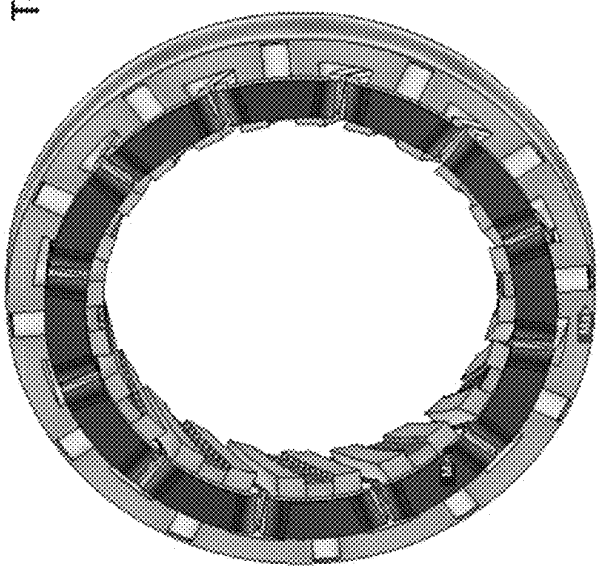

FIG. 41A

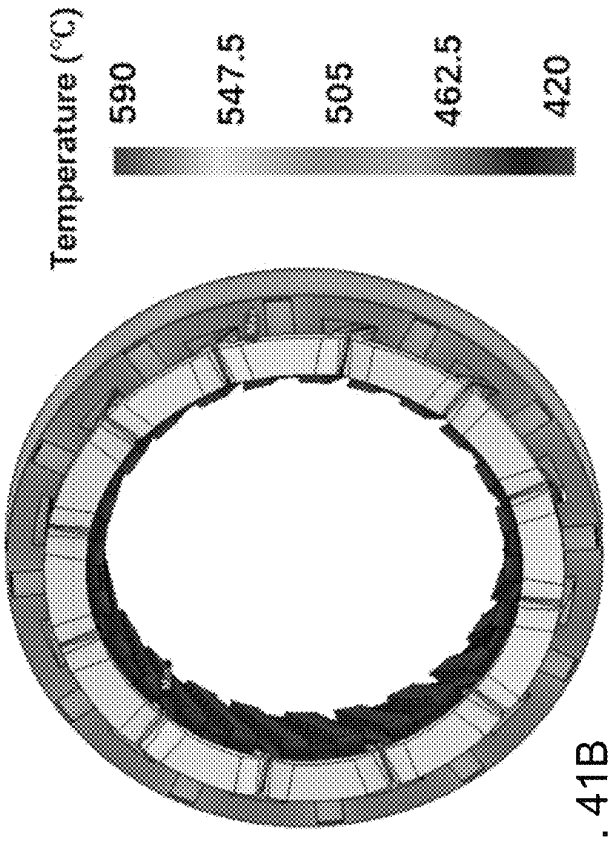

FIG. 41B

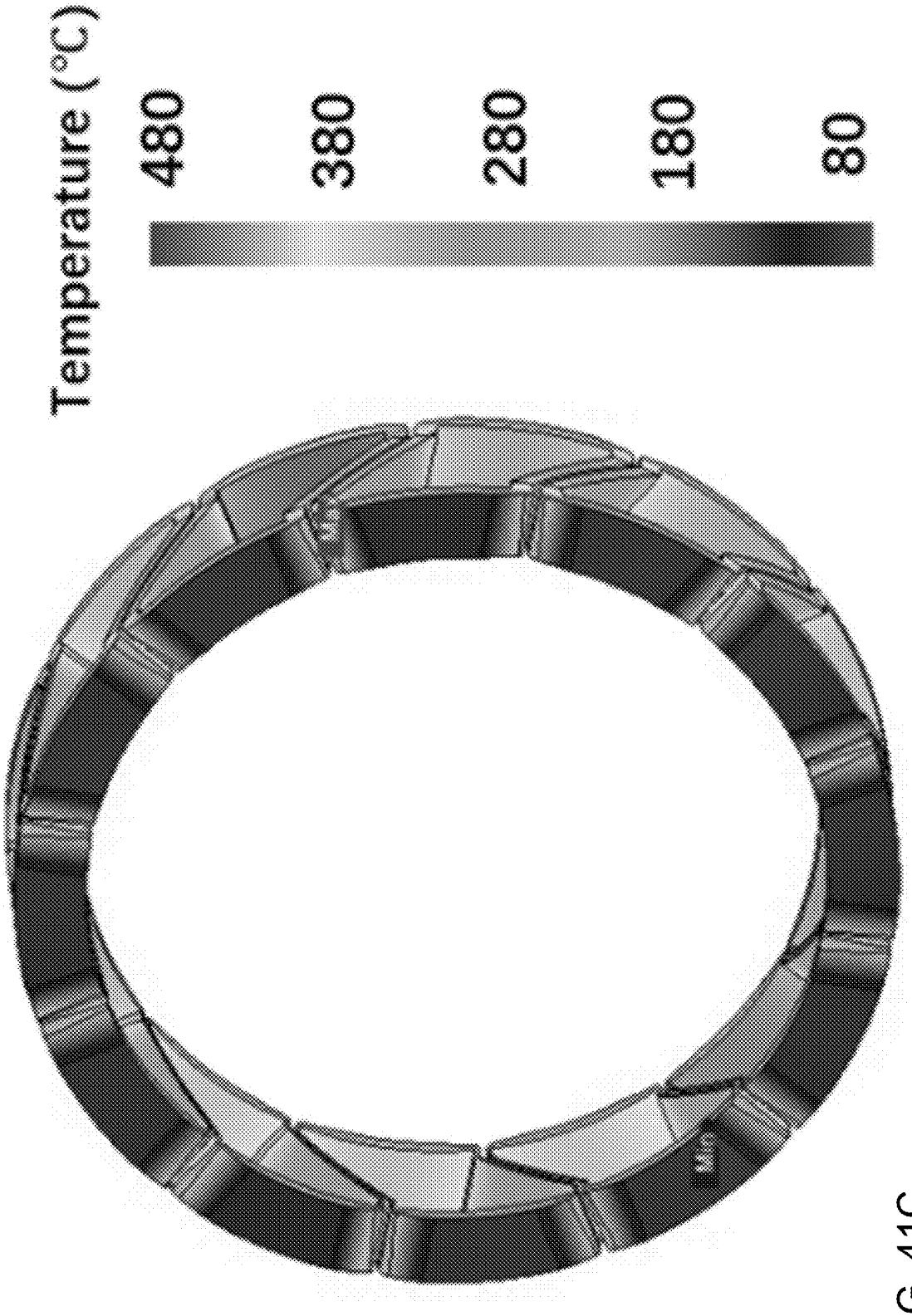

FIG. 41C

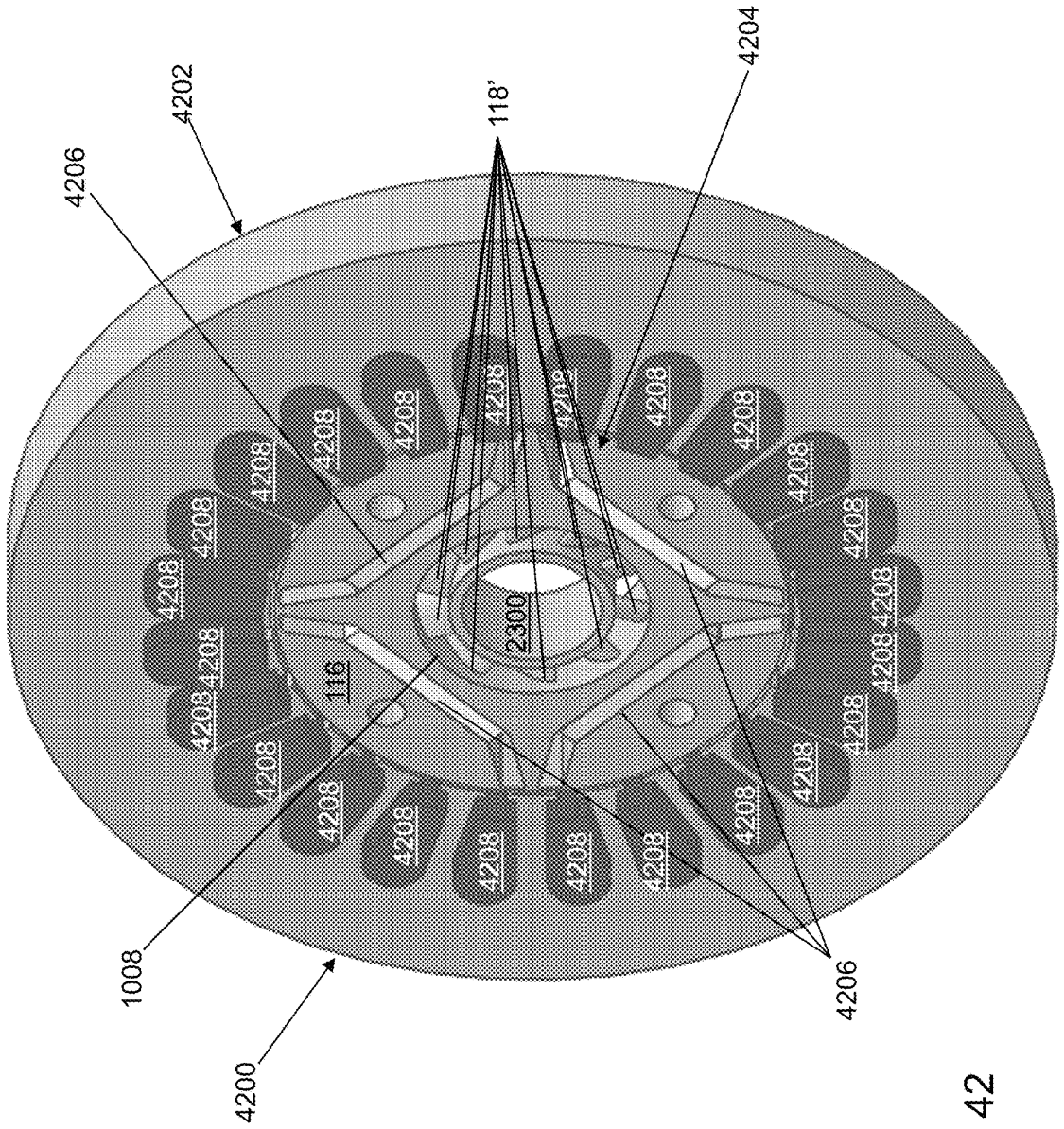

FIG. 42

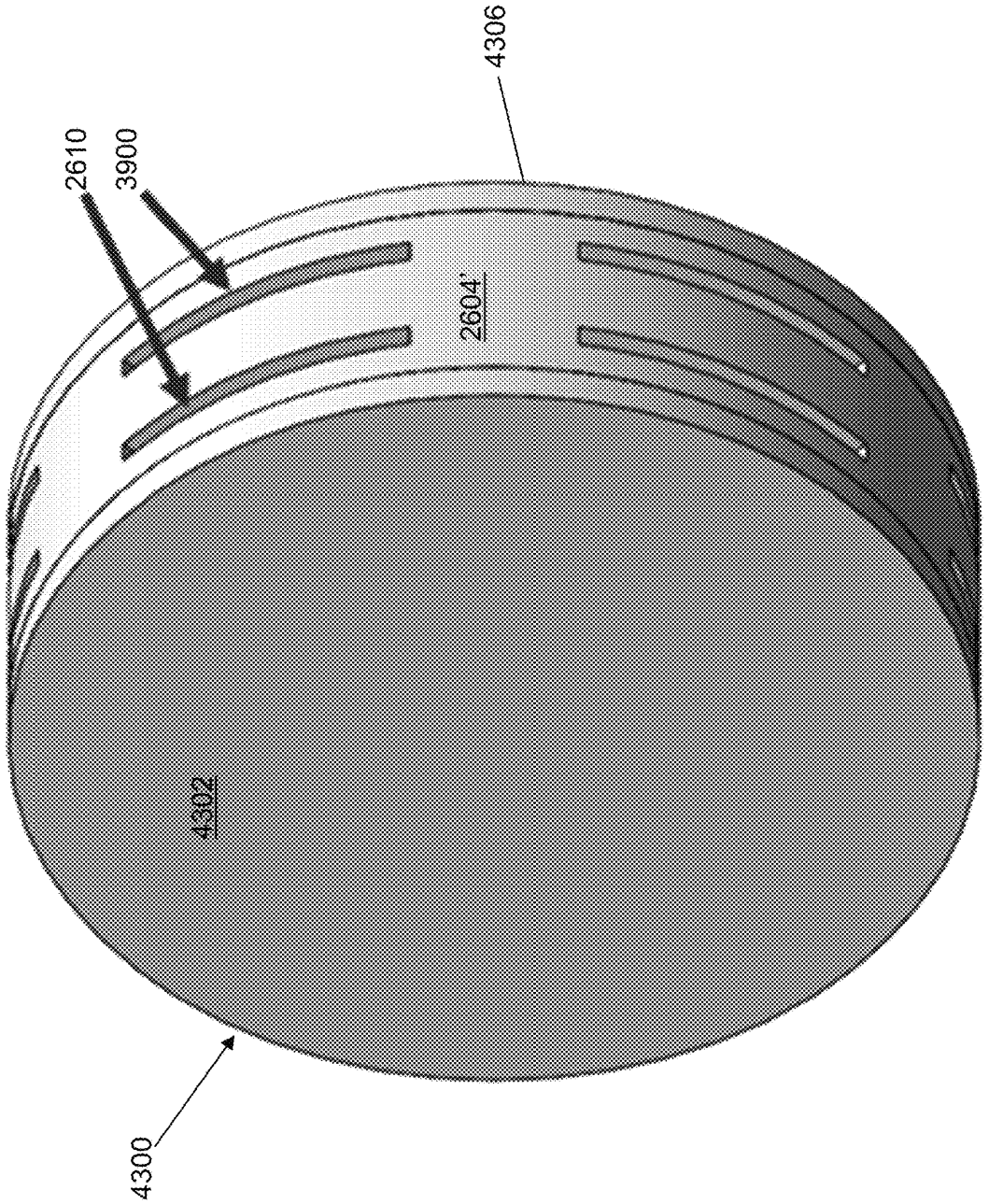

FIG. 43

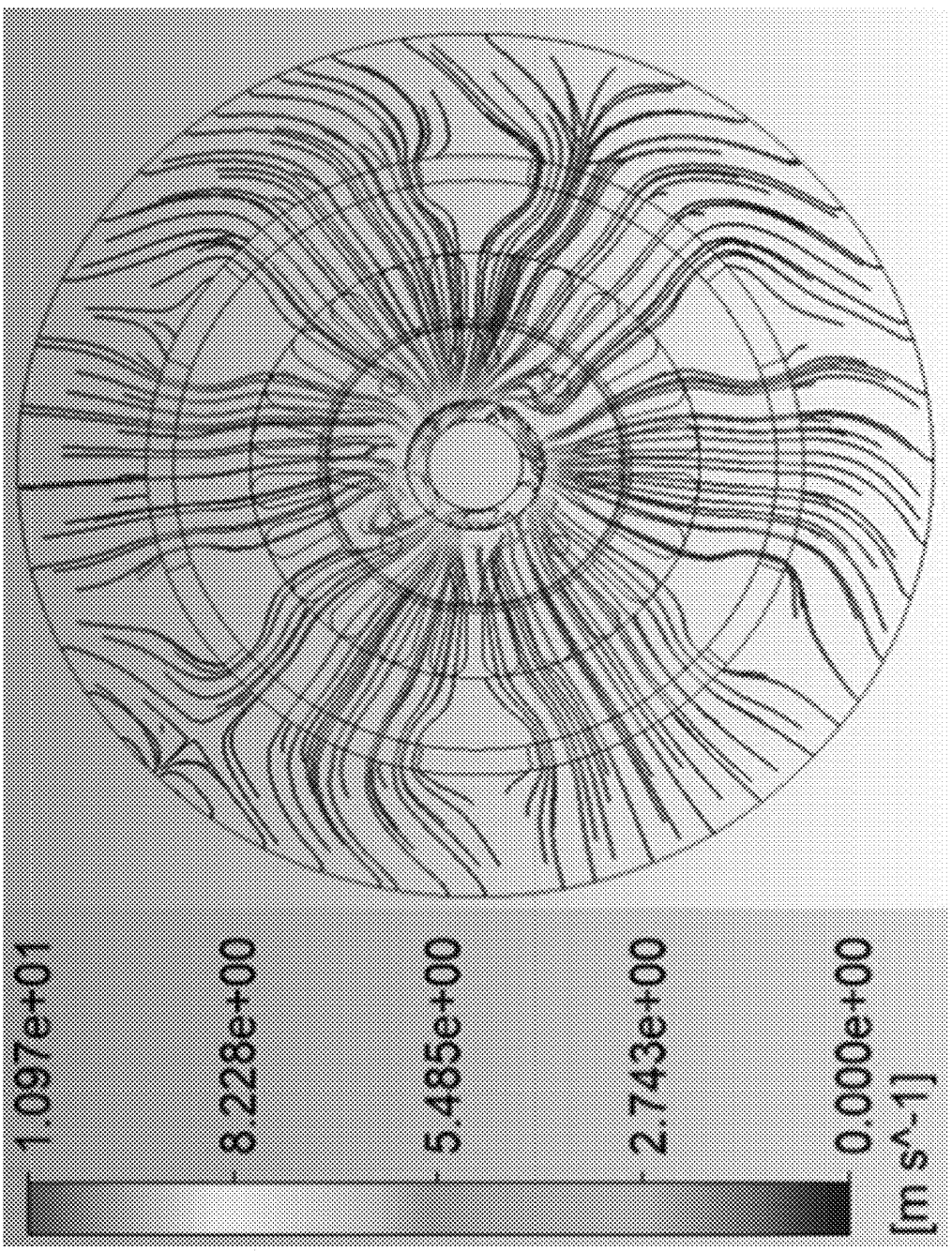

FIG. 44A

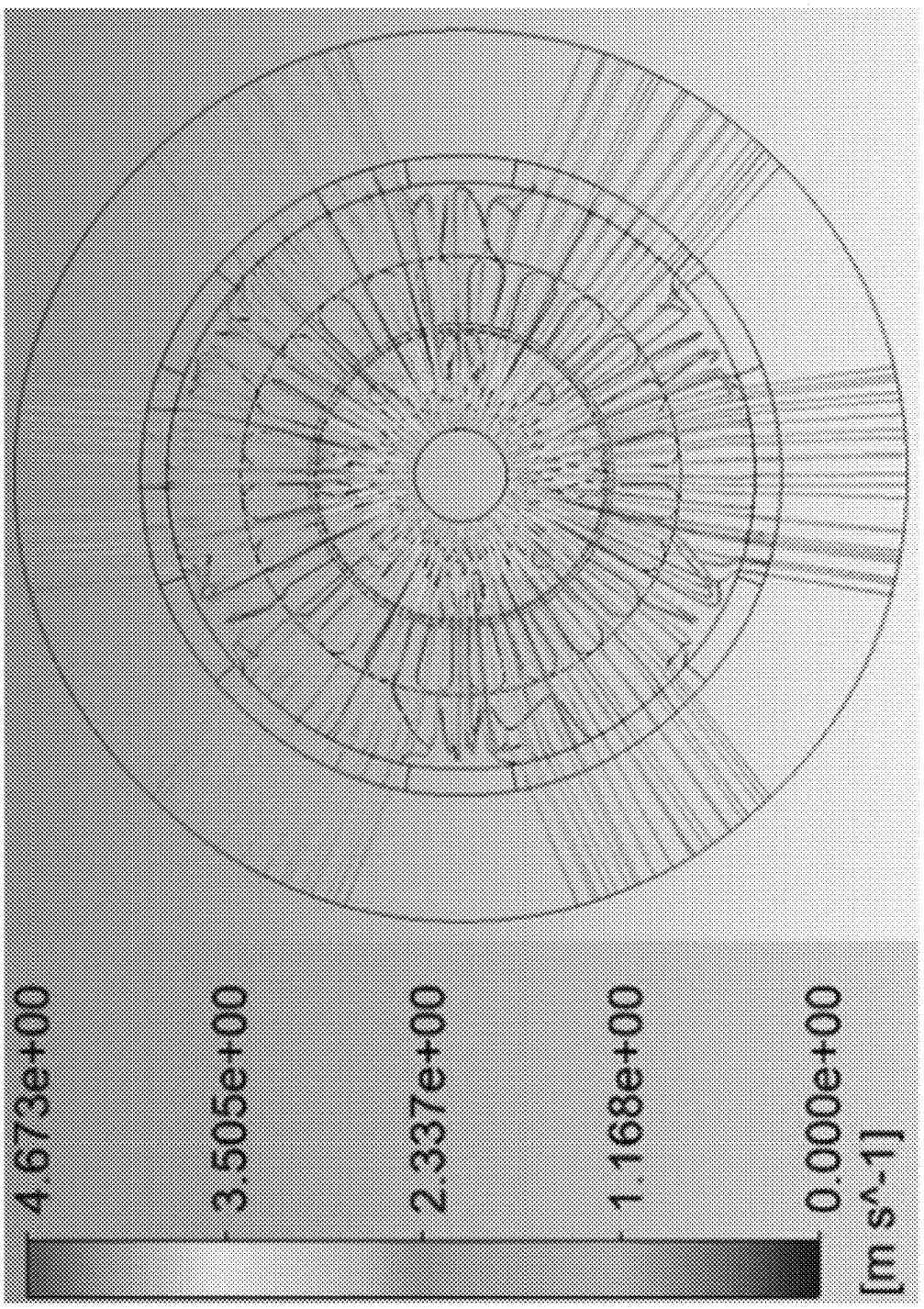

FIG. 44B

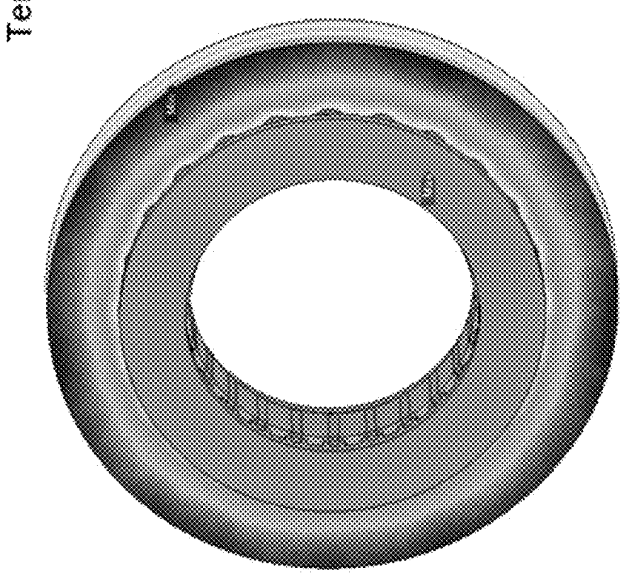

FIG. 45A

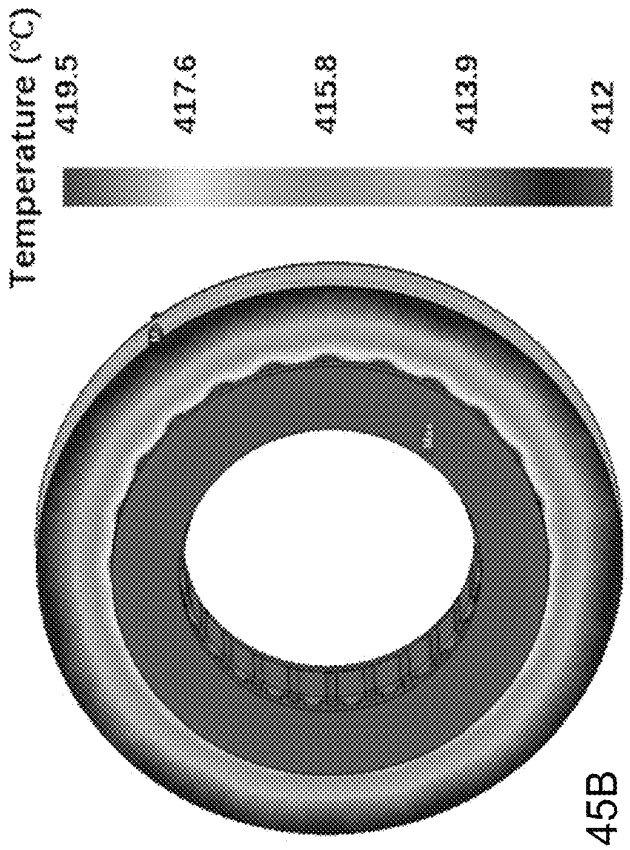

FIG. 45B

ELECTRICAL MACHINE COOLING WITH AXIAL AND RADIAL INLETS AND OUTLETS

CROSS REFERENCE TO RELATED APPLICATIONS

The present application claims priority to U.S. Provisional Patent Application No. 63/253,634 that was filed Oct. 8, 2021, the entire contents of which are incorporated herein by reference.

REFERENCE TO GOVERNMENT RIGHTS

This invention was made with government support under 1552942 awarded by the National Science Foundation. The government has certain rights in the invention.

BACKGROUND

Electrification in aerospace and automotive systems has attracted more and more attention in recent years to help reduce greenhouse gas emissions and mitigate climate change. Electrical machines need to have high power density, high efficiency, and be compact. In the machine design process, the thermal limit has become a dominant constraint because temperature-sensitive materials are often used to improve power and torque densities. A high winding temperature can lead to large resistance and copper loss.

Permanent magnet (PM) machines are widely used in many sectors (electric vehicles, wind generators, aircraft applications, industrial drives, HVAC) due to their high-power density, high efficiency, and compactness. Almost all electric and hybrid vehicles use PM motors. Conventional permanent magnet machines such as interior permanent magnet (IPM) machines and surface permanent magnet (SPM) machines have their magnets located on or buried in the rotor. Since permanent magnet materials are temperature sensitive, the cooling of the rotor is crucial to avoid the demagnetization of magnets.

Air-cooling and/or liquid-cooling techniques are commonly used for thermal management in electrical machines. Two particular methods, including forced air-cooling and water jacket cooling, focus on the stator and do not efficiently cool the rotor. Direct cooling of the rotor using spray cooling or in-shaft cooling, where oil is brought inside the shaft, is extremely complex and expensive. Similarly, induction motors need to be cooled because of the large conductor losses in the rotor. Therefore, appropriate thermal management is crucial for electrical machine operation. Existing solutions, such as liquid cooling, can be expensive or are not sufficient to keep the machine rotor and the copper windings at the proper temperatures.

SUMMARY

In an example embodiment, an electrical machine includes, but is not limited to, a rotor, a stator, a winding, and a housing. The rotor includes, but is not limited to, a rotor core configured to mount to a shaft for rotation of the rotor core and shaft together and a plurality of blades extending radially away from the rotor core. Each blade of the plurality of blades is curved axially along the rotor core. The stator includes, but is not limited to, a stator core, and a plurality of teeth extending from the stator core toward the rotor core. The plurality of teeth defines a plurality of slots between successive teeth of the plurality of teeth. The winding is wound through at least two slots of the plurality of slots. The stator is mounted radially relative to the rotor. The housing includes, but is not limited to, a front wall, a back wall, and a radial sidewall mounted between the front wall and the back wall to define an enclosure. A radial inlet aperture wall is formed circumferentially through the radial sidewall to form an opening through the radial sidewall. The rotor and the stator are mounted within the enclosure.

In another example embodiment, an electrical machine includes, but is not limited to, a hub, a rotor core, a stator, a winding, and a housing. The hub includes, but is not limited to, a hub core configured to mount to a shaft for rotation of the hub core and shaft together and a plurality of blades extending radially away from the hub core. Each blade of the plurality of blades is curved axially along the hub core. The rotor core is configured to mount to the plurality of blades and is mounted radially relative to the hub. The stator includes, but is not limited to, a stator core and a plurality of teeth extending from the stator core toward the rotor core. The plurality of teeth defines a plurality of slots between successive teeth of the plurality of teeth. The winding is wound through at least two slots of the plurality of slots. The stator is mounted radially relative to the rotor core. The housing includes, but is not limited to, a front wall, a back wall, and a radial sidewall mounted between the front wall and the back wall to define an enclosure. A radial inlet aperture wall is formed circumferentially through the radial sidewall to form an opening through the radial sidewall. The hub, the rotor core, and the stator are mounted within the enclosure.

Other principal features of the disclosed subject matter will become apparent to those skilled in the art upon review of the following drawings, the detailed description, and the appended claims.

BRIEF DESCRIPTION OF THE DRAWINGS

The patent or application file contains at least one drawing executed in color. Copies of this patent or patent application publication with color drawing(s) will be provided by the Office upon request and payment of the necessary fee.

Illustrative embodiments of the disclosed subject matter will hereafter be described referring to the accompanying drawings, wherein like numerals denote like elements.

FIG. **1** depicts a perspective view of an electrical machine in accordance with an illustrative embodiment.

FIG. **2** depicts a front view of the electrical machine of FIG. **1** in accordance with an illustrative embodiment.

FIG. **3** depicts a perspective view of a stator of the electrical machine of FIG. **1** in accordance with an illustrative embodiment.

FIG. **4** depicts a perspective view of a first rotor of the electrical machine of FIG. **1** in accordance with an illustrative embodiment.

FIG. **5** depicts a perspective view of a second rotor of the electrical machine of FIG. **1** in accordance with an illustrative embodiment.

FIG. **6** depicts a rotor blade shape and nomenclature for a rotor of the electrical machine of FIG. **1** in accordance with an illustrative embodiment.

FIG. **7** depicts a velocity diagram of a flow through a rotor of the electrical machine of FIG. **1** in accordance with an illustrative embodiment.

FIG. **8** depicts a combined velocity triangle for a rotor of the electrical machine of FIG. **1** showing a velocity increase in accordance with an illustrative embodiment.

FIG. **9** depicts a required power for rotor compression work as a function of mean blade diameter for a rotor blade

of a rotor of the electrical machine of FIG. **1** in accordance with an illustrative embodiment.

FIG. **10** depicts an exploded perspective view of an electrical machine in accordance with a second illustrative embodiment.

FIG. **11** depicts an exploded perspective view of the electrical machine in accordance with a third illustrative embodiment.

FIG. **12** depicts an exploded perspective view of the electrical machine in accordance with a fourth illustrative embodiment.

FIG. **13** depicts an exploded perspective view of the electrical machine in accordance with a fifth illustrative embodiment.

FIG. **14** depicts a perspective view of the electrical machine of FIG. **10** with a cascaded connection of multi-stage compressors in accordance with an illustrative embodiment.

FIG. **15** depicts a perspective view of a cascaded connection of two electrical machines of FIG. **10** with a cascaded connection of multi-stage compressors in accordance with an illustrative embodiment.

FIG. **16** depicts a back-electromotive force generated by the electrical machine of FIG. **1** as a function of the rotor position in accordance with an illustrative embodiment.

FIG. **17** depicts a cogging torque generated by the electrical machine of FIG. **1** as a function of a rotor position in accordance with an illustrative embodiment.

FIG. **18** depicts a torque generated by the electrical machine of FIG. **1** as a function of the rotor position in accordance with an illustrative embodiment.

FIG. **19** depicts a flow diagram illustrating examples of operations performed to determine parameters for the electrical machines of FIGS. **1** and **10-13** in accordance with an illustrative embodiment.

FIG. **20** depicts a perspective view of the electrical machine of FIG. **1** with different blade profiles in accordance with an illustrative embodiment.

FIG. **21** depicts a rotor blade shape and nomenclature for a rotor of the electrical machine of FIG. **20** in accordance with an illustrative embodiment.

FIG. **22** depicts a velocity diagram of a flow through the rotor of the electrical machine of FIG. **20** in accordance with an illustrative embodiment.

FIG. **23** depicts air flow through a hub with blades mounted interior of a rotor in accordance with an illustrative embodiment.

FIG. **24** depicts permanent magnets mounted to an exterior surface of the rotor of FIG. **23** in accordance with an illustrative embodiment.

FIG. **25** depicts permanent magnets mounted to an interior of a core of the rotor of FIG. **23** in accordance with an illustrative embodiment.

FIG. **26** depicts a perspective view of a housing for an electrical machine in accordance with an illustrative embodiment.

FIG. **27** depicts a perspective view of the housing of FIG. **26** with the electrical machine of FIG. **20** mounted within the housing in accordance with an illustrative embodiment.

FIG. **28**A depicts a front view of the housing of FIG. **26** with the electrical machine of FIG. **20** mounted within the housing in accordance with an illustrative embodiment.

FIG. **28**B depicts a side view of the housing of FIG. **26** with the electrical machine of FIG. **20** mounted within the housing in accordance with an illustrative embodiment.

FIG. **29** depicts a side cross-sectional view of the computational fluid dynamics simulation model of the housing of FIG. **26** with the electrical machine of FIG. **20** mounted within the housing in accordance with an illustrative embodiment.

FIG. **30** shows an inlet air flow velocity pattern within the housing of FIG. **26** with the electrical machine of FIG. **20** mounted within the housing in accordance with an illustrative embodiment.

FIG. **31** shows an outlet air flow velocity pattern within the housing of FIG. **26** with the electrical machine of FIG. **20** mounted within the housing in accordance with an illustrative embodiment.

FIG. **32** shows a front view of a housing to illustrate angle variations in alternative housing designs in accordance with an illustrative embodiment.

FIG. **33**A shows a side view of an inlet air flow velocity pattern within the housing of FIG. **26** with the electrical machine of FIG. **20** mounted within the housing with a 10-degrees radial inlet size in accordance with an illustrative embodiment.

FIG. **33**B shows a side view of an inlet air flow velocity pattern within the housing of FIG. **26** with the electrical machine of FIG. **20** mounted within the housing with a 20-degrees radial inlet size in accordance with an illustrative embodiment.

FIG. **33**C shows a side view of an inlet air flow velocity pattern within the housing of FIG. **26** with the electrical machine of FIG. **20** mounted within the housing with a 30-degrees radial inlet size in accordance with an illustrative embodiment.

FIG. **33**D shows a side view of an inlet air flow velocity pattern within the housing of FIG. **26** with the electrical machine of FIG. **20** mounted within the housing with a 40-degrees radial inlet size in accordance with an illustrative embodiment.

FIG. **34** shows a heat transfer coefficient comparison for the stator surface and the end winding surface that results from the inlet models with 10-degrees, 20-degrees, 30-degrees, and 40-degrees radial inlet sizes in accordance with an illustrative embodiment.

FIG. **35**A shows a pressure drop comparison through a front of the housing that results with six radial inlets of 10-degrees, 20-degrees, and 30-degrees and two axial inlets of 150-degrees, and six radial inlets of 30-degrees and two axial inlets of 130-degrees in accordance with an illustrative embodiment.

FIG. **35**B shows an end winding heat transfer coefficient comparison for the end winding front surface that results with six radial inlets of 10-degrees, 20-degrees, and 30-degrees and two axial inlets of 150-degrees, and six radial inlets of 30-degrees and two axial inlets of 130-degrees in accordance with an illustrative embodiment.

FIG. **35**C shows the front stator surface heat transfer coefficient comparison that results with six radial inlets of 10-degrees, 20-degrees, and 30-degrees and two axial inlets of 150-degrees, and six radial inlets of 30-degrees and two axial inlets of 130-degrees in accordance with an illustrative embodiment.

FIG. **36**A shows a front view of an inlet air flow velocity pattern within the housing of FIG. **26** with the electrical machine of FIG. **20** mounted inside the housing with six radial inlets of 10-degrees and two axial inlets of 150-degrees in accordance with an illustrative embodiment.

FIG. **36**B shows a front view of an inlet air flow velocity pattern within the housing of FIG. **26** with the electrical machine of FIG. **20** mounted inside the housing with six radial inlets of 20-degrees and two axial inlets of 150-degrees in accordance with an illustrative embodiment.

FIG. **36**C shows a front view of an inlet air flow velocity pattern within the housing of FIG. **26** with the electrical machine of FIG. **20** mounted inside the housing with six radial inlets of 30-degrees and two axial inlets of 150-degrees in accordance with an illustrative embodiment.

FIG. **36**D shows a front view of an inlet air flow velocity pattern within the housing of FIG. **26** with the electrical machine of FIG. **20** mounted inside the housing with six radial inlets of 30-degrees and two axial inlets of 130-degrees in accordance with an illustrative embodiment.

FIG. **37** shows a back view of a second housing with four axial outlets of 75-degrees in accordance with an illustrative embodiment.

FIG. **38**A shows an outlet air flow velocity pattern within the second housing of FIG. **37** with the electrical machine of FIG. **20** mounted inside the housing in accordance with an illustrative embodiment.

FIG. **38**B shows an end winding and stator total temperature distribution within the housing of FIG. **26** with the electrical machine of FIG. **20** mounted inside the housing with two axial outlets of 150-degrees in accordance with an illustrative embodiment.

FIG. **38**C shows an end winding and stator total temperature distribution within the second housing of FIG. **37** with the electrical machine of FIG. **20** mounted inside the housing with four axial outlets of 75-degrees in accordance with an illustrative embodiment.

FIG. **38**D shows a rear end winding and stator wall temperature distribution within the housing of FIG. **26** with the electrical machine of FIG. **20** mounted inside the housing with two axial outlets of 150-degrees in accordance with an illustrative embodiment.

FIG. **38**E shows a rear end winding and stator wall temperature distribution within the second housing of FIG. **37** with the electrical machine of FIG. **20** mounted inside the housing with four axial outlets of 75-degrees in accordance with an illustrative embodiment.

FIG. **38**F shows a pressure drop comparison across an exit of the housing with two axial outlets of 150-degrees and a rear of the housing with four axial outlets of 75-degrees in accordance with an illustrative embodiment.

FIG. **38**G shows a rear end winding surface and stator surface heat transfer coefficient comparison that results with two axial outlets of 150-degrees and with four axial outlets of 75-degrees in accordance with an illustrative embodiment.

FIG. **39** shows a perspective view of a third housing with axial inlets, radial inlets, axial outlets, and radial outlets in accordance with an illustrative embodiment.

FIG. **40**A shows a stator surface heat transfer coefficient comparison that results with six radial outlets of from 5-degrees to 40-degrees in accordance with an illustrative embodiment.

FIG. **40**B shows a stator surface heat transfer coefficient comparison that results from different fan volume flow rates in accordance with an illustrative embodiment.

FIG. **40**C shows an end winding surface heat transfer coefficient comparison that results with six radial outlets of from 5-degrees to 40-degrees in accordance with an illustrative embodiment.

FIG. **40**D shows an end winding surface heat transfer coefficient comparison that results from different fan volume flow rates in accordance with an illustrative embodiment.

FIG. **41**A shows a stator temperature contour plot with the housing of FIG. **26** in accordance with an illustrative embodiment.

FIG. **41**B shows a stator temperature contour plot without the housing of FIG. **26** in accordance with an illustrative embodiment.

FIG. **41**C shows a winding temperature distribution at 15 A_{rms}/mm^2 current density with the third housing of FIG. **39** in accordance with an illustrative embodiment.

FIG. **42** depicts a perspective view of an electrical machine with a hub with blades interior of the rotor in accordance with an illustrative embodiment.

FIG. **43** depicts a perspective view of a fourth housing with radial inlets and radial outlets in accordance with an illustrative embodiment.

FIG. **44**A shows a front view of an inlet air flow velocity pattern within the fourth housing of FIG. **43** with the electrical machine of FIG. **42** mounted inside the housing in accordance with an illustrative embodiment.

FIG. **44**B shows a back view of an outlet air flow velocity pattern within the fourth housing of FIG. **43** with the electrical machine of FIG. **42** mounted inside the housing in accordance with an illustrative embodiment.

FIG. **45**A shows a stator temperature distribution with the fourth housing of FIG. **43** in accordance with an illustrative embodiment.

FIG. **45**B shows a stator temperature distribution without the fourth housing in accordance with an illustrative embodiment.

DETAILED DESCRIPTION

Referring to FIG. **1**, a perspective view of an electrical machine **100** is shown in accordance with an illustrative embodiment. In the illustrative embodiment of FIG. **1**, electrical machine **100** is a radial flux switching permanent magnet machine (FSPM). Electrical machine **100** may include a stator **102**, a rotor **104**, and a plurality of windings **114**. In the illustrative embodiment, electrical machine **100** is a three-phase machine that can be configured as a generator or as a motor as understood by a person of skill in the art. In alternative embodiments, electrical machine **100** can be configured to support a fewer or a greater number of phases.

Use of directional terms, such as top, bottom, right, left, front, back, upper, lower, horizontal, vertical, behind, etc. are merely intended to facilitate reference to the various surfaces of the described structures relative to the orientations shown in the drawings and are not intended to be limiting in any manner unless otherwise indicated.

Electrical machine **100** may be used in various orientations. A shaft **106** may be mounted to extend parallel to a z-axis (shown referring to FIGS. **3** and **5**) that is perpendicular to an x-axis and a y-axis (shown referring to FIGS. **2**, **3**, **4**, and **5**). The x-axis and the y-axis are perpendicular to each other so that the x-axis, y-axis, and z-axis form an orthonormal coordinate system. The z-axis defines an axial direction that extends through a center of rotor **104**. In the illustrative embodiment of FIG. **1**, rotor **104** is mounted radially within stator **102**, and rotor **104** is mounted to shaft **106** for rotation. Rotor **104** is separated from stator **102** by an air gap **120**. In an alternative embodiment, stator **102** may be mounted radially within rotor **104**, and shaft **106** may or may not extend through a center of electrical machine **100**.

As used in this disclosure, the term "mount" includes join, unite, connect, couple, associate, insert, hang, hold, affix, attach, fasten, bind, paste, secure, bolt, screw, rivet, pin, nail, clasp, clamp, cement, fuse, solder, weld, glue, form over, slide together, layer, and other like terms. The phrases "mounted on" and "mounted to" include any interior or

exterior portion of the element referenced. These phrases also encompass direct mounting (in which the referenced elements are in direct contact) and indirect mounting (in which the referenced elements are not in direct contact, but are mounted together via intermediate elements). Elements referenced as mounted to each other herein may further be integrally formed together, for example, using a molding process as understood by a person of skill in the art. As a result, elements described herein as being mounted to each other need not be discrete structural elements. The elements may be mounted permanently, removably, or releasably.

Stator **102** may include a stator core **108**, a plurality of teeth **110**, and a plurality of magnets **112** that form a plurality of stator poles. Stator **102** has a generally circular cross section with a hollow core sized to accommodate shaft **106** and rotor **104**. Stator core **108** and the plurality of teeth **110** may be formed of a ferromagnetic material such as lamination steel, iron, cobalt, nickel, etc. Stator core **108** and the plurality of teeth **110** may be formed of laminations stacked in the axial direction. The laminations may be punched or laser cut. In the illustrative embodiment, the number of stator slots or stator poles of stator **102** is P_s=12 though stator **102** may include a fewer or a greater number of stator poles.

Rotor **104** has a generally circular cross section with a hollow core sized to accommodate shaft **106**. Rotor **104** may include a rotor core **116** and a plurality of blades **118** that form a plurality of rotor poles. The number of rotor poles may depend on the number of phases supported by electrical machine **100**. In the illustrative embodiment, the number of rotor blades or rotor poles of rotor **104** is P_r=10 though rotor **104** may include a fewer or a greater number of rotor poles. Rotor core **116** and the plurality of blades **118** may be formed of a ferromagnetic material such as lamination steel, iron, cobalt, nickel, etc. Rotor core **116** and the plurality of blades **118** may be formed of laminations stacked in the axial direction that is parallel to the z-axis. The laminations may be punched or laser cut.

Rotor **104** may control rotation of shaft **106** when electrical machine **100** is acting as a motor, and shaft **106** may control rotation of rotor **104** when electrical machine **100** is acting as a generator. Electrical machine **100** may be configured to act as both a generator and a motor or as only a generator or as only a motor.

The excitation frequency, f_e, of an FSPM machine is proportional to the number of rotor poles (p_r) as

$$f_e = \frac{np_r}{60},$$

where n is a rotational speed, for example, in revolutions per minute (RPM). A typical FSPM machine has P_s=12 and P_r=10 though a minimum number of stator slots is six for a three-phase machine because the number of stator slots is an even number and a multiple of the number of phases. The number of rotor poles can be 4, 5, 7, 8, etc. though not all of these combinations may be suitable for practical use.

Referring to FIG. **2**, a front view of electrical machine **100** is shown in accordance with an illustrative embodiment. Stator core **108** and the plurality of teeth **110** form a plurality of slots in which the plurality of windings **114** are wound. A winding of the plurality of windings **114** is wound over at least one magnet of the plurality of magnets **112** and through at least two slots of the plurality of slots. For example, in the illustrative embodiment of FIG. **2**, a first winding **114***a* is wound over a first magnet **112***a* and defines a first phase "A" winding. A second winding **114***b* is wound over a second magnet **112***b* and defines a second phase "A" winding. A third winding **114***c* is wound over a third magnet **112***c* and defines a third phase "A" winding. A fourth winding **114***d* is wound over a fourth magnet **112***d* and defines a fourth phase "A" winding. First winding **114***a* and second winding **114***b* may be connected in series. Third winding **114***c* and fourth winding **114***d* may be connected in series. First winding **114***a*, second winding **114***b*, third winding **114***c*, and fourth winding **114***d* may be connected in series in various orders. Similarly, the remaining windings are wound over the remaining magnets to form four phase "B" windings and four phase "C" windings. Each of the plurality of windings **114** may form a concentrated coil. Each winding of the plurality of windings **114** conducts a current in a positive or a negative direction.

The plurality of magnets **112** are permanent magnets formed of non-rare or rare earth elements such as ferrite, samarium-cobalt, neodymium-iron-boron, etc. The plurality of magnets **112** may be cast, sintered, molded, etc. Each magnet of the plurality of magnets **112** is magnetized to form a south (S) pole on a first side and a north (N) pole on a second side opposite the first side, wherein the magnetization direction is in a circumferential direction from the first side to the second side of the magnet relative to the generally circular cross section of stator **102**. The plurality of magnets **112** are mounted with N poles adjacent N poles and S poles adjacent S poles to form pole pairs. The pole pairs are formed at a regular pitch circumferentially around stator **102**. In the illustrative embodiment, the block arrows point from the north polarity to the south polarity.

Referring to FIG. **3**, a perspective view of stator **102** of electrical machine **100** is shown in accordance with an illustrative embodiment. Stator **102** has a hollow cylindrical shape with an aperture through a center of the cylinder. Stator core **108** and the plurality of teeth **110** may form a plurality of core pieces. In the illustrative three-phase embodiment, the plurality of core pieces includes four core pieces for each phase such that the plurality of core pieces includes a first core piece **108***a*, a second core piece **108***b*, a third core piece **108***c*, a fourth core piece **108***d*, a fifth core piece **108***e*, a sixth core piece **108***f*, a seventh core piece **108***g*, an eighth core piece **108***h*, a ninth core piece **108***i*, a tenth core piece **108***j*, an eleventh core piece **108***k*, and a twelfth core piece **108***l*. In the illustrative embodiment, each core piece of the plurality of core pieces has the same size and shape. In the illustrative embodiment, each core piece has a "C"-shape distributed circumferentially at a regular pitch around the z-axis and open towards rotor **104**. For example, third core piece **108***c* has a first tooth **300***c*, a second tooth **302***c*, and a core section **304***c*, and fourth core piece **108***d* has a first tooth **300***d*, a second tooth **302***d*, and a core section **304***d*. First tooth **300***c* and second tooth **302***c* extend from core section **304***c* to form a C-shaped face that opens towards the z-axis and rotor **104**. First tooth **300***d* and second tooth **302***d* extend from core section **304***d* to form a C-shaped face that opens towards the z-axis and rotor **104**. The hollow of the C-shape of each core piece defines a stator slot within which the plurality of windings **114** is wound. The slots are distributed at equal angles around a circumference of stator **102**.

In the illustrative embodiment of FIG. **3**, the plurality of magnets **112** are mounted between the teeth of adjacent core pieces. For example, a third magnet **112***c* fits in a slot formed between a first tooth **300***c* of third core piece **108***c* and second tooth **302***d* of fourth core piece **108***d*. The remaining magnets are similarly mounted and distributed circumfer-

entially around stator core **108**. For example, a first magnet **112***a* fits in a slot formed between first core piece **108***a* and second core piece **108***b*, a second magnet **112***b* fits in a slot formed between second core piece **108***b* and third core piece **108***c*; a fourth magnet **112***d* fits in a slot formed between fourth core piece **108***d* and fifth core piece **108***e*; a fifth magnet **112***e* fits in a slot formed between fifth core piece **108***e* and sixth core piece **108***f*; a sixth magnet **112***f* fits in a slot formed between sixth core piece **108***f* and seventh core piece **108***g*, a seventh magnet **112***g* fits in a slot formed between seventh core piece **108***g* and eighth core piece **108***h*; an eighth magnet **112***h* fits in a slot formed between eighth core piece **108***h* and ninth core piece **108***i*; a ninth magnet **112***i* fits in a slot formed between ninth core piece **108***i* and tenth core piece **108***j*; a tenth magnet **112***j* fits in a slot formed between tenth core piece **108***j* and eleventh core piece **108***k*; an eleventh magnet **112***k* fits in a slot formed between eleventh core piece **108***k* and twelfth core piece **108***l*; and a twelfth magnet **112***l* fits in a slot formed between twelfth core piece **108***l* and first core piece **108***a*.

In the illustrative embodiment, each magnet of the plurality of magnets **112** has the same size and shape. For example, each magnet of the plurality of magnets **112** has a rectangular shape in the x-y-plane though each magnet of the plurality of magnets **112** may have a truncated wedge shape or other polygonal and/or elliptical shape in the x-y-plane in alternative embodiments. The plurality of core pieces and the plurality of magnets **112** form the circular cross section of stator **102** in the x-y-plane with the z-axis extending axially through a center of the circular cross section of stator **102**.

Each magnet of the plurality of magnets **112** is curved in the x-y-plane in the direction of the z-axis to axially align the plurality of magnets **112** with an axially extending edge or face of a blade of the plurality of blades **118**. Being curved in the x-y-plane in the direction of the z-axis means that a location of each magnet of the plurality of magnets **112**, such as third magnet **112***c*, is at a different (x,y) coordinate value at each location along the z-axis. The (x,y) coordinate variation follows a continuous curve with a non-zero curvature value (not a straight line) between a front face of stator **102** and a back face of stator **102**. The continuous curve may be monotonic.

A stator pole width may or may not have the same value in the axial direction, i.e. the width may change, for example, as a trade-off between manufacturability and torque production. Each magnet of the plurality of magnets **112** and each core piece may be segmented in the axial direction such that the segmentation follows the curvature line.

Referring to FIG. **4**, a perspective view of rotor **104** is shown in accordance with an illustrative embodiment. Rotor core **116** has a hollow cylindrical shape with an aperture through a center of the cylinder. Rotor core **116** may include a rotor front face **400**, a rotor back face (not shown), a rotor interior surface **1008** (shown with reference to FIG. **10**), and a rotor exterior face **402**. Rotor exterior face **402** and rotor interior surface **1008** extend between rotor front face **400** and the rotor back face. Rotor front face **400** and the rotor back face are in the x-y-plane. Rotor interior surface **1008** and rotor exterior face **402** extend parallel to the z-axis or in the axial direction. Shaft **106** mounts to rotor interior surface **1008**. The plurality of blades **118** extend from rotor exterior face **402**. Of course, if stator **102** is mounted interior of rotor **104** instead of exterior as in the illustrative embodiment, the plurality of blades **118** would extend from rotor interior surface **1008**. The plurality of blades **118** extend from rotor exterior face **402** at a regular pitch circumferentially around rotor core **116**.

The plurality of blades **118** includes a first blade **118***a*, a second blade **118***b*, a third blade **118***c*, a fourth blade **118***d*, a fifth blade **118***e*, a sixth blade **118***f*, a seventh blade **118***g*, an eighth blade **118***h*, a ninth blade **118***i*, and a tenth blade **118***j* that each has the same size and shape. In alternative embodiments, the plurality of blades **118** may have a different size or shape. For example, sixth blade **118***f* includes a front face **404***f*, a back face (not shown), a first side face **406***f*, a second side face (not shown), and an exterior face **408***f*. First side face **406***f*, the second side face, and exterior face **408***f* extend between front face **404***f* and the back face. Front face **404***f* extends from rotor exterior face **402**, and the back face extends from the rotor back face. First side face **406***f* and the second side face extend from rotor exterior face **402**. Exterior face **408***f* extends between first side face **406***f* and the second side face and defines an axial edge of sixth blade **118***f*. In the illustrative embodiment of FIG. **4**, a rotor pole width of exterior face **408***f* changes in an axial direction with a curvature.

Air gap **120** is defined between exterior face **408***f* of sixth blade **118***f* and inner edges of each tooth of stator **102**. Air gap **120** is similarly defined between an exterior face **408** of each of first blade **118***a*, second blade **118***b*, third blade **118***c*, fourth blade **118***d*, fifth blade **118***e*, seventh blade **118***g*, eighth blade **118***h*, ninth blade **118***i*, and tenth blade **118***j* and the inner edges of each tooth of stator **102**.

Each blade of the plurality of blades **118** is shaped, sized, and/or positioned to carry a magnetic flux of electrical machine **100**. Each blade of the plurality of blades **118** is simultaneously shaped, sized, and/or positioned to act as an airfoil that compresses a gas when rotor **104** is rotated. Rotor **104** may be used as part of a gas compressor stage. The gas flows axially between successive blades of the plurality of blades **118**.

Referring to FIG. **5**, a perspective view of a second rotor **104***a* of electrical machine **100** is shown in accordance with an illustrative embodiment. Rotor core **116** has a hollow cylindrical shape with an aperture through a center of the cylinder. Rotor core **116** may include a rotor front face **400**, a rotor back face (not shown), and rotor interior surface **1008**. The plurality of blades **118** include a first airfoil blade **118***a*', a second airfoil blade **118***b*', a third airfoil blade **118***c*', a fourth airfoil blade **118***d*', a fifth airfoil blade **118***e*', a sixth airfoil blade **118***f*', a seventh airfoil blade **118**g', an eighth airfoil blade **118***h*', a ninth airfoil blade **118***i*', and a tenth airfoil blade **118***j*' that each has the same size and shape. First airfoil blade **118***a*', second airfoil blade **118***b*', third airfoil blade **118***c*', fourth airfoil blade **118***d*', fifth airfoil blade **118***e*', sixth airfoil blade **118***f*', seventh airfoil blade **118***g*', eighth airfoil blade **118***h*', ninth airfoil blade **118***i*', and tenth airfoil blade **118***j*' form fan-like airfoils to progressively compress the gas that flows between successive blades of the plurality of blades **118**.

The plurality of blades **118** are designed such that there is simultaneous energy conversion in both the electromagnetic domain and the fluid dynamic domain. The electromagnetic part of the blade design creates efficient energy conversion between electric energy supplied/generated by currents applied to the plurality of windings **114** and mechanical energy generated/supplied by rotating shaft **106**. The fluid dynamic design converts the kinetic energy from rotation of rotor **104** directly into a pressure rise in the gas that flows between successive blades of the plurality of blades **118**. The synergized design approach uses electrical machine sizing

equations and fluid dynamic equations to determine the power converted in each domain. The output power from electric energy is calculated based on the electrical machine sizing equation below:

$$P_{out} = \frac{\sqrt{2}}{2}\pi^3 K_{av} K_t K_{curve} \eta \left(\frac{f_e}{p_s}\right) B_{g,pk} A_{s,rms} D_{is}^2 L_e, \quad (1)$$

where K_{av} is a coefficient to scale peak flux density to average flux density, K_t is a stator tooth ratio number, K_{curve} is a curve factor, η is an efficiency value, $B_{g,pk}$ is a peak airgap flux density, $A_{s,rms}$ is an electric loading measured based on a root mean square (rms) current, D_{is} is an inner diameter of stator **102**, and L_e is an effective length of electrical machine **100**. A preliminary geometry of electrical machine **100** may be determined by choosing appropriate values of the key parameters, such as a diameter and a length of electrical machine **100**, $A_{s,rms}$, and $B_{g,pk}$, once a power and a speed rating are provided for electrical machine **100**. $B_{g,pk}$ may be limited by the saturation of steel, and $A_{s,rms}$ may be limited by the cooling of electrical machine **100**.

The plurality of blades **118** are shaped with a specific curvature with a specific input (angle of attack) and output angle. Referring to FIG. **6**, a rotor blade shape (curvature) and nomenclature is shown for rotor **104** or second rotor **104***a* of electrical machine **100** in accordance with an illustrative embodiment. For illustration, first blade **118***a* or first airfoil blade **118***a*' of the plurality of blades **118** is curved with an inlet attacking angle **600**, a chord length **602** of a chord line **603**, a turn angle **604**, an outlet attacking angle **606**, and a stagger angle **608**. Stagger angle **608** is an angle between chord line **603** and the z-axis (axial direction). Turn angle **604** of first blade **118***a* or first airfoil blade **118***a*' redirects an inlet flow velocity vector **610** to an outlet flow velocity vector **612**. Inlet flow velocity vector **610** is an inlet flow velocity of the gas with respect to first blade **118***a* or first airfoil blade **118***a*'. Outlet flow velocity vector **612** is an outlet flow velocity of the gas with respect to first blade **118***a* or first airfoil blade **118***a*'. A blade pitch **614** is a distance between a center of successive blades of the plurality of blades **118**. A rotation direction **616** defines a direction of rotation of the plurality of blades **118** resulting in a pressure side **618** and a suction side **620** for each blade of the plurality of blades **118**.

Referring to FIG. **7**, a velocity diagram of a gas flow through rotor **104** or second rotor **104***a* of electrical machine **100** is shown in accordance with an illustrative embodiment. A gas flow velocity vector **700** flowing into first blade **118***a* or first airfoil blade **118***a*' is assumed to have only an axial component. A blade speed vector **702** defines a blade speed at a middle blade diameter of each blade of the plurality of blades **118**. A gas flow outlet velocity vector **704** is an actual velocity of the gas exiting rotor **104** or second rotor **104***a*. It may be assumed that the axial gas flow velocity vector **700** remains constant. The torque, T_{shaft}, required in shaft **106** to compress the gas is proportional to a difference between tangential blade velocity and mass flow rate as shown below

$$T_{shaft} = r(V_{1.5} - V_1)_m \quad (2)$$

where m is the mass flow rate, r is a mean radius of first blade **118***a* or first airfoil blade **118***a*', and V_1 is the tangential component of gas flow velocity vector **700**, which is the tangential velocity of the mean blade for the rotor inlet, and $V_{1.5}$ is the tangential component of gas flow outlet velocity vector **704**, which is the tangential velocity of the mean blade for the rotor outlet.

Referring to FIG. **8**, a combined velocity triangle showing the tangential component of velocity increase is shown for rotor **104** or second rotor **104***a* of electrical machine **100** in accordance with an illustrative embodiment. A delta vector **800** completes the velocity triangle between gas flow velocity vector **700** and gas flow outlet velocity vector **704**. A magnitude **802** of delta vector **800** indicates a net increase of rotor tangential velocity provided by first blade **118***a* or first airfoil blade **118***a*'. Blade speed vector **702** has a blade speed magnitude **804**. The outlet gas also has a higher stagnation temperature as compared to an inlet stagnation temperature.

Referring to FIG. **9**, a required power for rotor compression work is shown as a function of mean blade diameter for first blade **118***a* or first airfoil blade **118***a*' in accordance with an illustrative embodiment.

Referring to FIG. **10**, an exploded perspective view of a second electrical machine **100***a* is shown in accordance with an illustrative embodiment. Second electrical machine **100***a* includes stator **102** and second rotor **104***a*. A diffuser **1000** is mounted to second electrical machine **100***a* to receive the gas compressed by the plurality of blades **118**. Diffuser **1000** is a stationary diffuser that reduces the speed of the gas and increases the pressure on the gas to further compress the gas.

Diffuser **1000** may include an outer core **1002**, an inner core **1004**, and a plurality of diffuser blades **1006**. For example, diffuser **1000** may include a first stator blade **1006***a*, a second stator blade **1006***b*, a third stator blade **1006***c*, etc. The plurality of diffuser blades **1006** are mounted between outer core **1002** and inner core **1004** to receive the gas output from second rotor **104***a* (or rotor **104**), to reduces the speed of the gas, to further increase the pressure on the gas, and to output the further compressed gas. The gas from the output of the diffuser can be guided to another stage of compression such as another axial or centrifugal compressor.

Referring again to FIG. **8**, the kinetic energy of the gas is converted into static pressure in diffuser **1000** where an outlet velocity **706** (shown referring to FIG. **7**) of the gas from diffuser **1000** is slowed down while the pressure is increased. To evaluate how much the pressure is increased by second rotor **104***a* and diffuser **1000**, a pressure ratio is calculated as

$$\frac{p_{o1.5}}{p_{o1}} = \left(\frac{T_{o1.5}}{T_{o1}}\right)^{k/(k-1)} \quad (3)$$

where $P_{o1.5}$ is a total diffuser outlet pressure, p_{o1} is a total rotor inlet pressure, T_{o1} is a total rotor inlet temperature of the gas, $T_{o1.5}$ is a total diffuser outlet temperature of the gas, and k is a ratio of specific heat. The two temperatures can be calculated as

$$T_{o1} = T_1 + \frac{V_1^2}{2c_p} \quad (4)$$

$$T_{o1.5} = T_{o2} = T_{o1} - \frac{1w_2}{2c_p} \quad (5)$$

where c_p is a constant pressure specific heat of the gas, T_1 is an inlet gas temperature, $1w_2$ is a work per unit mass done

by rotor **104** and diffuser **1000** from an inlet to second rotor **104***a* to an outlet from diffuser **1000**.

Referring to FIG. **11**, an exploded perspective view of a third electrical machine **100***b* is shown in accordance with an illustrative embodiment. In the illustrative embodiment of FIG. **11**, third electrical machine **100***b* is a doubly salient permanent magnet machine. Third electrical machine **100***b* may include a second stator **102***a*, second rotor **104***a* (or rotor **104**), and the plurality of windings **114**. In the illustrative embodiment, third electrical machine **100***b* is a three-phase machine that can be configured as a generator or as a motor as understood by a person of skill in the art. Diffuser **1000** is mounted to third electrical machine **100***b* to receive the gas compressed by the plurality of blades **118**.

Second stator **102***a* may include stator core **108**, the plurality of teeth **110**, and the plurality of magnets **112** that form a plurality of stator poles. Second stator **102***a* has a generally circular cross section with a hollow core sized to accommodate shaft **106** and second rotor **104***a* (or rotor **104**). The plurality of teeth **110** may have a different size and shape and number as compared to stator **102** as understood by a person of skill in the art. Unlike the plurality of magnets **112** of stator **102**, the plurality of magnets **112** of second stator **102***a* are mounted to extend in a radial direction through stator core **108** in axial alignment with a slot of the plurality of slots instead of through the plurality of teeth **110**. There also may be fewer or a greater number of magnets for the plurality of magnets **112** of second stator **102***a*. The plurality of windings **114** further may be wound through the plurality of slots of second stator **102***a* in a different manner than the plurality of windings **114** are wound through the plurality of slots of stator **102** as understood by a person of skill in the art.

Referring to FIG. **12**, an exploded perspective view of a fourth electrical machine **100***c* is shown in accordance with an illustrative embodiment. In the illustrative embodiment of FIG. **12**, fourth electrical machine **100***c* is a flux reversal permanent magnet machine. Fourth electrical machine **100***c* may include a third stator **102***b*, second rotor **104***a* (or rotor **104**), and the plurality of windings **114**. In the illustrative embodiment, fourth electrical machine **100***c* is a three-phase machine that can be configured as a generator or as a motor as understood by a person of skill in the art. Diffuser **1000** is mounted to fourth electrical machine **100***c* to receive the gas compressed by the plurality of blades **118**.

Third stator **102***b* may include stator core **108**, the plurality of teeth **110**, and the plurality of magnets **112** that form a plurality of stator poles. Third stator **102***b* has a generally circular cross section with a hollow core sized to accommodate shaft **106** and second rotor **104***a* (or rotor **104**). The plurality of teeth **110** may have a different size and shape and number as compared to stator **102** as understood by a person of skill in the art. Unlike the plurality of magnets **112** of stator **102**, the plurality of magnets **112** of second stator **102***a* are mounted to an exterior face of each tooth of the plurality of teeth **110** instead of through the plurality of teeth **110**. The exterior face of each tooth of the plurality of teeth **110** faces second rotor **104***a* (or rotor **104**). Air gap **120** separates the plurality of blades **118** from each magnet of the plurality of magnets **112**. There also may be fewer or a greater number of magnets for the plurality of magnets **112** of third stator **102***b*. The plurality of windings **114** further may be wound through the plurality of slots of third stator **102***b* in a different manner than the plurality of windings **114** are wound through the plurality of slots of stator **102** as understood by a person of skill in the art.

Referring to FIG. **13**, an exploded perspective view of a fifth electrical machine **100***d* is shown in accordance with an illustrative embodiment. In the illustrative embodiment of FIG. **13**, fifth electrical machine **100***d* is a switched reluctance machine. Fifth electrical machine **100***d* may include a fourth stator **102***c*, second rotor **104***a* (or rotor **104**), and the plurality of windings **114**. In the illustrative embodiment, fifth electrical machine **100***d* is a three-phase machine that can be configured as a generator or as a motor as understood by a person of skill in the art. Diffuser **1000** is mounted to fifth electrical machine **100***c* to receive the gas compressed by the plurality of blades **118**.

Fourth stator **102***c* may include stator core **108** and the plurality of teeth **110** that form a plurality of stator poles. Fourth stator **102***c* has a generally circular cross section with a hollow core sized to accommodate shaft **106** and second rotor **104***a* (or rotor **104**). The plurality of teeth **110** may have a different size and shape and number as compared to stator **102** as understood by a person of skill in the art. The plurality of windings **114** further may be wound through the plurality of slots of fourth stator **102***c* in a different manner than the plurality of windings **114** are wound through the plurality of slots of stator **102** as understood by a person of skill in the art.

Referring to FIG. **14**, a perspective view of second electrical machine **100***a* and diffuser **1000** is shown with a connection to a multi-stage compressor **1400** in accordance with an illustrative embodiment. Diffuser **1000** may not be included in an alternative embodiment. Multi-stage compressor **1400** is mounted to receive compressed gas from diffuser **1000**. Arrays of airfoils of multi-stage compressor **1400** may be set in rows, usually as pairs. For example, in each pair of compressors, one compressor of the pair may be rotating and the other compressor of the pair may be stationary. In the illustrative embodiment of FIG. **14**, multi-stage compressor **1400** includes a first rotating compressor **1402** paired with a first stationary compressor **1404**, a second rotating compressor **1406** paired with a second stationary compressor **1408**, and a third rotating compressor **1410** paired with a third stationary compressor **1412**. Multi-stage compressor **1400** may include a fewer or a greater number of arrays of airfoils.

The rotating airfoils or rotor blades of first rotating compressor **1402**, second rotating compressor **1406**, and third rotating compressor **1410** accelerate the gas received from a previous stage such as diffuser **1000**, first stationary compressor **1404**, and second stationary compressor **1408**, respectively. The stationary airfoils, also known as stators or vanes, of first stationary compressor **1404**, second stationary compressor **1408**, and third stationary compressor **1412** decelerate and redirect the flow direction of the gas, preparing it for the rotor blades of the next stage such as second rotating compressor **1406** and third rotating compressor **1410**. A cross-sectional area of a gas passage may diminish along multi-stage compressor **1400** to maintain an optimum axial Mach number. Beyond about five stages or a 4:1 design pressure ratio, a variable geometry may be used to further improve a compression of the gas.

The design for multi-stage compressor **1400** follows the same rules as outlined above for rotor **104** and second rotor **104***a* such that if the mean blade diameter stays constant, the power required for each successive stage is the same as the first stage assuming turn angle **604** and inlet flow velocity vector **610** remain the same. The pressure rise ratio normally decreases slightly for the later stages while the temperature

increases from stage to stage. If the blade mean diameter is allowed to change, the required power at each stage is calculated as:

$$P_{stage} = mr\omega\left[r\omega - V_1\tan\left(\arctan\left(\frac{d\omega}{2V_1}\right) - \theta\right)\right] \quad (6)$$

where θ is turn angle **604**, and ω is an angular speed of rotor **104**. The required power at a second stage as a function of rotor mean blade diameter is shown in FIG. **9**.

Referring to FIG. **15**, a perspective view of second electrical machine **100***a*, diffuser **1000**, a second instance **100***a***1** of second electrical machine **100***a*, and a second diffuser **1500** is shown with a connection to a second multi-stage compressor **1502** in accordance with an illustrative embodiment. Diffuser **1000** is mounted to receive compressed gas from second electrical machine **100***a*. Second instance **100***a***1** of second electrical machine **100***a* is mounted to receive compressed gas from diffuser **1000**. Second diffuser **1500** is mounted to receive compressed gas from second instance **100***a***1** of second electrical machine **100***a*. Second multi-stage compressor **1502** is mounted to receive compressed gas from second diffuser **1500**. In the illustrative embodiment of FIG. **15**, second multi-stage compressor **1502** includes first rotating compressor **1402** paired with first stationary compressor **1404** and second rotating compressor **1406** paired with a second stationary compressor **1408**. Second multi-stage compressor **1502** may include a fewer or a greater number of arrays of airfoils. Diffuser **1000** and/or second diffuser **1500** may not be included in alternative embodiments. A greater number of electrical machines **100** of the same or different type may be included in alternative embodiments.

The various dimensions of the elements of the electrical machines described herein may be determined based on desired rated performance characteristics using analytical sizing equations and finite element analysis using an electromechanical design tool. For example, referring to FIG. **16**, a back-electromotive force (back-EMF) generated by electrical machine **100** as a function of a rotor position is shown in accordance with an illustrative embodiment. Referring to FIG. **17**, a cogging torque generated by electrical machine **100** is shown in accordance with an illustrative embodiment. Referring to FIG. **18**, a torque generated by electrical machine **100** as a function of the rotor position is shown in accordance with an illustrative embodiment. The cogging torque, the back-EMF, and the torque were determined using finite element analysis and the parameter values listed in Table 1 below.

TABLE 1

Parameters	Values
Electrical machine power, P_{out} [kW]	40
Rotor speed n [krpm]	15
Hub diameter D_{hub} [mm]	103.2
Blade tip diameter D_{tip} [mm]	136.4
Stator curve slot pitch	1
Blade turn angle, θ [deg.]	30
Axial air velocity, V_1 [m/s]	170
Specific gas constant, $R_{specific}$ [J/(kg*K)]	287.1
Air pressure p_{o1} [kPa]	101.3
Air temperature, T_1 [K]	300
Mass rate of flow, ṁ [kg/s]	1.249
Torque required, T [Nm]	7.524
Power required, P [kW]	11.82
Inlet stagnation temperature, T_{o1} [K]	314.4
Rotor outlet stagnation temperature, $T_{o1.5}$ [K]	323.8
Ideal pressure rise	10.88%

Hub diameter D_{hub} is a diameter **500** (shown referring to FIG. **5**) of a yoke of rotor **104**. Blade tip diameter D_{tip} is an outer diameter **502** (shown referring to FIG. **5**) of rotor **104**. Axial air flux velocity V_1 is a magnitude of gas flow velocity vector **700** at an input to diffuser **1000**. Air pressure p_{o1} is a pressure at an inlet of diffuser **1000**. Air temperature T_1 is an input air temperature. Torque required, T, and power required, P, is a torque and a power, respectively, required to compress the gas. Ideal pressure rise is a percentage pressure increase at an output with respect to an inlet pressure. The airflow compression pressure rise of rotor **104** was calculated as 10.88%, which is in a typical range of 5% to 20% for a single stage compression using subsonic tip speed blades. The power required to compress the air is calculated to be 11.82 kW, so the remaining power supplied by the electrical machine can be used for additional rotating compressor stages. The proposed machine has a sinusoidal back-EMF and a small cogging torque, which is beneficial to improving efficiency.

To further refine the parameters of the electrical machines describe herein including a determination of an optimum curve angle for stator **102** and rotor **104** as well as the airfoil shape of the plurality of blades to achieve maximum pressure ratios without sacrificing the electromagnetic performance, multi-physics simulations that integrate the analysis of electromagnetic, thermal, and fluid dynamic aspects are performed for various operating stages using advanced co-simulation and analysis tools.

A flowchart for the multi-physics design is provided in FIG. **19**. In an operation, input parameters are defined. For example, in an operation **1900**, initial dimensions of electrical machine **100** design requirements are defined for electrical machine **100** in terms of axial air flow, electromagnetic torque, structure, and thermal properties.

In an operation **1902**, a computational fluid dynamics simulation of the defined electrical machine **100** is executed to determine axial airflow. In an operation **1904**, the determined axial air flow is verified against the design requirements. At this stage, fluid dynamic properties of the designed machine are validated.

In an operation **1906**, a finite element analysis simulation of the defined electrical machine **100** is executed to determine a torque production. In an operation **1908**, the determined torque production is verified against the design requirements. At this stage, the electromagnetic properties of the designed machine are validated.

In an operation **1910**, a determination is made concerning both fluid dynamics and electromagnetics to validate whether or not the determined axial air flow, compression ratio, and the determined torque production satisfy the design requirements. If the determined axial air flow, compression ratio, and the determined torque production satisfy the design requirements, processing continues in an operation **1914**. If the determined axial air flow, compression ratio, and the determined torque production do not satisfy the design requirements, processing continues in an operation **1912**.

In operation **1912**, dimensions of the plurality of blades **118** that form the plurality of rotor poles are modified, and processing continues in operation **1902** with the modified

dimensions. The curvature along with input (angle of attack) angle and output angle of the plurality of blades **118** are modified. The plurality of stator poles are also modified to have the average trajectory of the rotor curvature.

In operation **1914**, structural and thermal simulation of the defined electrical machine **100** is executed to determine that the structure of the machine meets various mechanical requirements such as vibration, stress, and reliability. Similarly, thermal design of electrical machine **100** should be such that the machine receives adequate cooling, and the materials used in the machine do not exceed its temperature rating.

In an operation **1916**, a determination is made concerning whether or not the determined torque, air flow, compression, thermal, vibration, stress, and reliability measures satisfy the design requirements. If the determined measures satisfy the design requirements, processing continues in an operation **1918**. If the determined measures do not satisfy the design requirements, processing continues in operation **1912**.

In operation **1918**, the design parameters for electrical machine **100** that satisfy the design requirements are output, for example, to a computer-readable medium or a computer display.

In conventional compressors, a drive motor is mounted separately from a compressor assembly often with additional gears or outlet casing since the motor is mounted so that the axial flow of the gas is not compromised. The drive motor along with its independent cooling mechanism adds additional losses in addition to weight and volume. The electrical machines described herein provide a reduced volume and utilize the pressure and temperature difference.

By incorporating electrical machine **100**, **100***a*, **100***b*, **100***c*, **100***d* at a low-pressure stage of a compressor, a natural cooling mechanism is provided for electrical machine **100**, **100***a*, **100***b*, **100***c*, **100***d* keeping the internal temperature and losses at a minimum. Because axial-flow compression is particularly advantageous for higher pressure ratios, multiple stages of compression can be achieved by cascading electrical machine **100**, **100***a*, **100***b*, **100***c*, **100***d* with one or more diffuser **1000**. To further increase a discharge pressure, an axial flow compressor can be combined with a radial flow stage at the axial stage outlet.

Referring to FIG. **20**, a perspective view is shown of electrical machine **100** with a second plurality of blades **118'** that have a different blade profile than those shown in FIG. **1** in accordance with an illustrative embodiment. Similar to FIGS. **6** and **7**, the blade nomenclature and related angles of the second plurality of blades **118'** are shown in FIGS. **21** and **22**. The second plurality of blades **118'** includes a first blade **1181***a*, a second blade **1181***b*, a third blade **1181***c*, etc. that each have the same size and shape. The thermodynamic performance can be evaluated using analytical calculations based on vector diagrams as well as three-dimensional (3-D) computational fluid dynamics (CFD) simulation. The velocity triangle shown in FIG. **22** is used to calculate a flow inlet velocity, a flow outlet velocity, and a total pressure ratio of a rotor stage. The subscripts 1 and 1.5 refer to the inlet and outlet of the rotor stage, respectively. A power required for flow compression is given by $P_{comp}=\omega\dot{m}r(V_{u1.5}-V_{u1})$, where ω is a rotor rotational speed, in is a mass flow rate, r is a rotor mid-radius, and V_{u1}, $V_{u1.5}$ are tangential components of V_1 and $V_{1.5}$, respectively, in the velocity triangle shown in FIG. **22**, where V_1 is indicated by gas flow velocity vector **700**, $V_{1.5}$ is indicated by gas flow outlet velocity vector **704**, V_{u1} is indicated by blade speed vector **702**, and $V_{u1.5}$ is indicated by delta vector **800**. The pressure ratio from the inlet to the outlet of the rotor stage can be calculated using

$$\frac{P_{o1.5}}{P_{o1}}=\left(\frac{T_{o1.5}}{T_{o1}}\right)^{\frac{k}{k-1}},$$

where P_o is a stagnation pressure in Pascals (Pa), T_o is a stagnation temperature in Kelvin (K), and k is the specific heat ratio of air. The stagnation temperature at the inlet is computed using

$$T_{o1}=T_1+\frac{V_1^2}{2c_p},$$

and the stagnation temperature at the outlet is computed using

$$T_{o1}=T_2=T_{o1}-\frac{w_{12}}{c_p},$$

where T_1 is an inlet flow temperature, c_p is a constant-pressure specific heat of gas, and w_{12} is a work done to a flow from the blade which is computed using

$$w_{12}=\frac{P_{comp}}{\dot{m}}.$$

To achieve a symmetric back-EMF waveform, a balanced force on rotor **104**, and to limit the fundamental frequency, a 12/10 stator slot and rotor pole combination FSPM topology may be used. A sizing equation for torque calculation is determined using

$$T_{out}=\frac{\sqrt{2}}{4}\pi^2K_mK_tK_{curve}\eta\left(\frac{N_r}{N_s}\right)B_{g,pk}A_{s,rms}D_{is}^2L_e,$$

where K_m is a linkage flux factor, K_t is a stator tooth width ratio, K_{curve} is a curvature factor, η is a machine electrical efficiency, N_s and N_r are a number of stator slot and rotor poles, respectively, $B_{g,pk}$ is a peak airgap flux density in Tesla, $A_{s,rms}$ is an electric loading in A_{rms}/meter, D_{is} is a stator inner diameter in meters (m), and L_e is an effective length in meters. From the perspective of electrical machine **100**, stagger angle **608** is equivalent to skewing rotor **104**. Stator **102** and the plurality of magnets **112** may also be skewed to maximize torque production capability. A circumferential skew angle of stator **102**, α_s, may be computed using

$$\alpha_s=2\arcsin\left(\frac{0.5l_e\tan\gamma}{r}\right),$$

where l_e is a stator stack length and r is a stator inner radius. Ten segmentations may be applied to the plurality of magnets **112** to reduce magnet losses.

The design parameters and performance of electrical machine **100** with the second plurality of blades **118'** are listed in Table 2.

TABLE 2

Parameters and Performance	Value
Stator outer diameter [mm]	300
Stator stack length [mm]	30
Airgap length [mm]	1
Rotor tip diameter [mm]	200
Machine speed [rpm]	10,000
Fundamental frequency [Hz]	1666.7
Current density [A_{rms}/mm^2]	5
Winding turns per coil	5
Blade chord length [mm]	76
Stagger angle [deg]	38
Total pressure ratio calculated by velocity triangle	1.029
Compression power [kW]	2.66
Peak flux linkage [mWb]	10.2
Back-EMF [V_{rms}]	76.2
Average loaded torque [Nm]	28.7
Output power [kW]	30
Magnet loss [W]	359
Copper loss [W]	190
Stator iron loss [W]	356
Rotor iron loss [W]	150
Motor efficiency [%]	96.6

Referring to FIG. **23**, an air intake flow **2306** and an air outtake flow **2308** are shown entering and exiting a hub **2300** with the second plurality of blades **118'** mounted to rotor interior surface **1008** of rotor core **116** in accordance with an illustrative embodiment. Instead of extending radially outward from rotor core **116** of rotor **104**, the second plurality of blades **118'** extend radially outward from a hub exterior radial surface **2304** of hub **2300** and radially inward from rotor interior surface **1008** of rotor core **116**. As a result, the second plurality of blades **118'** are positioned between hub **2300** and rotor core **116**. Shaft **106** may mount to a hub interior radial surface **2302** of hub **2300**. The second plurality of blades **118'** are mounted to rotor core **116** so that rotor **104'** rotates with shaft **106** and hub **2300** when hub **2300** is mounted to shaft **106**. As shaft **106** rotates hub **2300** and rotor core **116**, the second plurality of blades **118'** produce airflow around hub **2300** by pulling air as indicated by air intake flow **2306** toward hub **2300** and expelling air as indicated by air outtake flow **2308**.

Adding hub **2300** does not change how the plurality of magnets **112** are mounted to rotor core **116**. For example, referring to FIG. **24**, a second plurality of magnets **2400** are mounted to an exterior surface of rotor core **116** in accordance with an illustrative embodiment. As another example, referring to FIG. **25**, a third plurality of magnets **2500** are mounted to interior apertures formed in rotor core **116** in accordance with an illustrative embodiment. A similar arrangement can be applied to induction machines and synchronous reluctance machines.

Rotor core **116** often rotates at high speed. When the plurality of blades **118** or the second plurality of blades **118'** that form the rotor poles are shaped into airfoils, or the second plurality of blades **118'** are mounted to hub **2300** and mounted within rotor core **116**, rotor core **116** can function as a fan that draws air from a front part of electrical machine **100** and pushes the air to a rear part of electrical machine **100**. In this process, an interior portion of the rotor iron, the second plurality of magnets **2400**, and the third plurality of magnets **2500** can be cooled. Since for many types of PM machines, the permanent magnets are located on rotor **104**, cooling the rotor iron also facilitates the cooling of the magnets. A number of blades and the airfoil shape can be adjusted to achieve an optimal cooling effect.

In addition to cooling the rotor iron, rotor core **116** also has the potential to facilitate end winding cooling as well as cooling the stator surface facing the end windings. When inlets and outlets are designed in a housing within which electrical machine **100** is mounted, the plurality of blades **118** or the second plurality of blades **118'** draw the ambient air into the housing and push the air out through the outlet. The position of inlets and outlets can be designed strategically so that the flow is forced past the end winding areas which need the most cooling. For example, when radial inlets are placed above the end windings, the air is pulled across the stator steel and around end windings as well as end winding surfaces (typically copper) before entering the rotor stage and cooling the inner part of the rotor surface.

For example, referring to FIG. **26**, a perspective view is shown of a housing **2600** in accordance with an illustrative embodiment. Housing **2600** may include a front wall **2602**, a radial sidewall **2604**, and a back wall **2606** that form an enclosure. Typically, front wall **2602** and back wall **2606** are circular in cross-section axially, and radial sidewall **2604** has a hollow circular shape though other shapes including elliptical and polygonal shapes may be used in alternative embodiments. Axial inlet aperture walls **2608** are formed in front wall **2602**. In the illustrative embodiment, the axial inlet aperture walls **2608** form arcs relative to a center of front wall **2602** that extend axially through front wall **2602**. Radial inlet aperture walls **2610** are formed in radial sidewall **2604** and also form arcs relative to a center of radial sidewall **2604** and extend circumferentially around radial sidewall **2604**. Axial outlet aperture walls **2612** are formed in back wall **2606**. In the illustrative embodiment, the axial outlet aperture walls **2612** form arcs relative to a center of back wall **2606** that extend axially through back wall **2606**. Air is pulled into the axial inlet aperture walls **2608** as indicated by a first air intake flow **2306-1** and a second air intake flow **2306-2** and into the radial inlet aperture walls **2610** as indicated by a third air intake flow **2306-3** toward hub **2300** and expelled as indicated by air outtake flow **2308**.

Referring to FIG. **27**, a perspective view is shown of housing **2600** with electrical machine **100** mounted therein in accordance with an illustrative embodiment. Referring to FIG. **28**A, a front view is shown of housing **2600** with electrical machine **100** mounted therein in accordance with an illustrative embodiment. Referring to FIG. **28**B, a side view is shown of housing **2600** with electrical machine **100** mounted therein in accordance with an illustrative embodiment. Referring to FIG. **29**, a side cross-sectional view is shown of the 3-D CFD model of housing **2600** with electrical machine **100** mounted therein in accordance with an illustrative embodiment.

Referring to FIG. **28**A, a radial angle **2800** defines an angle spanned by the axial inlet aperture walls **2608** that have a radial width **2802**. A radial separation angle **2804** separates adjacent axial inlet apertures. In alternative embodiments, the axial inlet aperture walls **2608** can have alternative shapes. A fewer or a greater number of axial inlet apertures may be formed by the axial inlet aperture walls **2608**. For example, in the illustrative embodiment, the axial inlet aperture walls **2608** define two axial apertures. Preferably, the axial inlet aperture walls **2608** are positioned in front of the plurality of blades **118** or the second plurality of blades **118'**. In an illustrative embodiment, the axial outlet aperture walls **2612** are sized, shaped, and positioned in and through back wall **2606** similar to the axial inlet aperture walls **2608** relative to front wall **2602** though this is not required.

Referring to FIG. **28**B, a radial arclength **2810** defines an arclength of each radial inlet aperture of the radial inlet aperture walls **2610**. An axial width **2812** defines a width of

each radial inlet aperture of the radial inlet aperture walls **2610** in the axial direction. A radial separation arclength **2814** separates adjacent radial inlet apertures. In alternative embodiments, the radial inlet aperture walls **2610** can have alternative shapes. A fewer or a greater number of radial inlet apertures may be formed by the radial inlet aperture walls **2610**. For example, in the illustrative embodiment, the radial inlet aperture walls **2610** define six radial apertures evenly distributed circumferentially around radial sidewall **2604**. Preferably, the radial inlet aperture walls **2610** are positioned above a front portion of the end windings of the plurality of windings **114**. Though not shown in the illustrative embodiment of housing **2600**, radial outlet aperture walls may be formed in radial sidewall **2604**.

Rotation of the plurality of blades **118** or the second plurality of blades **118'** draws ambient air from an exterior of housing **2600** into electrical machine **100** through the radial and/or axial inlets. Then, air passes over the front end winding and stator surface and is accelerated by the rotating blades towards the rotor stage. Finally, air exits housing **2600** through radial and/or axial outlets and cools the rear end winding and stator surface. In this process, self-cooling can be achieved from forced convection provided by the high-speed flow. It is desirable to have a small pressure drop associated with the air flow through housing **2600** so that the delivered pressure rise is close to the pressure rise produced at rotor **104**. The light shaded arrows show the air flow direction.

3-D CFD simulations were performed to evaluate the convective heat transfer coefficient at different surfaces for electrical machine **100**. To simplify the model and improve accuracy, the axial and radial inlets and the axial outlets were analyzed in separate models.

Referring to FIG. **30**, an inlet air flow velocity pattern is shown relative to housing **2600** with electrical machine **100** mounted therein in accordance with an illustrative embodiment. Referring to FIG. **31**, an outlet air flow velocity pattern is shown relative to housing **2600** with electrical machine **100** mounted therein in accordance with an illustrative embodiment. In FIG. **30**, it can be observed that the air drawn into the radial inlet aperture walls **2610** and the axial inlet aperture walls **2608** has a large velocity that passes over the end winding and stator surfaces. In the outlet model shown in FIG. **31**, the flow leaving the fan zone has a high velocity and directly exits housing **260** through the axial outlet aperture walls **2612**. In those regions without an adjacent outlet, airflow is blocked and flows to the region above the rear end winding and stator surface, cooling these surfaces.

The area, location, and the number of the axial inlet aperture walls **2608** and of the axial outlet aperture walls **2612** can be adjusted to guide flow direction and achieve a desired cooling effect. For example, referring to FIG. **32**, an illustrative housing includes two axial inlet apertures each with a radial angle **2800** of 150-degrees and six radial inlet apertures with a radial arclength **2810** of 20-degrees. Four inlet models were simulated. Each inlet model included the two axial inlet apertures each with a radial angle **2800** of 150-degrees. A first inlet model included the six radial inlet apertures with a radial arclength **2810** of 10-degrees. A second inlet model included the six radial inlet apertures with a radial arclength **2810** of 20-degrees. A third inlet model included the six radial inlet apertures with a radial arclength **2810** of 30-degrees. A fourth inlet model included the six radial inlet apertures with a radial arclength **2810** of 40-degrees.

Referring to FIG. **33**A, a side view of an inlet air flow velocity pattern using the first inlet model is shown in accordance with an illustrative embodiment. Referring to FIG. **33**B, a side view is shown of an inlet air flow velocity pattern using the second inlet model is shown in accordance with an illustrative embodiment. Referring to FIG. **33**C, a side view is shown of an inlet air flow velocity pattern using the third inlet model is shown in accordance with an illustrative embodiment. Referring to FIG. **33**D, a side view is shown of an inlet air flow velocity pattern using the fourth inlet model is shown in accordance with an illustrative embodiment.

It can be observed that the flow velocity above the end winding surface varies for different radial inlet areas. The heat transfer boundary conditions are calculated based on the CFD simulation using a heat transfer coefficient

$$h = \frac{q}{T_{wall} - T_{ref}},$$

where q is the heat flux on the surface, T_{wall} is the wall temperature, and T_{ref} is the bulk temperature of the surrounding fluid. The maximum wall temperature is used in the calculation of the heat transfer coefficient since the hot spot temperature is most crucial in the design, which results in a minimum heat transfer coefficient. The local bulk temperature is used as the reference temperature, which has a value close to the inlet flow temperature for most flow rates of interest.

The heat transfer coefficient associated with the four inlet models as a function of fan volume flow rate is shown in FIG. **34**. A first curve **3400** shows the heat transfer coefficient on the stator surface using the first inlet model. A second curve **3401** shows the heat transfer coefficient on the end windings using the first inlet model. A third curve **3402** shows the heat transfer coefficient on the stator surface using the second inlet model. A fourth curve **3403** shows the heat transfer coefficient on the end windings using the second inlet model. A fifth curve **3404** shows the heat transfer coefficient on the stator surface using the third inlet model. A sixth curve **3405** shows the heat transfer coefficient on the end windings using the third inlet model. A seventh curve **3406** shows the heat transfer coefficient on the stator surface using the fourth inlet model. An eighth curve **3407** shows the heat transfer coefficient on the end windings using the fourth inlet model.

The end winding surface has a larger heat transfer coefficient than the stator surface. The second inlet model has the largest end winding heat transfer coefficient; whereas, the fourth inlet model has the largest stator surface heat transfer coefficient. The same analysis can be conducted for different axial inlet areas. Through the combination of radial inlet and axial inlet areas, a desired heat transfer coefficient for the end winding and stator surfaces can be achieved.

A pressure drop was calculated based on a difference between a pressure at the housing inlet and the blade inlet. In the CFD simulation, the boundary condition at the housing inlet is set as the inlet pressure, and the fan zone inlet is set as a mass flow rate at the outlet. The mass flow rate is based on the inlet volume flow rate to the rotor which is varied. An inlet design **1** was based on the first inlet model; an inlet design **2** was based on the second inlet model; an inlet design **3** was based on the third inlet model; and an inlet design **4** included the six radial inlet apertures with a radial

arclength **2810** of 30-degrees and the two axial inlet apertures each with a radial angle **2800** of 130-degrees.

Referring to FIG. **35**A, a pressure drop comparison is shown at a front of housing **260** for each inlet design. A first curve **3500** shows the front housing pressure drop using inlet design **1**. A second curve **3501** shows the front housing pressure drop using inlet design **2**. A third curve **3502** shows the front housing pressure drop using inlet design **3**. A fourth curve **3503** shows the front housing pressure drop using inlet design **4**. It can be observed that inlet design **1** has the largest pressure drop and inlet design **3** has the smallest. For the same axial inlet area, the pressure drop in the housing decreases with an increase in the radial inlet area. Comparing the housing pressure drops associated with inlet design **3** and design **4**, the trend is the same for different axial inlet areas

Referring to FIG. **35**B, an end winding heat transfer coefficient comparison is shown in accordance with an illustrative embodiment. A first curve **3510** shows the heat transfer coefficient on the end winding surface using the inlet design **1**. A second curve **3511** shows the heat transfer coefficient on the end winding surface using the inlet design **2**. A third curve **3512** shows the heat transfer coefficient on the end winding surface using the inlet design **3**. A fourth curve **3513** shows the heat transfer coefficient on the end winding surface using the inlet design **4**.

Referring to FIG. **35**C, a stator surface heat transfer coefficient comparison is shown in accordance with an illustrative embodiment. A first curve **3520** shows the heat transfer coefficient on the stator surface using the inlet design **1**. A second curve **3521** shows the heat transfer coefficient on the stator surface using the inlet design **2**. A third curve **3522** shows the heat transfer coefficient on the stator surface using the inlet design **3**. A fourth curve **3523** shows the heat transfer coefficient on the stator surface using the inlet design **4**.

Referring to FIG. **36**A, a front view is shown of an inlet air flow velocity pattern using inlet design **1** in accordance with an illustrative embodiment. Referring to FIG. **36**B, a front view is shown of an inlet air flow velocity pattern using inlet design **2** in accordance with an illustrative embodiment. Referring to FIG. **36**C, a front view is shown of an inlet air flow velocity pattern using inlet design **3** in accordance with an illustrative embodiment. Referring to FIG. **36**D, a front view is shown of an inlet air flow velocity pattern using inlet design **4** in accordance with an illustrative embodiment. FIGS. **36**A-**36**D show the radial inlet flow streamlines at volume flow rate of 1.14 m^3/s.

Most of the flow entering the radial inlets directly enters the fan zone after passing the stator and end winding surfaces. There is a small amount of flow swirling in the regions not directly adjacent to the inlets. The inlet design **1** has the smallest heat transfer coefficients due to the small radial inlet area and associated reduction in the flow in the housing. The heat transfer coefficients of inlet design **2** are slightly larger than those of design **3** and **4**. It is found that larger radial inlets do not necessarily lead to larger heat transfer coefficients. The smaller flow area can result in higher flow velocity. As shown in FIG. **36**B, the flow velocity above the end windings is approximately 110 m/s; whereas in FIG. **36**C, the flow velocity is around 96 m/s. Inlet designs **3** and **4** have the same radial inlet area, but design **4** has smaller axial inlets. At the same fan zone volume flow rate, the axial inlet volume flow rate reduces with the decrease of axial inlet area. Therefore, the radial inlet volume flow rate will increase. With constant radial inlet area, larger volume flow rate means higher flow velocity. As shown in FIG. **36**D, the flow velocity above the end winding surface is about 105 m/s in inlet design **4**, which is higher than 96 m/s in design **3**.

Similar to housing inlets, the housing outlet can be designed into axial and radial outlets, and the area and structure of the outlets can be adjusted. Referring to FIG. **37**, a back view is shown of housing **2600** with the axial outlet aperture walls **2612** defining four axial apertures with radial angle **2800** equal to 75-degrees in accordance with an illustrative embodiment. The total radial angle is the same as the axial outlet aperture walls **2612** defining two axial apertures with radial angle **2800** equal to 150-degrees. FIG. **38**A shows the outlet air flow velocity pattern relative to housing **2600** with electrical machine **100** mounted therein for housing **2600** with the axial outlet aperture walls **2612** defining four axial apertures with radial angle **2800** equal to 75-degrees as compared to FIG. **31** that shows the outlet air flow velocity pattern relative to housing **2600** with electrical machine **100** mounted therein for housing **2600** with the axial outlet aperture walls **2612** defining two axial apertures with radial angle **2800** equal to 150-degrees. Due to the different outlet structures, the rear end winding and stator surface have an uneven temperature distribution, which is shown referring to FIGS. **38**B and **38**C that show the total temperature and FIGS. **38**D and **38**E that show the wall temperature. The flow leaving the fan zone has a high velocity and directly exits housing **2600** through the outlet apertures. In those regions without an adjacent outlet, airflow is blocked and flows to the region above the rear end winding and stator surface, cooling these surfaces. The area away from the outlets has a lower temperature than the area close to the outlet apertures due to the increased cooling on these surfaces. In the two axial outlets model, the flow entering the end winding and stator region has a higher velocity, which can lead to a larger heat transfer coefficient. However, with the same amount of heat flux on stator and end winding surfaces, in the four axial outlet apertures model, the highest temperature is 326 K which is lower than 345 K in the two axial outlet apertures model.

Referring to FIG. **38**F, a pressure drop comparison is shown at a rear of the housing that results from outlet design **1** that is housing **2600** with the axial outlet aperture walls **2612** defining two axial apertures with radial angle **2800** equal to 150-degrees and outlet design **2** that is housing **2600** with the axial outlet aperture walls **2612** defining four axial apertures with radial angle **2800** equal to 75-degrees in accordance with an illustrative embodiment. A first curve **3800** shows the front housing pressure drop using outlet design **1**. A second curve **3801** shows the front housing pressure drop using outlet design **2**. The housing design with two axial apertures has approximately 20% larger pressure drop in the housing than the design with four axial apertures.

Referring to FIG. **38**G, a heat transfer coefficient comparison is shown between outlet design **1** and outlet design **2** in accordance with an illustrative embodiment. A first curve **3810** shows the end winding heat transfer coefficient using outlet design **1**. A second curve **3811** shows the stator surface heat transfer coefficient using outlet design **1**. A third curve **3812** shows the end winding heat transfer coefficient using outlet design **2**. A fourth curve **3813** shows the stator surface heat transfer coefficient using outlet design **2**. Since the heat transfer coefficients are calculated using the maximum wall temperature, outlet design **2** has a larger end winding and stator surface heat transfer coefficient than design **1**.

Referring to FIG. **39**, a perspective view is shown of a second housing **2600'** in accordance with an illustrative

embodiment. Second housing **2600'** may include front wall **2602**, a second radial sidewall **2604'**, and back wall **2606** that form an enclosure. The radial inlet aperture walls **2610** are formed in second radial sidewall **2604'** and form arcs relative to a center of second radial sidewall **2604'** and extend circumferentially around second radial sidewall **2604'**. Radial outlet aperture walls **3900** are also formed in second radial sidewall **2604'** and form arcs relative to a center of second radial sidewall **2604'** and extend circumferentially around second radial sidewall **2604'**. The radial inlet aperture walls **2610** and the radial outlet aperture walls **3900** may have the same or different shapes with the same or different areas and axial locations. A number of the radial inlet aperture walls **2610** and the radial outlet aperture walls **3900** further may be the same or different. In the illustrative embodiment, a number of the radial inlet aperture walls **2610** and a number of the radial outlet aperture walls **3900** is six. The radial outlet aperture walls **3900** have a greater radial arclength **2810** and axial width **2812** relative to the radial inlet aperture walls **2610**. As a result, an area of the radial outlet aperture walls **3900** is greater than an area of the radial inlet aperture walls **2610**.

CFD simulations were performed with radial arclength **2810** for the radial inlet aperture walls **2610** of between 5-degrees and 40-degrees at 5-degree increments. The curve fitting results for end winding and stator surface heat transfer coefficients are shown in Table 3, where v is the average flow velocity in the stator.

TABLE 3

Radial inlet circumferential angle (deg)	Stator surface analytical model	End winding analytical model
5	h_{stator} = 3.38v + 41.4	$h_{winding}$ = 3.61v + 41.22
10	h_{stator} = 3.42v + 49.3	$h_{winding}$ = 4.08v + 43.9
15	h_{stator} = 3.5v + 46.9	$h_{winding}$ = 4.35v + 37.5
20	h_{stator} = 3.73v + 49.2	$h_{winding}$ = 4.94v + 36.1
25	h_{stator} = 3.9v + 48.6	$h_{winding}$ = 4.88v + 42.8
30	h_{stator} = 4v + 49.5	$h_{winding}$ = 4.98v + 44.6
40	h_{stator} = 4.28v + 49.3	$h_{winding}$ = 4.96v + 44.4

From the equations shown in Table 3, at different radial inlet circumferential angles, there is an almost constant offset. For the stator surface, the coefficient for velocity is increasing as the radial inlet angle increases. For end winding surface, however, the heat transfer coefficient first increases then approximately stays the same after 20-degrees. The constant heat transfer coefficient is due to the air swirling above the end windings. Optimization can also be done using the analytical model to find the desired inlet and outlet design.

Referring to FIG. **40**A, a first stator surface heat transfer coefficient comparison is shown that results from different radial inlet models in accordance with an illustrative embodiment. A first curve **4000** shows the stator surface heat transfer coefficient using the radial inlet aperture walls **2610** having a radial arclength **2810** of 5-degrees. A second curve **4001** shows the stator surface heat transfer coefficient using the radial inlet aperture walls **2610** having a radial arclength **2810** of 10-degrees. A third curve **4002** shows the stator surface heat transfer coefficient using the radial inlet aperture walls **2610** having a radial arclength **2810** of 15-degrees. A fourth curve **4003** shows the stator surface heat transfer coefficient using the radial inlet aperture walls **2610** having a radial arclength **2810** of 20-degrees. A fifth curve **4004** shows the stator surface heat transfer coefficient using the radial inlet aperture walls **2610** having a radial arclength **2810** of 25-degrees. A sixth curve **4005** shows the stator surface heat transfer coefficient using the radial inlet aperture walls **2610** having a radial arclength **2810** of 30-degrees. A seventh curve **4006** shows the stator surface heat transfer coefficient using the radial inlet aperture walls **2610** having a radial arclength **2810** of 40-degrees.

Referring to FIG. **40**B, a stator surface heat transfer coefficient comparison is shown for various fan volume flow rates in accordance with an illustrative embodiment. A first curve **4010** shows the stator surface heat transfer coefficient for a fan volume flow rate of 1.14 m^3/s. A second curve **4011** shows the stator surface heat transfer coefficient for a fan volume flow rate of 0.93 m^3/s. A third curve **4012** shows the stator surface heat transfer coefficient for a fan volume flow rate of 0.78 m^3/s. A fourth curve **4013** shows the stator surface heat transfer coefficient for a fan volume flow rate of 0.62 m^3/s. A fifth curve **4014** shows the stator surface heat transfer for a fan volume flow rate of 0.47 m^3/s. A sixth curve **4015** shows the stator surface heat transfer coefficient for a fan volume flow rate of 0.31 m^3/s.

Referring to FIG. **40**C, a first end winding surface heat transfer coefficient comparison is shown that results from different outlet models in accordance with an illustrative embodiment. A first curve **4020** shows the end winding heat transfer coefficient using the radial inlet aperture walls **2610** having a radial arclength **2810** of 5-degrees. A second curve **4021** shows the end winding heat transfer coefficient using the radial inlet aperture walls **2610** having a radial arclength **2810** of 10-degrees. A third curve **4022** shows the end winding heat transfer coefficient using the radial inlet aperture walls **2610** having a radial arclength **2810** of 15-degrees. A fourth curve **4023** shows the end winding heat transfer coefficient using the radial inlet aperture walls **2610** having a radial arclength **2810** of 20-degrees. A fifth curve **4024** shows the end winding heat transfer coefficient using the radial inlet aperture walls **2610** having a radial arclength **2810** of 25-degrees. A sixth curve **4025** shows the end winding heat transfer coefficient using the radial inlet aperture walls **2610** having a radial arclength **2810** of 30-degrees. A seventh curve **4026** shows the end winding heat transfer coefficient using the radial inlet aperture walls **2610** having a radial arclength **2810** of 40-degrees.

Referring to FIG. **40**D, a second end winding surface heat transfer coefficient comparison is shown that results from different outlet models in accordance with an illustrative embodiment. A first curve **4030** shows the end winding heat transfer coefficient for a fan volume flow rate of 1.14 m^3/s. A second curve **4031** shows the end winding heat transfer coefficient for a fan volume flow rate of 0.93 m^3/s. A third curve **4032** shows the end winding heat transfer coefficient for a fan volume flow rate of 0.78 m^3/s. A fourth curve **4033** shows the end winding heat transfer coefficient for a fan volume flow rate of 0.62 m^3/s. A fifth curve **4034** shows the end winding heat transfer for a fan volume flow rate of 0.47 m^3/s. A sixth curve **4035** shows the end winding heat transfer coefficient for a fan volume flow rate of 0.31 m^3/s. From FIG. **40**A and FIG. **40**C, it can be observed that the surface heat transfer coefficient has a linear relationship with stator average flow velocity.

To verify the self-cooling function, a thermal finite element analysis (FEA) was conducted with inlet design **2** (six radial inlets of 20-degrees and two axial inlets of 150-degrees) and outlet design **2** (four axial outlets of 75-degrees). The machine parameters and thermal boundary conditions are shown in Table 4.

TABLE 4

Parameters	Value
Stator outer diameter [mm]	300
Rotor tip diameter [mm]	200
Machine speed [rpm]	10,000
Current density [A_{rms}/mm^2]	5
Output power [kW]	30
Total loss [W]	1055
Efficiency [%]	96.6
Front end winding surface heat transfer coefficient [W/m^2-K]	278
Rear end winding surface heat transfer coefficient [W/m^2-K]	152
Front stator surface heat transfer coefficient [W/m^2-K]	230
Rear stator surface heat transfer coefficient [W/m^2-K]	150
Stator inner surface heat transfer coefficient [W/m^2-K]	433.9
Rotor surface heat transfer coefficient [W/m^2-K]	435.7
In slot surface heat transfer coefficient [W/m^2-K]	832.4
Stator outer surface heat transfer coefficient [W/m^2-K]	5

A Nomex **410** slot liner was used in the design, which has a thickness of 0.179 mm and a thermal conductivity of 0.149 W/m-K. The equivalent heat transfer coefficient from the in-slot winding to stator core **108** can then be calculated using the thermal conductivity and thickness of the slot liner. For natural convection of the housing, the convective heat transfer coefficient of the stator outer surface is set as 5 W/m^2-K. The output power of the machine is 30 kW, where the total loss is 1055 W. The temperature distribution in stator **102** is shown in FIG. **41**A. The rotor temperature is much lower than the stator temperature and therefore is not shown in FIG. **41**A. Since both stator front and rear surfaces are cooled by air, the middle part of the stator iron has the highest temperature. The maximum temperature of the permanent magnets is 111° C., which is in the acceptable range.

If there is no forced convection from the air entering the housing, the stator inner surface and rotor surface heat transfer coefficients are set as 100 W/m^2-K to account for the high rotational speed, and the other end winding and stator surfaces are set to have heat transfer coefficients of 5 W/m^2-K. In this case, as shown in FIG. **41**B, the maximum magnet temperature can be as high as 475-degrees Celsius. Active cooling with a water jacket would need to be included in the design to cool the machine. The effect of using a water jacket can be simulated by increasing the heat transfer coefficient of the stator outer surface. It is found that the water jacket can effectively cool the stator iron and permanent magnets. The maximum magnet temperature can be reduced to 139-degrees Celsius when the stator outer surface heat transfer coefficient is 300 W/m^2-K. However, the end windings cannot be cooled by the water jacket. Even when the stator outer surface heat transfer coefficient is 10,000 W/m^2-K, the maximum end winding temperature is still around 350-degrees Celsius.

In the FEA simulation, RECOMA 35E samarium cobalt magnets from Arnold Magnetic Technologies were used that have a maximum operating temperature of 350-degrees Celsius. Since the maximum magnet temperature is 111-degrees Celsius at 5 A_{rms}/mm^2 current density, the current density of the integrated machine is increased to explore the potential of its improved cooling capability. The total loss, maximum magnet temperature, and maximum winding temperature at different current densities are shown in Table 5. At a current density of 15 A_{rms}/mm^2, the maximum magnet temperature is 340-degrees Celsius. However, the maximum winding temperature is very high. The temperature distribution in the windings at 15 A_{rms}/mm^2 is shown in FIG. **41**C. It can be observed in FIG. **41**C that the end winding surfaces have a relatively low temperature due to the cooling from the airflow. The in-slot windings, however, have higher temperature. This issue can be solved by using foil windings or adding scaffolds or other openings to the windings to allow air flow and further reduce the winding temperature.

TABLE 5

Current density [A_{rms}/mm^2]	5	5	10	15
Total loss [W]	1055	1055	2367	4147
Cooling method	Self-cooling	No self-cooling	Self-cooling	Self-cooling
Maximum magnet temperature [° C.]	111	475	212	340
Maximum winding temperature [° C.]	99	589	235	463

Referring to FIG. **42**, a perspective view is shown of a sixth electrical machine **4200** with hub **2300** with the second plurality of blades **118'** interior of a third rotor **4204** in accordance with an illustrative embodiment. Sixth electrical machine **4200** may include a fifth stator **4202** that included a second plurality of windings **4208** mounted in slots formed a plurality of teeth. A fourth plurality of magnets **4206** are mounted within a rotor core of third rotor **4204**.

Sixth electrical machine **4200** implemented as a 24-slot 4-pole IPM machine with hub **2300** was used to verify the cooling effect. The machine design parameters and performances are listed in Table 6 below.

TABLE 6

Parameters and Performances	Value
Stator outer diameter [mm]	112
Stator inner diameter [mm]	56
Rotor outer diameter [mm]	55
Rotor inner diameter [mm]	15
Blade tip diameter [mm]	25.3
Blade hub diameter [mm]	17.7
Stack length [mm]	10
Pole number	4
Slot number	24
Speed [rpm]	5,000
Winding turns per phase	35
Current density [A_{rms}/mm^2]	10
Average torque [Nm]	0.7
Fan power [W]	0.014
Output power [W]	367
Copper loss [W]	22
Stator iron loss [W]	3.4
Rotor iron loss [W]	0.1
Efficiency	93.5%

There are flux barriers designed in third rotor **4204**, which are air voids to prevent the flow of flux between the fourth plurality of magnets **4206**. At 5,000 rpm, 10 A_{rms}/mm^2 current density, the machine's output power is 367 W with an efficiency of 93.5%. The fan power associated with the second plurality of blades **118'** is 0.014 W, which is very small because of the small fan size. For the IPM machine, since the magnets are inserted in the rotor iron, there is limited space for hub **2300** and the second plurality of blades **118'**. For other machine types, such as the SPM machine, the fan size can be larger, providing more cooling effect.

Referring to FIG. **43**, a perspective view is shown of a second housing **4300** in accordance with an illustrative embodiment. Second housing **4300** may include a solid front wall **4302**, second radial sidewall **2604'**, and a solid back wall **4306** that form an enclosure. The radial inlet aperture walls **2610** and the radial outlet aperture walls **3900** are formed in second radial sidewall **2604'**. In the illustrative embodiment, of FIG. **43**, the radial inlet aperture walls **2610**

and the radial outlet aperture walls **3900** have the same shape and size and are positioned at the same axial locations. Air flow enters second housing **4300** and passes over the front end winding, fifth stator **4202**, and third rotor **4204**. Then, the flow is accelerated in the rotor stage and exits second housing **4300** after passing the rear surfaces. In this process, a small amount of flow also goes into the flux barrier space, cooling the surrounding surfaces. The CFD model is separated into the front and rear parts to simplify the model and improve accuracy.

Referring to FIG. **44**A, a front view is shown of an inlet air flow velocity pattern within second housing **4300** with sixth electrical machine **4200** mounted therein in accordance with an illustrative embodiment. Referring to FIG. **44**B, a back view is shown of an outlet air flow velocity pattern within second housing **4300** with sixth electrical machine **4200** mounted therein in accordance with an illustrative embodiment.

Steady state thermal FEA was performed for sixth electrical machine **4200**. The heat transfer coefficients associated with different surfaces are listed in Table 7.

TABLE 7

Surface	Heat transfer coefficient [W/m^2-k]	Surface	Heat transfer coefficient [W/m^2-k]
Front end winding surface	29	Front rotor surface	25
Rear end winding surface	18	Rear rotor surface	12
Front stator surface	22	Rotor flux barrier surface	16
Rear stator surface	9	Air gap surface	10
Rotor blade hub surface	100		

The thermal analysis as conducted at 10 A_{rms}/mm^2 current density. The machine output power, losses, and maximum temperatures are shown in Table 8. Since for sixth electrical machine **4200**, the losses on third rotor **4204** are minimal, the fourth plurality of magnets **4206** have a low temperature. Copper loss is the largest loss in sixth electrical machine **4200**. As shown in Table 8, at 10 A_{rms}/mm^2 with self-cooling provided by hub **2300** and the radial inlet aperture walls **2610** and the radial outlet aperture walls **3900**, the maximum winding temperature is 94-degrees Celsius. The maximum stator temperature is very close to the maximum winding temperature. Thus, even with a small fan zone with a minimum fan power, fifth stator **4202** and the end windings can still be effectively cooled by the produced airflow.

TABLE 8

Current density [A_{rms}/mm^2]	10	10
Cooling method	Self-cooling hub 2300/ second housing 4300	No self-cooling
Output power [W]	367	367
Copper loss [W]	22	43
Stator iron loss [W]	3.4	3.4
Rotor iron loss [W]	0.1	0.1
Maximum winding temperature [° C.]	94	453
Maximum magnet temperature [° C.]	107	467

Referring to FIG. **45**A, a stator temperature distribution is shown for sixth electrical machine **4200** with self-cooling in accordance with an illustrative embodiment. Referring to FIG. **45**B, a stator temperature distribution is shown for sixth electrical machine **4200** without self-cooling in accordance with an illustrative embodiment. FIGS. **45**A and **45**B shows the stator temperature distribution at 10 A_{rms}/mm^2. Without self-cooling, the maximum winding temperature under this operating condition can be as high as 453-degrees Celsius. This temperature is not attainable with copper wires. Without the cooling effect from the airflow, a more complex cooling scheme such as spray cooling of end windings may be necessary, which is more expensive and requires a complex arrangement that includes a pump for creating oil flow, scavenge system, filtering, etc.

As the current density of the electrical machine increases, adequate cooling is needed for windings, especially end windings, which are often the hot spots in the machine. Thermal management of the electrical machine's rotor is critical for permanent magnet machines to protect permanent magnets from demagnetization. For induction motors, where there are windings on the rotor, the temperature rise on the rotor needs to be limited to protect the winding insulation. Traditional cooling methods such as using a water jacket can effectively cool the stator iron from the machine's outer surface. However, the coolant cannot reach the rotor and end windings except by adding additional cooling paths, which will increase the machine's complexity. Oil-spray cooling is another common cooling method to cool the rotor, which also results in a complicated machine assembly structure. In addition, these methods also lead to a reduction of motor efficiency since the pump and the chiller consume a higher amount of power than a fan. These added components also increase the system volume and reduce the machine's power density. They also lower the system reliability.

The plurality of blades **118** and the second plurality of blades **118'** solve these issues by combining a fan with the rotor structure to provide direct cooling to the rotor iron. With radial inlets on the housing, the end windings can also be effectively cooled by the airflow. The plurality of blades **118** and the second plurality of blades **118'** further reduce the rotor weight. The area and position of inlets and outlets can be optimized to guide the flow to the hot spots that need cooling depending on the electrical machine architecture.

The term "air" is used herein to reference any gas. The word "illustrative" is used herein to mean serving as an example, instance, or illustration. Any aspect or design described herein as "illustrative" is not necessarily to be construed as preferred or advantageous over other aspects or designs. Further, for the purposes of this disclosure and unless otherwise specified, "a" or "an" means "one or more". Still further, in the detailed description, using "and" or "or" is intended to include "and/or" unless specifically indicated otherwise.

The foregoing description of illustrative embodiments of the disclosed subject matter has been presented for purposes of illustration and of description. It is not intended to be exhaustive or to limit the disclosed subject matter to the precise form disclosed, and modifications and variations are possible in light of the above teachings or may be acquired from practice of the disclosed subject matter. The embodiments were chosen and described in order to explain the principles of the disclosed subject matter and as practical applications of the disclosed subject matter to enable one skilled in the art to utilize the disclosed subject matter in various embodiments and with various modifications as suited to the particular use contemplated. It is intended that the scope of the disclosed subject matter be defined by the claims appended hereto and their equivalents.

What is claimed is:

1. An electrical machine comprising:

a rotor comprising

a rotor core configured to mount to a shaft for rotation of the rotor core and shaft together; and

a plurality of blades extending radially away from the rotor core;

a stator comprising

a stator core; and

a plurality of teeth extending from the stator core toward the rotor core, wherein the plurality of teeth defines a plurality of slots between successive teeth of the plurality of teeth;

a winding wound through the plurality of slots, wherein the stator is mounted radially relative to the rotor; and

a housing comprising

a front wall;

a back wall;

a radial sidewall mounted between the front wall and the back wall to define an enclosure;

a plurality of radial inlet aperture walls formed circumferentially around the radial sidewall; and

a plurality of radial outlet aperture walls formed circumferentially around the radial sidewall,

wherein an area of each of the plurality of radial outlet aperture walls is greater than an area of each of the plurality of radial inlet aperture walls,

wherein a number of the plurality of radial inlet aperture walls is same as a number of the plurality of radial outlet aperture walls.

2. The electrical machine of claim 1, wherein the plurality of radial inlet aperture walls are positioned above a front portion of the winding.

3. The electrical machine of claim 1, wherein the plurality of radial inlet aperture walls are evenly distributed circumferentially around the radial sidewall.

4. The electrical machine of claim 1, wherein the plurality of radial inlet aperture walls are aligned axially to encircle the radial sidewall.

5. The electrical machine of claim 1, wherein the area of each of the plurality of radial outlet aperture walls is greater than the area of each of the plurality of radial inlet aperture walls because an arclength of each of the plurality of radial outlet aperture walls is greater than an arclength of each of the plurality of radial inlet aperture walls.

6. The electrical machine of claim 1, wherein each radial inlet aperture wall of the plurality of radial inlet aperture walls has a radial arclength of greater than or equal to twenty degrees relative to a center of the rotor core.

7. The electrical machine of claim 6, wherein each radial inlet aperture wall of the plurality of radial inlet aperture walls has a radial arclength of less than or equal to 170 degrees relative to the center of the rotor core.

8. The electrical machine of claim 1, wherein each of the plurality of radial outlet aperture walls is axially offset from each of the plurality of radial inlet aperture walls between the front wall and the back wall.

9. The electrical machine of claim 1, wherein each radial outlet aperture wall of the plurality of radial outlet aperture walls is centered axially relative to a respective radial inlet aperture wall of the plurality of radial inlet aperture walls.

10. The electrical machine of claim 1, wherein the area of each of the plurality of radial outlet aperture walls is greater than the area of each of the plurality of radial inlet aperture walls because an axial width of each of the plurality of radial outlet aperture walls is greater than an axial width of each of the plurality of radial inlet aperture walls.

11. The electrical machine of claim 1, wherein each of the plurality of radial inlet aperture walls and each of the plurality of radial outlet aperture walls has an arc shape relative to a center of the radial sidewall.

12. The electrical machine of claim 1, further comprising an axial inlet aperture wall formed through the front wall to form a first opening through the front wall.

13. The electrical machine of claim 12, wherein a plurality of axial inlet aperture walls is formed through the front wall to form a plurality of openings through the front wall, wherein the axial inlet aperture wall is one of the plurality of axial inlet aperture walls.

14. The electrical machine of claim 13, wherein the plurality of axial inlet aperture walls is formed to align axially with the plurality of blades.

15. The electrical machine of claim 13, wherein each axial inlet aperture wall of the plurality of axial inlet aperture walls has a common shape and size with a radial arclength of greater than or equal to 75 degrees and less than or equal to 150 degrees relative to a center of the front wall.

16. The electrical machine of claim 13, further comprising a plurality of axial outlet aperture walls, wherein each axial outlet aperture wall of the plurality of axial outlet aperture walls is formed circumferentially through the back wall to form second openings through the back wall.

17. The electrical machine of claim 16, wherein each axial outlet aperture wall of the plurality of axial outlet aperture walls is centered axially relative to a respective axial inlet aperture wall of the plurality of axial inlet aperture walls.

18. An electrical machine comprising:

a hub comprising

a hub core configured to mount to a shaft for rotation; and

a plurality of blades extending radially away from the hub core;

a rotor core configured to mount to the plurality of blades;

a stator comprising

a stator core; and

a plurality of teeth extending from the stator core toward the rotor core, wherein the plurality of teeth defines a plurality of slots between successive teeth of the plurality of teeth;

a winding wound through the plurality of slots, wherein the stator is mounted radially relative to the rotor; and

a housing comprising

a front wall;

a back wall;

a radial sidewall mounted between the front wall and the back wall to define an enclosure, wherein the hub, the rotor core, and the stator are mounted within the enclosure;

a plurality of radial inlet aperture walls formed circumferentially around the radial sidewall; and

a plurality of radial outlet aperture walls formed circumferentially around the radial sidewall,

wherein an area of each of the plurality of radial outlet aperture walls is greater than an area of each of the plurality of radial inlet aperture walls,

wherein a number of the plurality of radial inlet aperture walls is same as a number of the plurality of radial outlet aperture walls.

19. The electrical machine of claim 18, wherein the plurality of radial inlet aperture walls are positioned above a front portion of the winding.

20. The electrical machine of claim 18, wherein the plurality of radial inlet aperture walls are evenly distributed circumferentially around the radial sidewall.

* * * * *